

CONSTRAINTS ON PRIMORDIAL BLACK HOLES

Bernard Carr,^{1,2,*} Kazunori Kohri,^{3,4,5,6,†} Yuuiti Sendouda,^{7,‡} and Jun'ichi Yokoyama^{2,5,§}

¹*School of Physics and Astronomy, Queen Mary University of London, Mile End Road, London E1 4NS, UK*

²*Research Center for the Early Universe (RESCEU),*

Graduate School of Science, The University of Tokyo, Tokyo 113-0033, Japan

³*KEK Theory Center, IPNS, KEK, Tsukuba, Ibaraki 305-0801, Japan*

⁴*The Graduate University for Advanced Studies (SOKENDAI), Tsukuba, Ibaraki 305-0801, Japan*

⁵*Kavli Institute for the Physics and Mathematics of the Universe,*

The University of Tokyo, Kashiwa, Chiba 277-8568, Japan

⁶*Rudolf Peierls Centre for Theoretical Physics, The University of Oxford, 1 Keble Road, Oxford OX1 3NP, UK*

⁷*Graduate School of Science and Technology, Hirosaki University, Hirosaki, Aomori 036-8561, Japan*

(Dated: Thursday 11th November, 2021, 04:20)

We update the constraints on the fraction of the Universe going into primordial black holes (PBHs) over the mass range 10^{-5} – 10^{50} g. Those smaller than $\sim 10^{15}$ g would have evaporated by now due to Hawking radiation, so their abundance at formation is constrained by the effects of evaporated particles on big bang nucleosynthesis, the cosmic microwave background (CMB), the Galactic and extragalactic γ -ray and cosmic ray backgrounds and the possible generation of stable Planck mass relics. PBHs larger than $\sim 10^{15}$ g are subject to a variety of constraints associated with gravitational lensing, dynamical effects, influence on large-scale structure, accretion and gravitational waves. We discuss the constraints on both the initial collapse fraction and the current fraction of the cold dark matter in PBHs at each mass scale but stress that many of the constraints are associated with observational or theoretical uncertainties and some are no longer applicable. We also consider indirect constraints associated with the amplitude of the primordial density fluctuations, such as second-order tensor perturbations and μ -distortions arising from the effect of acoustic reheating on the CMB, but these only apply if PBHs are created from the high- σ peaks of nearly Gaussian fluctuations. Finally we discuss how the constraints are modified if the PBHs have an extended mass function, this being relevant if PBHs provide some combination of the dark matter, the LIGO/Virgo coalescences and the seeds for cosmic structure.

CONTENTS

I. Introduction	3
A. Overview	3
B. PBH formation	4
1. Collapse from inhomogeneities	4
2. Soft equation of state	4
3. Critical collapse	5
4. Collapse of cosmic loops	5
5. Bubble collisions	5
6. Collapse of scalar field	5
7. Collapse of domain walls	5
C. Mass and density fraction of PBHs	6
D. Evaporation of PBHs	7
1. Mass loss and evaporation timescale	8
2. Primary and secondary emission	9
II. Constraints on evaporating PBHs	10
A. Big bang nucleosynthesis	10
1. Modern studies	11
2. Lithium-7	12
B. Cosmic microwave background	13

* B.J.Carr@qmul.ac.uk

† kohri@post.kek.jp

‡ sendouda@hirosaki-u.ac.jp

§ yokoyama@resceu.s.u-tokyo.ac.jp

1. Generation of entropy	13
2. CMB spectral distortions	13
3. CMB anisotropies	13
C. Cosmic ray and γ -ray backgrounds	14
1. Extragalactic γ -ray background	14
2. Galactic γ -ray background	17
3. Galactic positrons and antiprotons	18
4. Extragalactic antiprotons	19
5. Annihilation-line radiation	20
6. Emission of other particles	20
7. Reionisation and 21 cm signature	21
D. PBH explosions	22
1. Gamma-ray bursts and photosphere effects	22
2. High energy cosmic rays showers	23
E. Higgs instability	23
F. Planck mass relic constraints	23
III. Constraints on non-evaporated PBHs	24
A. Evaporation Constraints	25
B. Lensing Constraints	26
1. Femtolensing and picolensing	27
2. Microlensing of stars	27
3. Microlensing of supernovae	29
4. Quasar microlensing and millilensing	29
5. Microlensing of Mira variables, pulsars and fast radio bursts	30
C. Dynamical Constraints	30
1. Collisions	31
2. Neutron stars and white dwarfs	32
3. Wide binaries	32
4. Disruption of globular clusters and dwarf galaxies	33
5. Disc heating	34
6. Tidal streams	34
7. Dynamical friction effect on halo objects	34
8. Disruption and tidal distortion of galaxies in clusters	34
9. Intergalactic PBHs	35
D. Cosmic Structure Constraints	35
1. Lyman- α systems	36
2. Galaxies and clusters of galaxies	36
3. First baryonic clouds	37
4. Clusters of PBHs	37
E. Accretion and μ -distortion constraints	38
1. Accretion during radiation-dominated era	38
2. Limit from ionisation and thermal history	39
3. μ distortion	40
F. Gravitational Wave Constraints	41
1. Gravitational wave background	41
2. PBHs and the LIGO/Virgo events	42
3. Constraints from second order tensor perturbations	43
IV. Constraints for monochromatic and extended PBH mass functions	44
A. PBH mass function	46
B. Constraints for extended PBH mass function	48
V. Conclusion	50
Acknowledgments	51
References	52

I. INTRODUCTION

A. Overview

Primordial black holes (PBHs) have been a source of intense interest for more than 50 years [1], despite the fact that there is still no evidence for them. One reason for this interest is that only PBHs could be small enough for Hawking radiation to be important [2]. This has not yet been confirmed experimentally but this discovery is generally recognised as one of the key developments in 20th century physics and Hawking was only led to it through contemplating the properties of PBHs. Indeed, those smaller than about 10^{15} g would have evaporated by now but could still have many interesting cosmological consequences.

PBHs larger than 10^{15} g are unaffected by Hawking radiation but have also attracted interest because of the possibility that they provide the dark matter which comprises 25% of the critical density [3], an idea that goes back to the earliest days of PBH research [4]. Since PBHs formed in the radiation-dominated era, they are not subject to the well-known big bang nucleosynthesis (BBN) constraint that baryons can have at most 5% of the critical density [5]. They should therefore be classed as non-baryonic and from a dynamical perspective they behave like any other cold dark matter (CDM) candidate. There is still no compelling evidence that PBHs provide the dark matter, but nor is there for any of the more traditional CDM candidates.

Despite the lack of evidence for them, PBHs have been invoked to explain numerous cosmological features. For example, evaporating PBHs have been invoked to explain the extragalactic [6] and Galactic [7] γ -ray backgrounds, antimatter in cosmic rays [8], the annihilation line radiation from the Galactic centre [9], the reionization of the pregalactic medium [10] and some short-period gamma-ray bursts [11]. Non-evaporating PBHs – even if they do not provide the dark matter – have been invoked to explain lensing effects, the heating of the stars in our Galactic disc, the seeds for the supermassive black holes in galactic nuclei [12], the generation of large-scale structure through Poisson fluctuations [13], effects on the thermal and ionization history of the Universe [14] and – most recently – the LIGO/Virgo gravitational wave bursts [15–18]. Indeed, if the PBHs have an extended mass function, they might explain a multitude of cosmic conundra [19].

There are usually other possible explanations for these features, so there is still no definitive evidence for PBHs. Nevertheless, studying each of these effects allows one to place interesting constraints on the number of PBHs of mass M and this in turn places constraints on the cosmological models which would generate them. We will be discussing all these constraints in this review. For evaporating PBHs these are usually expressed as constraints on the fraction of the universe collapsing into PBHs at their formation epoch, denoted as $\beta(M)$. Indeed, this must be less than 10^{-18} over the entire mass range 10^9 – 10^{15} g. For non-evaporating ones they are most usefully expressed as constraints on the fraction of the dark matter in PBHs, denoted as $f(M)$. Despite the hope of many people that PBHs could provide the dark matter, it was already clear a decade ago that there are only a few mass windows where this is possible [20]: the asteroid range (10^{16} – 10^{17} g), the sublunar range (10^{20} – 10^{26} g) and the intermediate-mass range (10 – $10^3 M_\odot$). Since then, interest in PBHs as dark matter has increased – primarily because of the LIGO/Virgo events – and the lowest and highest mass windows have narrowed and perhaps been excluded entirely. On the other hand, the middle mass window has opened due to a weakening of some constraints. In practice, PBHs are expected to have an extended mass function but whether this makes it easier or more difficult for them to provide the dark matter has been the subject of some dispute.

In this review, we discuss all the PBH constraints, summarizing our results as excluded regions in the $\beta(M)$ and $f(M)$ planes. Similar diagrams have been produced by numerous authors – indeed almost every paper on PBHs now includes such a diagram – and we should particularly draw attention to the recent review of PBHs by Sasaki *et al.* [21]. However, we hope this review will be more comprehensive and up-to-date than the others. For example, Ref. [21] puts more emphasis on gravitational waves but does not discuss the limits on evaporating PBHs.

We should stress at the outset that the limits are constantly changing as a result of both observational and theoretical developments, so our claim for comprehensiveness may be short-lived. We will also discuss *all* claimed limits – even those which are no longer believed – because this is historically illuminating. Even wrong calculations are worth recording because this may avoid their being repeated in the future. In fact, all of the limits come with certain caveats and few can be regarded as 100% secure. (For example, the evaporation constraints assume the validity of Hawking radiation, even though there is still no direct observational evidence for this.) While we emphasize which limits have gone away or are questionable, we do not attempt to specify the confidence levels precisely, this sometimes being a rather contentious task anyway.

Since our primary purpose is the constraints, we will only include a brief discussion of the PBH formation mechanisms and there will little attempt to describe the more positive aspects of PBHs (i.e. the numerous ways in which they can probe the early Universe, high energy physics or even quantum gravity). However, this broader range of topics is covered in two other forthcoming reviews: one on PBHs and dark matter (Carr & Kuhnel, in preparation) and another on all aspects of PBHs (Carr, in preparation). So all these works should be regarded as complementary.

B. PBH formation

Black holes with a wide range of masses could have formed in the early Universe as a result of the great compression associated with the big bang [22, 23]. A comparison of the cosmological density at a time t after the big bang with the density associated with a black hole of mass M suggests that such PBHs would have a mass of order

$$M \sim \frac{c^3 t}{G} \sim 10^{15} \left(\frac{t}{10^{-23} \text{ s}} \right) \text{ g}. \quad (1)$$

This roughly corresponds to the Hubble mass at time t . PBHs could thus span an enormous mass range: those formed at the Planck time (10^{-43} s) would have the Planck mass (10^{-5} g), whereas those formed at 1 s would be as large as $10^5 M_\odot$, comparable to the mass of the holes thought to reside in galactic nuclei. By contrast, black holes forming at the present epoch could never be smaller than about $1 M_\odot$. The high density of the early Universe is a necessary but not sufficient condition for PBH formation. One possibility is that they formed from large inhomogeneities – either primordial, in the sense that they were fed into the initial conditions of the universe, or arising spontaneously in an initially smooth universe through quantum effects during an inflationary epoch. Another possibility is that some sort of phase transition may have enhanced PBH formation from primordial inhomogeneities or triggered it even if there were none. We now briefly discuss these various formation scenarios.

1. Collapse from inhomogeneities

Many PBH formation scenarios depend on the development of inhomogeneities of some kind. Overdense regions could then stop expanding and recollapse [24–26]. Whatever the source of the fluctuations, they would need to be large in order to ensure that the overdense region can collapse against the pressure. The overdensity δ when the region enters the horizon must exceed some critical value δ_c , which a simple analytic argument suggests is around $1/3$ in the radiation era [24]. More precise numerical and analytic calculations indicate values in the range $1/3$ to 0.45 , depending on the spatial profile of the perturbed region [27–31]. Shibata and Sasaki [32] describe the formation condition using the compaction function, whose maximum may provide a better criterion for collapse, and in this case the critical value lies in the small range between 0.37 and 0.43 , depending on the shape of the perturbed region [33, 34]. Nakama *et al.* [35] performed extensive numerical calculations of PBH formation, starting with initial profiles characterized by five parameters but concluding that just two of them are important: the radial integral of curvature profile in the central region and the size of the transition region. The former takes a single critical value of 0.42 when the transition region is small enough. The most natural source of the fluctuations would be quantum effects during inflation. Although any PBHs formed before the end of inflation (i.e. with mass exceeding about 1 g) will be diluted exponentially, the inflationary fluctuations themselves could generate PBHs and in most scenarios the PBHs would form immediately after reheating. In the simplest (single scalar field) scenario, the inflationary fluctuations are expected to have a power-law form and – since the fluctuations are only 10^{-5} on the CMB scale – they would need to be “blue” for PBH formation. However, the observed fluctuations are red, so one needs a more complicated scenario, in which one either has running of the spectral index or some feature in the power spectrum at the PBH scale. Numerous studies have been made of such scenarios (e.g. [36–48]) but we will not discuss them further here.

2. Soft equation of state

Whatever the source of the inhomogeneities, PBH formation would be enhanced if some phase transitions led to a sudden reduction in the pressure – for example, if the early Universe went through a dustlike phase at early times as a result of being dominated by non-relativistic particles for a period [49–51] or undergoing slow reheating after inflation [52, 53]. In such cases, the effect of pressure in stopping collapse is unimportant and the probability of PBH formation just depends upon the fraction of regions which are sufficiently spherical to undergo collapse. For a given spectrum of primordial fluctuations, this means that there may just be a narrow mass range – associated with the period of the soft equation of state – in which the PBHs form. Recently Kokubu *et al.* [54] have investigated PBH formation in a matter-dominated era and identified the threshold for black hole formation by considering the finite speed of propagation for information. They obtain a collapse fraction which is larger by an order of magnitude than the one derived in earlier work [49–51], assuming instantaneous propagation of information.

3. Critical collapse

When the density perturbation approaches the threshold value δ_c required for PBH formation, a critical phenomenon occurs in which the black hole mass scales as $(\delta - \delta_c)^\gamma$ and therefore extends down to arbitrarily small scales [55, 56]. Here the exponent γ is independent of the density profile and just depends on the equation of state (0.35 in the radiation case). Most of the density is in PBHs with the horizon mass but they also have a low mass tail with a power law [57–59]. Because δ_c is sensitive to the equation of state ($p = w \rho c^2$), even a slight reduction in w can enhance PBH production. For example, this may happen at the Quantum Chromodynamics (QCD) era [60–62] and applying the critical collapse analysis then predicts the mass function very precisely [63].

4. Collapse of cosmic loops

In the cosmic string scenario, one expects some strings to self-intersect and form cosmic loops. A typical loop will be larger than its Schwarzschild radius by the factor $(G\mu)^{-1}$, where μ is the string mass per unit length. Observations imply that $G\mu$ must be less than of order 10^{-6} . However, as discussed by many authors [64–69], there is still a small probability that a cosmic loop will get into a configuration in which every dimension lies within its Schwarzschild radius. This probability depends upon both μ and the string correlation scale. Note that the holes form with equal probability at every epoch, so they should have an extended mass spectrum. Black holes might also form through the collapse of string necklaces [70, 71].

5. Bubble collisions

Bubbles of broken symmetry might arise at any spontaneously broken symmetry epoch and many people have suggested that PBHs could form as a result of bubble collisions [72–78]. However, this happens only if the bubble formation rate per Hubble volume is finely tuned: if it is much larger than the Hubble rate, the entire Universe undergoes the phase transition immediately and there is not time to form black holes; if it is much less than the Hubble rate, the bubbles are very rare and never collide. The holes should have a mass of order the horizon mass at the phase transition, so PBHs forming at the Grand Unified Theory (GUT) epoch would have a mass of 10^3 g, those forming at the electroweak unification epoch would have a mass of 10^{28} g, and those forming at the QCD (quark-hadron) phase transition would have mass of around $1 M_\odot$. The production of PBHs from bubble collisions at the end of 1st order inflation has also been studied.

6. Collapse of scalar field

Cotner *et al.* have argued that a scalar condensate can form in the early Universe and collapse into Q-balls before decaying [79]. If the Q-balls dominate the energy density for some period, the statistical fluctuations in their number density can lead to PBH formation [80]. For a general charged scalar field, this can generate PBHs over the mass range allowed by observational constraints and with sufficient abundance to account for the dark matter and the LIGO observations. If the scalar field is associated with supersymmetry, the mass range must be below 10^{23} g. The fragmentation of the inflaton into oscillons can also lead to PBH production, plausibly in the sublunar range [81, 82].

7. Collapse of domain walls

The collapse of sufficiently large closed domain walls produced at a 2nd order phase transition in the vacuum state of a scalar field, such as might be associated with inflation, could lead to PBH formation [83–85]. These PBHs would have a small mass for a thermal phase transition but they could be much larger if one invoked a non-equilibrium scenario. Indeed, they could then span a wide range of masses, with a fractal structure of smaller PBHs clustered around larger ones [86]. Vilenkin and colleagues have argued that bubbles formed during inflation would (depending on their size) form either black holes or baby universes connected to our universe by wormholes [87, 88]. In this case, the PBH mass function would be very broad and extend to very high masses [89, 90].

In some of these scenarios, the PBH mass spectrum is expected to be narrow and centred around the mass given by Eq. (1) with t corresponding to the time at which the PBH scale reenters the horizon in the inflationary model

or to the time of the relevant cosmological phase transition otherwise. In this case, one expects a monochromatic mass spectrum. However, there are some circumstances in which the spectrum would be extended and this means that the constraint on one mass-scale would also imply a constraint on neighbouring scales. For example, we have seen that PBHs may be much smaller than the horizon size if they form as a result of critical phenomena or during a matter-dominated phase and in these cases their spectrum could extend well below the horizon mass. If the PBHs form from inflationary fluctuations, they will generically have a lognormal mass function [91]. It used to be claimed that a PBH could not be much larger than the value given by Eq. (1) at formation else it would be a separate closed universe rather than part of our universe [23]. This interpretation is misleading because the PBH mass necessarily goes to zero when the size of the overdensity region becomes too large [92] but there is still an effective upper limit to the mass of PBH forming at a given epoch and this is of order the horizon size [93]. Another point is that if the PBHs with M close to the mass M_* of those evaporating at the present epoch have a spread of masses $\Delta M \sim M_*$, one would expect evaporation to lead to a residual spectrum with $n_{\text{PBH}} \propto M^3$ for $M < M_*$ [6].

C. Mass and density fraction of PBHs

In the following discussion, we assume that the standard Lambda Cold Dark Matter (Λ CDM) model applies, with the age of the Universe being $t_0 = 13.8$ Gyr and the Hubble parameter being $H_0 \equiv 100h \text{ km s}^{-1} \text{ Mpc}^{-1}$ with $h = 0.67$ [94]. We also put $c = \hbar = k_B = 1$. The Friedmann equation implies that the density ρ and temperature T during the radiation era are given by

$$H^2 = \frac{8\pi G}{3} \rho = \frac{4\pi^3 G}{45} g_* T^4, \quad (2)$$

where g_* counts the number of relativistic degrees of freedom. This can be integrated to give

$$t \approx 0.738 \left(\frac{g_*}{10.75} \right)^{-1/2} \left(\frac{T}{1 \text{ MeV}} \right)^{-2} \text{ s}, \quad (3)$$

where g_* and T are normalised to their values at the start of the BBN epoch. Since we are only considering PBHs which form during the radiation era (the ones generated before inflation being diluted to negligible density), the initial PBH mass M is related to the particle horizon mass M_{PH} by

$$M = \gamma M_{\text{PH}} = \frac{4\pi}{3} \gamma \rho R_{\text{PH}}^3 = \frac{\gamma c^3 t}{G} \approx 2.03 \times 10^5 \gamma \left(\frac{t}{1 \text{ s}} \right) M_\odot. \quad (4)$$

Here the penultimate expression applies *exactly* in a radiation Universe (for which $R_{\text{PH}} = 2ct$) and γ is a numerical factor (somewhat below 1) which depends on the details of gravitational collapse. For much of the following discussion, we will assume that the PBHs all have the same mass M or at least a mass width ΔM no larger than M . This simplifies the analysis considerably and suffices providing we only require limits on the PBH abundance at particular values of M . If the PBHs have an extended mass function, as is more plausible, the analysis of the constraints is more complicated and we discuss this case later.

Assuming adiabatic cosmic expansion after PBH formation, the ratio of the PBH number density to the entropy density, n_{PBH}/s , is conserved. Using the relation $\rho_r = 3sT/4$, the fraction of the Universe's mass in PBHs at their formation time is then related to their number density $n_{\text{PBH}}(t)$ during the radiation era by

$$\beta(M) \equiv \frac{\rho_{\text{PBH}}(t_i)}{\rho(t_i)} = \frac{4M}{3T_i} \frac{n_{\text{PBH}}(t)}{s(t)} \approx 7.99 \times 10^{-29} \gamma^{-1/2} \left(\frac{g_{*i}}{106.75} \right)^{1/4} \left(\frac{M}{M_\odot} \right)^{3/2} \left(\frac{n_{\text{PBH}}(t_0)}{1 \text{ Gpc}^{-3}} \right), \quad (5)$$

where the subscript “i” indicates values at the epoch of PBH formation and we have assumed $s = 8.54 \times 10^{85} \text{ Gpc}^{-3}$ today. g_{*i} is now normalised to the value of g_* at around 10^{-5} s since it does not increase much before that in the Standard Model and most PBHs are likely to form before then. We can also express this as

$$\beta(M) \approx 7.06 \times 10^{-18} \gamma^{-1/2} \left(\frac{h}{0.67} \right)^2 \left(\frac{g_{*i}}{106.75} \right)^{1/4} \Omega_{\text{PBH}}(M) \left(\frac{M}{10^{15} \text{ g}} \right)^{1/2}, \quad (6)$$

where $\Omega_{\text{PBH}} \equiv \rho_{\text{PBH}}/\rho_{\text{crit}}$ is the current density parameter of the PBHs. This can also be obtained using the relation

$$\Omega_{\text{PBH}} = \beta \Omega_{\text{CMB}} (1+z) \sim 10^6 \beta \left(\frac{t}{\text{s}} \right)^{-1/2} \sim 10^9 \beta \left(\frac{M}{M_\odot} \right)^{-1/2}, \quad (7)$$

where $\Omega_{\text{CMB}} \approx 5 \times 10^{-5}$ is the density parameter of the cosmic microwave background (CMB) and we have used Eq. (1). The $(1+z)$ factor can be understood as arising because the radiation density scales as $(1+z)^4$, whereas the PBH density scales as $(1+z)^3$.

Since β always appears in combination with $\gamma^{1/2} g_{*i}^{-1/4} h^{-2}$, it is convenient to define a new parameter

$$\beta'(M) \equiv \gamma^{1/2} \left(\frac{g_{*i}}{106.75} \right)^{-1/4} \left(\frac{h}{0.67} \right)^{-2} \beta(M), \quad (8)$$

where g_{*i} and h can be specified very precisely but γ is rather uncertain. Note that the relationship between β and Ω_{PBH} must be modified if the universe ever deviates from the standard radiation-dominated behaviour – for example, if there is a dust-like stage for some extended early period or a second inflationary phase or if there are extra dimensions [95] or if the gravitational constant ever varies [96–98].

Any limit on Ω_{PBH} places a constraint on $\beta(M)$ or $\beta'(M)$. For non-evaporating PBHs with $M > 10^{15}$ g, one constraint comes from requiring that Ω_{PBH} be less than the cold dark matter (CDM) density, $\Omega_{\text{CDM}} = 0.264 \pm 0.006$ with $h = 0.67$ [94], so the 3σ upper limit is $\Omega_{\text{PBH}} < \Omega_{\text{CDM}} < 0.282$. Much stronger constraints are associated with PBHs smaller than 10^{15} g since these would have evaporated by now. For example, the γ -ray limit implies $\beta(10^{15} \text{ g}) \lesssim 10^{-28}$ and this is the strongest constraints on β over all mass ranges. Other ones are associated with the generation of entropy, modifications to the cosmological production of light elements and the cosmic microwave background (CMB) anisotropies. There are also constraints below 10^6 g based on the (uncertain) assumption that evaporating PBHs leave stable Planck mass relics, an issue which is discussed later.

The constraints on $\beta(M)$ were first brought together by Novikov *et al.* [99] 40 years ago. Besides the entropy, BBN, γ -ray background and density limit, they included a strong constraint above $10^{15} M_{\odot}$ associated with the upper limit on the CMB dipole anisotropy. An updated version of this diagram appeared in Ref. [53] about 15 years later but was essentially the same, apart from the omission of the dipole constraint (which was outside the considered mass range) and the addition of the ‘relics’ constraint. Because of their historical interest, both diagrams are shown in Fig. 1. Subsequently, this diagram has frequently been revised as the relevant effects have been studied in greater detail. For example, Josan *et al.* [100] produced a comprehensive version a decade ago and we also produced a version around that time in Ref. [101] (henceforth CKSY), covering both the evaporating and non-evaporating PBHs. However, there have been many further developments since then, on both the observational and theoretical front. An updated review of the constraints as of a few years ago can be found in Ref. [102] and the present discussion might be regarded as another (albeit more comprehensive) update. The important qualitative point of all such diagrams is that the value of $\beta(M)$ must be tiny over every mass range, even if the PBH density is large today, so any cosmological model which would entail an appreciable fraction of the Universe going into PBHs is immediately excluded.

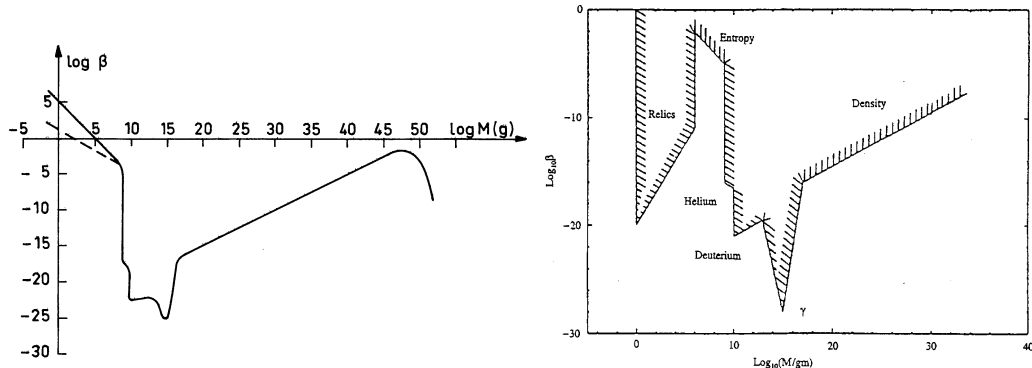


FIG. 1. Constraints on $\beta(M)$ from Refs. [99] in 1979 and [53] in 1994.

D. Evaporation of PBHs

The realization that PBHs might be small prompted Hawking to study their quantum properties. This led to his famous discovery [103] that black holes radiate thermally with a temperature

$$T_{\text{BH}} = \frac{\hbar c^3}{8\pi G M k_B} \sim 10^{-7} \left(\frac{M}{M_{\odot}} \right)^{-1} \text{ K}, \quad (9)$$

so they evaporate completely on a timescale

$$\tau(M) \sim \frac{G^2 M^3}{\hbar c^4} \sim 10^{64} \left(\frac{M}{M_\odot} \right)^3 \text{ yr}. \quad (10)$$

More precise expressions are given below but this implies that only PBHs smaller than about 10^{15} g would have evaporated by the present epoch, so Eq. (1) implies that this effect could be important only for ones which formed before 10^{-23} s. Since PBHs with a mass of around 10^{15} g would be producing photons with energy of order 100 MeV at the present epoch, the observational limit on the γ -ray background intensity at 100 MeV immediately implies that their density could not exceed about 10^{-8} times the critical density [6]. This suggests that there is little chance of detecting their final explosive phase at the present epoch, at least in the Standard Model of particle physics. Nevertheless, the γ -ray background limit does not preclude PBHs having important cosmological effects [104].

1. Mass loss and evaporation timescale

From Eq. (9) the temperature of a black hole with mass $M \equiv M_{10} \times 10^{10}$ g is

$$T_{\text{BH}} \approx 1.06 M_{10}^{-1} \text{ TeV}. \quad (11)$$

This assumes that the hole has no charge or angular momentum, since charge and angular momentum are usually assumed to be lost through quantum emission on a shorter timescale than the mass, although this may fail at the Planck scale [105]. The emission is not exactly black-body but depends upon the spin and charge of the emitted particle, the average energy for neutrinos, electrons and photons being $4.22 T_{\text{BH}}$, $4.18 T_{\text{BH}}$ and $5.71 T_{\text{BH}}$, respectively [106].

The mass loss rate of an evaporating black hole can be expressed as

$$\frac{dM_{10}}{dt} = -5.34 \times 10^{-5} f(M) M_{10}^{-2} \text{ s}^{-1}. \quad (12)$$

Here $f(M)$ is a measure of the number of emitted particle species, normalised to unity for a black hole with $M \gg 10^{17}$ g, this emitting only particles which are (effectively) massless: photons, three generations of neutrinos and antineutrinos, and gravitons. The contribution of each relativistic degree of freedom to $f(M)$ is [107]

$$\begin{aligned} f_{s=0} &= 0.267, & f_{s=1} &= 0.060, & f_{s=3/2} &= 0.020, & f_{s=2} &= 0.007, \\ f_{s=1/2} &= 0.147 \text{ (neutral)}, & f_{s=1/2} &= 0.142 \text{ (charge } \pm e). \end{aligned} \quad (13)$$

Holes in the mass range $10^{15} \text{ g} < M < 10^{17} \text{ g}$ emit electrons but not muons, while those in the range $10^{14} \text{ g} < M < 10^{15} \text{ g}$ also emit muons, which subsequently decay into electrons and neutrinos. The latter range is relevant for the PBHs which are completing their evaporation at the present epoch.

Once M falls to around 10^{14} g, a black hole can also begin to emit hadrons. However, hadrons are composite particles made up of quarks held together by gluons. For temperatures exceeding the QCD confinement scale, $\Lambda_{\text{QCD}} = 250\text{--}300$ MeV, one would expect these fundamental particles to be emitted rather than composite particles. Only pions would be light enough to be emitted below Λ_{QCD} . Above this temperature, the particles radiated can be regarded as asymptotically free, leading to the emission of quarks and gluons [108]. Since there are 12 quark degrees of freedom per flavour and 16 gluon degrees of freedom, one would expect the emission rate (i.e., the value of f) to increase suddenly once the QCD temperature is reached. If one includes just u , d and s quarks and gluons, Eq. (13) implies that their contribution to f is $3 \times 12 \times 0.14 + 16 \times 0.06 \approx 6$, compared to the pre-QCD value of about 2. Thus the value of f roughly quadruples, although there will be a further increase in f at somewhat higher temperatures due to the emission of the heavier quarks. After their emission, quarks and gluons fragment into further quarks and gluons until they cluster into the observable hadrons when they have travelled a distance $\Lambda_{\text{QCD}}^{-1} \sim 10^{-13}$ cm. This is much larger than the size of the hole, so gravitational effects can be neglected.

If we sum up the contributions from all the particles in the Standard Model up to 1 TeV, corresponding to $M_{10} \sim 1$, this gives $f(M) = 15.35$. Integrating the mass loss rate over time then gives a lifetime

$$\tau \approx 407 \left(\frac{f(M)}{15.35} \right)^{-1} M_{10}^3 \text{ s}. \quad (14)$$

The mass of a PBH evaporating at time τ after the big bang is then

$$M \approx 1.35 \times 10^9 \left(\frac{f(M)}{15.35} \right)^{1/3} \left(\frac{\tau}{1 \text{ s}} \right)^{1/3} \text{ g}. \quad (15)$$

The critical mass for which τ equals the age of the Universe is denoted by M_* . For the currently favoured age of 13.8 Gyr, one finds

$$M_* \approx 1.02 \times 10^{15} \left(\frac{f_*}{15.35} \right)^{1/3} \text{ g} \approx 5.1 \times 10^{14} \text{ g}, \quad (16)$$

where the last step assumes $f_* = 1.9$, the value associated with the temperature $T_{\text{BH}}(M_*) = 21 \text{ MeV}$. At this temperature muons and some pions are emitted, so the value of f_* accounts for this. Although QCD effects are initially small for PBHs with $M = M_*$, only contributing a few percent, it should be noted that they become important once M falls to

$$M_q \approx 0.4 M_* \approx 2 \times 10^{14} \text{ g}, \quad (17)$$

since the peak energy becomes comparable to Λ_{QCD} then. This means that an appreciable fraction of the time-integrated emission from the PBHs evaporating at the present epoch goes into quark and gluon jet products.

It should be stressed that the above analysis is not exact because the value of $f(M)$ in Eq. (15) should really be the weighted average of $f(M)$ over the lifetime of the black hole. The more precise calculations of MacGibbon [107, 109] give the slightly smaller value $M_* = 5.00 \times 10^{14} \text{ g}$. However, the weighted average is well approximated by $f(M)$ unless one is close to a particle mass threshold. For example, since the lifetime of a black hole of mass $0.4 M_*$ is roughly $0.25 \times (0.4)^3 = 0.016$ that of an M_* black hole, one expects the value of M_* to be overestimated by a few percent. This explains the small difference from MacGibbon's calculation.

2. Primary and secondary emission

Particles injected from PBHs have two components: the *primary* component, which is the direct Hawking emission, and the *secondary* component, which comes from the decay of gauge bosons or heavy leptons and the hadrons produced by fragmentation of primary quarks and gluons. For example, the photon spectrum can be written as

$$\frac{d\dot{N}_\gamma}{dE_\gamma}(E_\gamma, M) = \frac{d\dot{N}_\gamma^{\text{pri}}}{dE_\gamma}(E_\gamma, M) + \frac{d\dot{N}_\gamma^{\text{sec}}}{dE_\gamma}(E_\gamma, M), \quad (18)$$

with similar expressions for other particles. In order to treat QCD fragmentation, CKSY use the PYTHIA code (version 6), a Monte Carlo event generator constructed to fit hadron fragmentation for centre-of-mass energies $\sqrt{s} \lesssim 200 \text{ GeV}$. The pioneering work of MacGibbon and Webber used the HERWIG code but obtained similar results [108].

The spectrum of secondary photons is peaked around $E_\gamma \simeq m_{\pi^0}/2 \approx 68 \text{ MeV}$, because it is dominated by the 2γ -decay of soft neutral pions which are practically at rest. The peak flux can be expressed as

$$\frac{d\dot{N}_\gamma^{\text{sec}}}{dE_\gamma}(E_\gamma = m_{\pi^0}/2) \simeq 2 \sum_{i=q,g} \mathcal{B}_{i \rightarrow \pi^0}(\bar{E}, E_{\pi^0}) \frac{\bar{E}}{m_{\pi^0}} \frac{d\dot{N}_i^{\text{pri}}}{dE_i}(E_i \simeq \bar{E}), \quad (19)$$

where $\mathcal{B}_{q,g \rightarrow \pi^0}(E_{\text{jet}}, E_{\pi^0})$ is the fraction of the jet energy E_{jet} going into neutral pions of energy E_{π^0} . This is of order 0.1 and fairly independent of jet energy. If we assume that most of the primary particles have the average energy $\bar{E} \approx 4.4 T_{\text{BH}}$, the last factor becomes $d\dot{N}_i^{\text{pri}}/dE_i \approx 1.6 \times 10^{-3} \hbar^{-1}$. Thus the energy dependence of Eq. (19) comes entirely from the factor \bar{E} and is proportional to the Hawking temperature. The emission rates of primary and secondary photons for four typical temperatures are shown in Fig. 2.

It should be noted that the time-integrated ratio of the secondary flux to the primary flux increases rapidly once M goes below M_* . This is because a black hole with $M = M_*$ will emit quarks efficiently once its mass gets down to the value M_q given by Eq. (17) and this corresponds to an appreciable fraction of its original mass. On the other hand, a PBH with somewhat larger initial mass, $M = (1 + \mu) M_*$, will today have a mass [101]

$$m \equiv M(t_0) \approx (3\mu)^{1/3} M_* \quad (\mu \ll 1). \quad (20)$$

Here we have assumed $f(M) \approx f_*$, which should be a good approximation for $m > M_q$ since the value of f only changes slowly above the QCD threshold. However, m falls below M_q for $\mu < 0.02$ and if we assume that f jumps discontinuously from f_* to αf_* at this mass, then Eq. (20) must be reduced by a factor $\alpha^{1/3}$. The fact that this happens only for $\mu < 0.02$ means that the fraction of the black hole mass going into secondaries falls off sharply above M_* . The ratio of the secondary to primary peak energies and the ratio of the time-integrated fluxes are shown in Fig. 3. Relation (20) is important if one is considering the effects of PBHs evaporating at the present epoch (e.g. the local γ -ray background generated by PBHs in the Galactic halo).

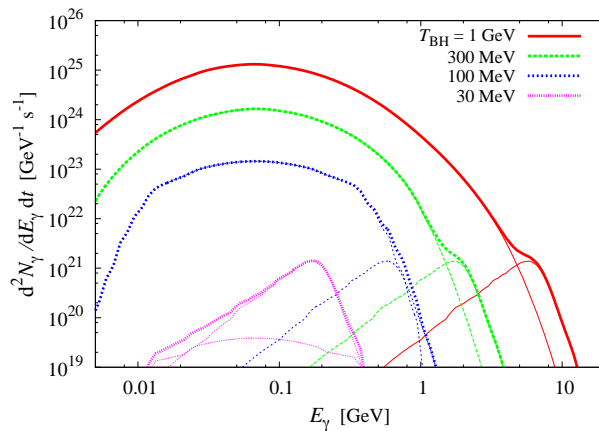


FIG. 2. Instantaneous emission rate of photons for four typical black hole temperatures, from Ref. [101]. For each temperature, the curve with the right (left) peak represents the primary (secondary) component and the thick curve denotes their sum.

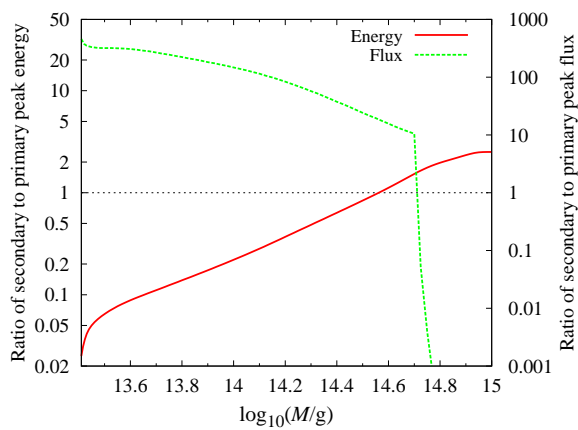


FIG. 3. Ratios of secondary to primary peak energies (solid) and fluxes (dotted), from Ref. [101].

II. CONSTRAINTS ON EVAPORATING PBHS

In this section we discuss the constraints on evaporating PBHs. The results are summarised in Fig. 4, which is an update of Fig. 6 of Ref. [101]. The important point is that the BBN and photon background limits are the most stringent ones over almost the entire mass range 10^9 – 10^{17} g. There is just a small range 10^{13} – 10^{14} g where the CMB anisotropy damping limit dominates and another range 10^{15} – 10^{16} g where the Galactic positron limit dominates. Obviously none of these constraints would apply if there were no Hawking radiation, the only constraint then coming from the condition $\Omega_{\text{PBH}} < 1$. In this context, Raidal *et al.* have suggested that large primordial curvature fluctuations could collapse into horizonless exotic compact objects (ECOs) instead of PBHs [110]. In this case, they either do not evaporate at all or they do so much more slowly, so only the dynamical constraints apply and this opens up a much larger parameter space.

A. Big bang nucleosynthesis

PBHs with $M \sim 10^{10}$ g and $T_{\text{BH}} \sim 1$ TeV have a lifetime $\tau \sim 10^3$ s and therefore evaporate at the epoch of cosmological nucleosynthesis. The effect of these evaporations on BBN has been a subject of long-standing interest. Injection of high-energy neutrinos and antineutrinos [111] changes the weak interaction freeze-out time and hence

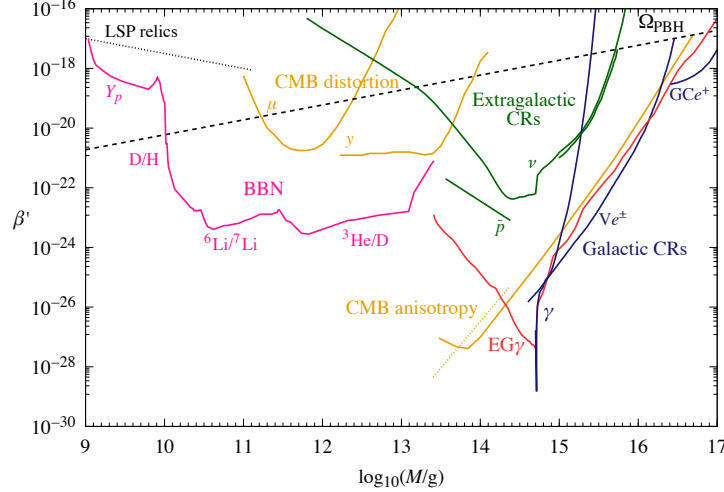


FIG. 4. Combined BBN (pink) and EGB (red) limits, compared to other constraints on evaporating PBHs from LSP relics (grey), the CMB spectral distortions and anisotropies (yellow), extragalactic antiprotons and neutrinos (green) and the Galactic γ -ray background, e^\pm annihilations in the Galactic centre and e^\pm observations by Voyager 1 (blue). The dotted line is the only constraint if there is no Hawking radiation.

the neutron-to-proton ratio at the onset of BBN, which changes ^4He production. Since PBHs with $M = 10^9\text{--}10^{13}\text{ g}$ evaporated during or after BBN, the baryon-to-entropy ratio at nucleosynthesis would be increased, resulting in overproduction of ^4He and underproduction of D [112]. Emission of high-energy nucleons and antinucleons [113] increases the primordial deuterium abundance due to capture of free neutrons by protons and spallation of ^4He . The emission of photons by PBHs with $M > 10^{10}\text{ g}$ dissociates the deuterons produced in nucleosynthesis [114]. The limits associated with these effects are shown in Fig. 1.

Observational data on both the light element abundances and the neutron lifetime have changed since these early papers. Much more significant, however, have been developments in our understanding of the fragmentation of quark and gluon jets from PBHs into hadrons. Most of the hadrons created decay almost instantaneously compared to the timescale of nucleosynthesis but long-lived ones (such as pions, kaons and nucleons) remain long enough in the ambient medium to leave an observable signature on BBN. These effects were first discussed by Kohri and Yokoyama [115] for the relatively low mass PBHs evaporating in the early stages of BBN but the analysis has now been extended to incorporate the effects of heavier PBHs evaporating after BBN [101], the hadrons and high energy photons from these PBHs further dissociating synthesised light elements.

1. Modern studies

High energy particles emitted by PBHs modify the standard BBN scenario in three different ways: (1) high energy mesons and antinucleons induce extra interconversion between background protons and neutrons even after the weak interaction has frozen out in the background Universe; (2) high energy hadrons dissociate light elements synthesised in BBN, thereby reducing ^4He and increasing D, T, ^3He , ^6Li and ^7Li ; (3) high energy photons generated in the cascade further dissociate ^4He to increase the abundance of lighter elements even more.

The PBH constraints depend on three parameters: the initial baryon-to-photon ratio η_i , the PBH initial mass M or (equivalently) its lifetime τ , and the initial PBH number density normalised to the entropy density, $Y_{\text{PBH}} \equiv n_{\text{PBH}}/s$. From Eq. (5) this is related to the initial mass fraction β' by

$$\beta' = 5.4 \times 10^{21} \left(\frac{\tau}{1\text{ s}} \right)^{1/2} Y_{\text{PBH}}. \quad (21)$$

The parameters β' , τ and Y_{PBH} all depend on M but we suppose a monochromatic mass function in what follows. The initial baryon-to-photon ratio is set to the present one $\eta = (6.225 \pm 0.170) \times 10^{-10}$, after allowing for entropy production from PBH evaporations and photon heating due to e^+e^- annihilations.

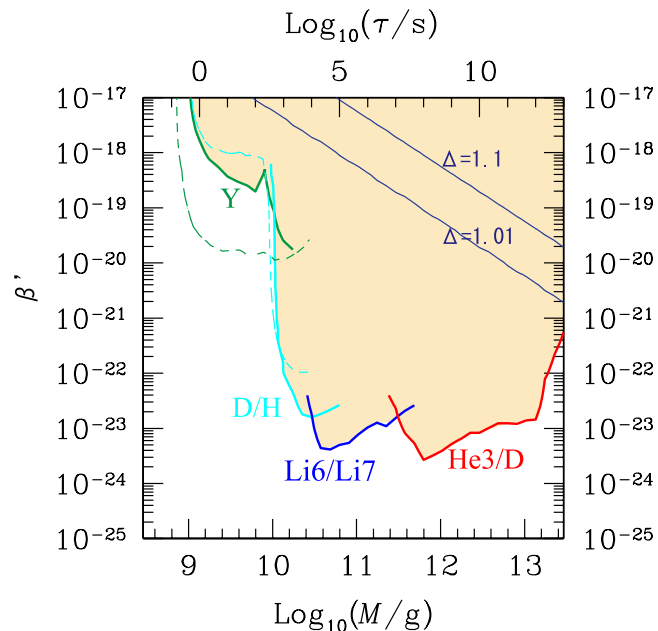


FIG. 5. Upper bounds on $\beta'(M)$ required for success of BBN model, from Ref. [101]. The broken lines give the earlier limit from Ref. [115] and the blue lines give the entropy production limit.

Figure 5 summarises the results of these calculations (see CKSY for further details). PBHs with lifetime smaller than 10^{-2} s are free from BBN constraints because they evaporate well before weak freeze-out and leave no trace. PBHs with $M \approx 10^9\text{--}10^{10}$ g and lifetime $\tau \approx 10^{-2}\text{--}10^2$ s are constrained by the extra interconversion between protons and neutrons due to emitted mesons and antinucleons, which increases the n/p freeze-out ratio as well as the final ${}^4\text{He}$ abundance. For $\tau \approx 10^2\text{--}10^7$ s, corresponding to $M \approx 10^{10}\text{--}10^{12}$ g, hadro-dissociation processes become important and the debris deuterons and non-thermally produced ${}^6\text{Li}$ put strong constraints on $\beta(M)$. Finally, for $\tau = 10^7\text{--}10^{12}$ s, corresponding to $M > 10^{12}\text{--}10^{13}$ g, energetic neutrons decay before inducing hadrodissociation. Instead, photodissociation processes are operative and the most stringent constraint comes from overproduction of ${}^3\text{He}$. However, even these effects become insignificant after 10^{12} s.

These computations involved Monte-Carlo simulations and included experimental and observational uncertainties in the baryon number and reaction and decay rates to obtain error bars in the light element abundances. These bounds should therefore be much more conservative than the ones obtained without these uncertainties. We adopted the upper bound on the abundance of ${}^3\text{He}/\text{D}$ rather than ${}^3\text{He}/\text{H}$ since it is more reliable. Because ${}^3\text{He}$ is both produced and destroyed in low-mass stars, the observed local value of ${}^3\text{He}/\text{H}$ does not imply an upper bound on the primordial component [116]. However, the ${}^3\text{He}/\text{D}$ observed in the solar system should give a reasonable upper bound on the primordial value because this increases with cosmic time [117]. In addition, we included both hadronic and radiative emissions; these can occur together and cancel each other, which reduces the constraint overlapping regions. Reference [118] claims stronger BBN constraints on evaporating PBHs but does not consider these effects.

For comparison, Fig. 5 shows the much weaker constraint imposed by the entropy production from evaporating PBHs [112]. These are labelled by the value of Δ , which is the ratio of the entropy density after and before PBH evaporations. We also show as a broken line the BBN limits obtained earlier by Kohri and Yokoyama [115]. The helium limit is weaker because the helium abundance is now known to be smaller, while the deuterium limit is stronger because hadrodissociation of helium produces more deuterium.

2. Lithium-7

Overproduction of ${}^7\text{Li}$ by a factor ~ 3 is the most serious issue with the standard cosmological model [119]. Astrophysical solutions have so far failed. Particle decay models reduce lithium via neutron injection but generically overproduce D [120], for which there are increasingly precise constraints. Therefore more exotic particle decays –

involving neutron-triggered destruction of ${}^7\text{Be}$, followed by γ -ray destruction of excess D – have been suggested, notably those associated with leptophilic metastable massive particle of mass $\sim 10\text{ MeV}$ [121]. However, PBHs evaporating at $\sim 10^2\text{--}10^4\text{ s}$ might provide a plausible alternative. For example, PBHs with an extended mass function around 10^{12} g could provide an early injection of neutrons, followed by soft γ -rays. This combination could destroy some ${}^7\text{Be}$ at $\sim 10^2\text{ s}$, avoiding overproduction of ${}^7\text{Li}$, and subsequently destroy excess D at $\sim 10^3\text{--}10^4\text{ s}$.

B. Cosmic microwave background

1. Generation of entropy

The effects of PBH evaporations on the CMB (Cosmic Microwave Background) were first analysed by Zel'dovich and Starobinskii [113]. They pointed out that photons from PBHs smaller than 10^9 g are emitted sufficiently early to be completely thermalised and merely contribute to the photon-to-baryon ratio. The requirement that this does not exceed the observed ratio of around 10^9 leads to a limit

$$\beta'(M) < 10^9 \left(\frac{M}{M_{\text{Pl}}} \right)^{-1} \approx 10^{-5} \left(\frac{M}{10^9\text{ g}} \right)^{-1} \quad (M < 10^9\text{ g}), \quad (22)$$

so only PBHs below 10^4 g could generate *all* of the CMB. This limit is not shown in Fig. 4 because it is very weak.

2. CMB spectral distortions

Zel'dovich and Starobinskii [113] also noted that photons from PBHs in the range $10^{11}\text{ g} < M < 10^{13}\text{ g}$, although partially thermalised, will produce noticeable distortions in the CMB spectrum unless

$$\beta'(M) < \left(\frac{M}{M_{\text{Pl}}} \right)^{-1} \approx 10^{-16} \left(\frac{M}{10^{11}\text{ g}} \right)^{-1} \quad (10^{11}\text{ g} < M < 10^{13}\text{ g}), \quad (23)$$

this corresponding to the fraction of the density in PBHs being less than unity at evaporation. In the intermediate mass range, $10^9\text{--}10^{11}\text{ g}$, there is a transition from limit (22) to the much stronger limit (23). Subsequently the form of these distortions has been analysed in greater detail. If an appreciable number of photons are emitted after the freeze-out of double-Compton scattering ($t \gtrsim 7 \times 10^6\text{ s}$), corresponding to $M > 10^{11}\text{ g}$, the distribution of the CMB photons develops a non-zero chemical potential, leading to a μ -distortion. On the other hand, if the photons are emitted after the freeze-out of the single-Compton scattering ($t \gtrsim 3 \times 10^9\text{ s}$), corresponding to $M > 10^{12}\text{ g}$, the distribution is modified by a y -distortion. These constraints were first calculated in the context of decaying particle models [122]. In the PBH context, recent calculations of Tashiro and Sugiyama [123] show that the CMB distortion constraints are of order $\beta'(M) < 10^{-21}$ for some range of M . The precise form of the constraints is shown by the brown lines in Fig. 4. We note that they are weaker than the BBN constraint but stronger than the constraint given by Eq. (23).

There are also CMB distortion constraints associated with the accretion of larger non-evaporating black holes and PBH evaporations could be potentially constrained by their effect on the form of the recombination lines in the CMB spectrum [124], just as in the annihilating dark matter scenario [125, 126].

3. CMB anisotropies

Another constraint on PBHs evaporating after the time of recombination is associated with the damping of small-scale CMB anisotropies. The limit can be obtained by modifying an equivalent calculation for decaying particles, as described by Zhang *et al.* [127]. Their constraint can be written in the form

$$\log_{10} \zeta < -10.8 - 0.50x + 0.085x^2 + 0.0045x^3, \quad x \equiv \log_{10} \left(\frac{\Gamma}{10^{-13}\text{ s}^{-1}} \right), \quad (24)$$

where Γ is the decay rate, which corresponds to $\tau(M)^{-1}$ in our case, and ζ is the fraction of the CDM in PBHs, which is simply related to $\beta(M)$, times the fraction of the emitted energy which goes into heating the matter. The last factor, which includes the effects of the electrons and positrons as well as the photons, will be denoted by f_{H} and

depends on the redshift [128, 129]. Most of the heating will be associated with the electrons and positrons; they are initially degraded by inverse Compton scattering off the CMB photons but after scattering have an energy

$$\gamma^2 E_{\text{CMB}} \approx 300 \left(\frac{\gamma}{10^3} \right)^2 (1+z) \text{ eV} \approx 5 \times 10^5 \left(\frac{M}{10^{13} \text{ g}} \right)^{-2} (1+z) \text{ eV} \approx 20 (1+z)^2 \text{ eV}, \quad (25)$$

where γ is the Lorentz factor and in the last expression we assume that the mass of a PBH evaporating at redshift z in the matter-dominated era is $M \approx M_* (1+z)^{-1/2}$. Since this energy is always above the ionization threshold for hydrogen (13.6 eV), we can assume that the heating of the electrons and positrons is efficient before reionization. Using Eq. (5) for $\beta(M)$ and Eq. (14) for $\tau(M)$, one can now express Eq. (24) as a limit on $\beta(M)$. In the mass range of interest, the rather complicated cubic expression in M can be fitted by the approximation

$$\beta'(M) < 3 \times 10^{-30} \left(\frac{f_{\text{H}}}{0.1} \right)^{-1} \left(\frac{M}{10^{13} \text{ g}} \right)^{3.1} \quad (2.5 \times 10^{13} \text{ g} \lesssim M \lesssim 2.4 \times 10^{14} \text{ g}), \quad (26)$$

where $f_{\text{H}} \approx 0.1$ is the fraction of emission which comes out in electrons and positrons. Here the lower mass limit corresponds to black holes evaporating at recombination and the upper one to those evaporating at a redshift 6 [130], after which the ionisation ensures the opacity is too low for the emitted electrons and positrons to heat the matter.

Equation (26) is stronger than all the other available limits in this mass range but had not been pointed out before CKSY. Recently it has been studied more carefully by Poulin *et al.* [131], who compute CMB anisotropy constraints on electromagnetic energy injection over a large range of timescales. They apply their formalism for PBHs with mass $10^{13.5} - 10^{16.8}$ g, showing that the constraints are comparable to the γ -ray background ones and dominate below around 10^{14} g. Stöcker *et al.* [132] have followed up on this work, using the Boltzmann code CLASS. Their bounds are several orders of magnitude stronger than the EGB limit in the range $3 \times 10^{13} < M/g < 3 \times 10^{14}$ and exclude PBHs with a monochromatic mass distribution in the range $3 \times 10^{13} < M/g < 2 \times 10^{16}$ from containing all of the dark matter. Future CMB or 21 cm experiments could improve these limits models even more [133]. Poulter *et al.* [134] have extended these constraints to the case in which the PBHs have an extended mass function.

C. Cosmic ray and γ -ray backgrounds

1. Extragalactic γ -ray background

One of the earliest works that applied the theory of black hole evaporation to astrophysics was carried out by Page and Hawking [6]. They used the diffuse EGB observations to constrain the mean cosmological number density of PBHs which are completing their evaporation at the present epoch to be less than 10^4 pc^{-3} . This corresponds to an upper limit on Ω_{PBH} of around 10^{-8} . The limit was subsequently refined by MacGibbon and Carr [128] who considered how it is modified by including quark and gluon emission and inferred $\Omega_{\text{PBH}} \leq (7.6 \pm 2.6) \times 10^{-9} h^{-2}$, corresponding to a 2σ upper limit of $1.3 \times 10^{-8} h^{-2}$. Later they used EGRET observations to derive a slightly stronger limit $\Omega_{\text{PBH}} \leq (5.1 \pm 1.3) \times 10^{-9} h^{-2}$ [135] or a 2σ upper limit of $7.7 \times 10^{-9} h^{-2}$. Using the modern value of h gives $\Omega_{\text{PBH}} \leq 1.5 \times 10^{-8}$ and this corresponds to $\beta'(M_*) < 6 \times 10^{-26}$ from Eq. (6). They also inferred from the form of the γ -ray spectrum that PBHs could not provide the *dominant* contribution to the background.

The photon emission has a primary and secondary component and these are calculated according to the prescription of Sec. ID 2. The relative magnitude of these two components is sensitive to the PBH mass and this affects the associated $\beta'(M)$ limit. In order to determine the present background spectrum of particles generated by PBH evaporations, we must integrate over the lifetime of the black holes, allowing for the fact that particles generated in earlier cosmological epochs will be redshifted in energy by now.

If the PBHs all have the same initial mass M , and if we approximate the number of emitted photons in the energy bin $\Delta E_\gamma \simeq E_\gamma$ by $\dot{N}_\gamma(E_\gamma) \simeq E_\gamma (d\dot{N}_\gamma/dE_\gamma)$, then the emission rate per volume at cosmological time t is

$$\frac{dn_\gamma}{dt}(E_\gamma, t) \simeq n_{\text{PBH}}(t) E_\gamma \frac{d\dot{N}_\gamma}{dE_\gamma}(M(t), E_\gamma), \quad (27)$$

where the t -dependence of M just reflects the evaporation. Since the photon energy and density are redshifted by factors $(1+z)^{-1}$ and $(1+z)^{-3}$, respectively, the present number density of photons with energy $E_{\gamma 0}$ is

$$n_{\gamma 0}(E_{\gamma 0}) = n_{\text{PBH}0} E_{\gamma 0} \int_{t_{\min}}^{\min(t_0, \tau)} dt (1+z) \frac{d\dot{N}_\gamma}{dE_\gamma}(M(t), (1+z) E_{\gamma 0}), \quad (28)$$

where t_{\min} corresponds to the earliest time at which the photons freely propagate and $n_{\text{PBH}0}$ is the current PBH number density for $M > M_*$ or the number density they would have now had they not evaporated for $M < M_*$. The photon flux is

$$I \equiv \frac{c}{4\pi} n_{\gamma 0}. \quad (29)$$

The calculated present-day fluxes of primary and secondary photons are shown in Fig. 6, where the number density $n_{\text{PBH}0}$ for each M has the maximum value consistent with the observations.

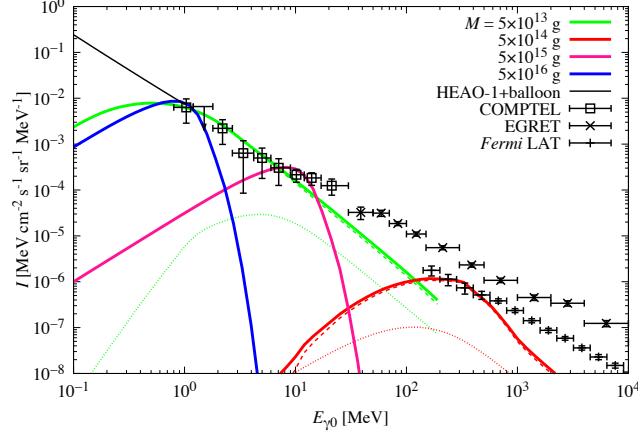


FIG. 6. Fluxes corresponding to the upper limit on the PBH abundance for various values of M , from Ref. [101] but updated. All PBHs produce primary photons but $M \lesssim M_*$ ones also produce secondary photons, giving a stronger constraint on β .

Note that the highest energy photons are associated with PBHs of mass M_* . Photons from PBHs with $M > M_*$ are at lower energies because they are cooler, while photons from PBHs with $M < M_*$ are at lower energies because (although initially hotter) they are redshifted. The spectral shape depends on the mass M and can be easily understood. PBHs with $M > M_*$ have a rather sharp peak, well approximated by the instantaneous black-body emission of the primary photons, while holes with $M \leq M_*$ have an $E_{\gamma 0}^{-2}$ fall-off for $E_{\gamma 0} \gg T_{\text{BH}}/[1 + z(\tau)]$ due to the final phases of evaporation [107].

The relevant observations come from HEAO 1 and other balloon observations in the 3–500 keV range, COMPTEL in the 0.8–30 MeV range, EGRET in the 30–100 MeV range and Fermi-LAT in the 100 MeV–820 GeV range. All the observations are shown in Fig. 6. The origin of the diffuse X-ray and γ -ray backgrounds is thought to be primarily distant astrophysical sources, such as blazars, and in principle one should remove these contributions before calculating the PBH constraints. This is the strategy adopted by Barrau *et al.* [136], who thereby obtain a limit $\Omega_{\text{PBH}} \leq 3.3 \times 10^{-9}$. CKSY do not attempt such a subtraction, so their constraints on $\beta'(M)$ may be overly conservative.

In order to analyse the spectra of photons emitted from PBHs, different treatments are needed for PBHs with initial masses below and above M_* . We saw in Sec. ID 2 that PBHs with $M > M_*$ can never emit secondary photons at the present epoch, whereas those with $M \leq M_*$ will do so once M falls below $M_q \approx 2 \times 10^{14}$ g. One can use simple analytical arguments to derive the form of the primary and secondary peak fluxes. The observed X-ray and γ -ray spectra correspond to $I^{\text{obs}} \propto E_{\gamma 0}^{-(1+\epsilon)}$ where ϵ lies between 0.1 and 0.4. For $M < M_*$, the limit is determined by the secondary flux and one can write the upper bound on β' as

$$\beta'(M) \lesssim 3 \times 10^{-27} \left(\frac{M}{M_*} \right)^{-5/2-2\epsilon} \quad (M < M_*). \quad (30)$$

For $M > M_*$, secondary photons are not emitted and one obtains a limit

$$\beta'(M) \lesssim 4 \times 10^{-26} \left(\frac{M}{M_*} \right)^{7/2+\epsilon} \quad (M > M_*). \quad (31)$$

These M -dependences explain qualitatively the slopes in Fig. 7. The limit bottoms out at 4×10^{-28} but we note that it strengthens by a factor of 7 below the mass M_* because of secondary emission. There is also a narrow band

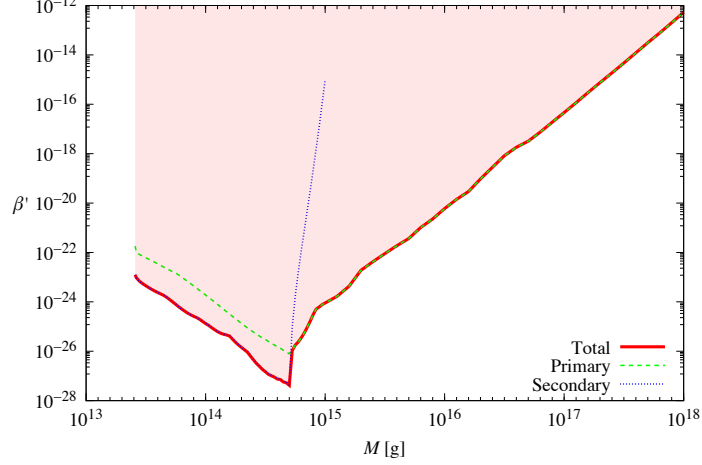


FIG. 7. Upper bounds on $\beta'(M)$ from the extragalactic photon background, from Ref. [101] but updated, with no other contributors to the background having been subtracted.

$M_* < M < 1.005 M_*$ in which PBHs have not yet completed their evaporation even though their current mass is below the mass $M_q \approx 0.4 M_*$ at which quark and gluon jets are emitted. From Eq. (5), the associated limit on the density parameter is $\Omega_{\text{PBH}}(M_*) \leq 5 \times 10^{-10}$. Note that this is a factor of 3 stronger than the limit given in CKSY.

We stress that the discontinuity in the EGB constraint at the mass M_* is entirely a consequence of the (probably unrealistic) assumption that the PBHs have a monochromatic mass function and even a tiny mass width ΔM would suffice to smear this out. Indeed, many derivations of the EGB constraint - including the original Page–Hawking calculation - assume that the PBHs have a power-law mass function. In this case, the discontinuity is removed and the stronger ($M < M_*$) limit pertains. Nevertheless, the discontinuity is still interesting in principle and the issue of non-monochromaticity will be even more important when we consider the Galactic background constraint.

Finally, we determine the mass range over which the γ -ray constraint applies. Since photons emitted at sufficiently early times cannot propagate freely, there is a minimum mass M_{min} below which the above constraint is inapplicable. The dominant interactions between γ -rays and the background Universe in the relevant energy range are pair-production off hydrogen and helium nuclei. For the opacity appropriate for a 75 % hydrogen and 25 % helium mix [6], the redshift below which there is free propagation is given by [128]

$$1 + z_{\text{max}} \approx 1155 \left(\frac{h}{0.67} \right)^{-2/3} \left(\frac{\Omega_b}{0.05} \right)^{-2/3}, \quad (32)$$

with the nucleon density parameter Ω_b being normalised to the modern value. The condition $\tau(M_{\text{min}}) = t(z_{\text{max}})$ then gives

$$M_{\text{min}} = \left(\frac{t(z_{\text{max}})}{t_0} \right)^{1/3} \left(\frac{f(M_{\text{min}})}{f_*} \right)^{1/3} M_* \approx 3 \times 10^{13} \text{ g}. \quad (33)$$

The limit is therefore extended down to this mass in Fig. 7. It goes above the density constraint $\Omega_{\text{PBH}}(M) < 0.25$ for $M > 7 \times 10^{16} \text{ g}$.

Ballesteros *et al.* [137] have recently improved this bound and extended its mass range by better modeling of the combined AGN and blazar emission in the MeV range. They also estimate the constraints from any future X-ray experiment capable of identifying a significantly larger number of astrophysical sources contributing to the diffuse background in this energy range. Note that Arbey *et al.* [138] have extended the EGB constraint on PBHs with masses 10^{13} – 10^{18} g from a monochromatic distribution of Schwarzschild black holes to an extended distribution of rotating Kerr black holes, showing that the lower part of this mass window can be closed for near-extremal black holes. See also Ref. [139] for constraints on spinning PBHs through superradiance.

2. Galactic γ -ray background

If PBHs of mass M_* are clustered inside our own Galactic halo, as expected, then there should also be a Galactic γ -ray background and, since this would be anisotropic, it should be separable from the extragalactic background. The ratio of the anisotropic to isotropic intensity depends on the Galactic longitude and latitude, the Galactic core radius and the halo flattening. Some time ago Wright [140] claimed that such a halo background had been detected in EGRET observations between 30 MeV and 120 MeV [141] and attributed this to PBHs. His detailed fit to the data, subtracting various other known components, required the PBH clustering factor to be $(2\text{--}12) \times 10^5 h^{-1}$, comparable to that expected, and the local PBH explosion rate to be $\mathcal{R} = 0.07\text{--}0.42 \text{ pc}^{-3} \text{ yr}^{-1}$. A later analysis of EGRET data between 70 MeV and 150 MeV, assuming a variety of distributions for the PBHs, was given by Lehoucq *et al.* [7]. In the isothermal model, which gives the most conservative limit, the Galactic γ -ray background requires $\mathcal{R} \leq 0.06 \text{ pc}^{-3} \text{ yr}^{-1}$. They claimed that this corresponds to $\Omega_{\text{PBH}}(M_*) \leq 2.6 \times 10^{-9}$, which from Eq. (6) implies $\beta'(M_*) < 1.4 \times 10^{-26}$, a factor of 30 above the extragalactic background constraint (30). Lehoucq *et al.* themselves claimed that it corresponds to $\beta'(M_*) < 1.9 \times 10^{-27}$ but this is because they use an old and rather inaccurate formula relating Ω_{PBH} and β .

It should be stressed that the Lehoucq *et al.* analysis does not constrain PBHs of *initial* mass M_* because these no longer exist. Rather it constrains PBHs of *current* mass M_* and, from Eq. (20) with $m = M_*$, this corresponds to an initial mass of $1.26 M_*$. However, as shown below, this value of M does not correspond to the strongest limit on $\beta(M)$. This contrasts to the situation with the extragalactic background, where the strongest constraint on $\beta(M)$ comes from the time-integrated contribution of the M_* black holes. There would also be a Galactic contribution from PBHs which were slightly *smaller* than M_* but sufficiently distant for their emitted particles to have only just reached us; since the light-travel time across the Galaxy is $t_{\text{gal}} \sim 10^5 \text{ yr}$, this corresponds to PBHs initially smaller than M_* by $(t_{\text{gal}}/3 t_0) M_* \sim 10^{-5} M_*$, so this extra contribution is negligible.

To examine this issue more carefully, we note that Eq. (20) implies that the emission from PBHs with initial mass $(1 + \mu) M_*$ currently peaks at an energy $E \approx 100 (3\mu)^{-1/3} \text{ MeV}$ for $\mu < 1$, which is in the range 70–150 MeV for $0.7 > \mu > 0.08$. (Note that secondary emission can be neglected in this regime, this only being important for $\mu < 0.02$.) So these black holes correspond to the “tail” population discussed in Sec. II C 1 and have a mass function $dn/dm \propto m^2$. This means that the interpretation of the Galactic γ -ray limit is sensitive to the non-monochromaticity in the PBH mass function, so we must distinguish between the various situations described later in Sec. IV. In particular, we need to distinguish between mass functions which centre at M_* and some higher value of M . In the present context, we assume that the mass function is narrow, so that $\beta(M)$ can be defined as the integral over the entire mass width.

The peak energy is above 150 MeV for $\mu < 0.08$, so the γ -ray band is in the Rayleigh–Jeans region. The flux of an individual hole scales as $m^3 \propto \mu$ in this regime. Although this flux must be weighted by the number density of the holes, $n(m) \propto m^3 \propto \mu$ for $\mu \ll 1$, this factor is necessarily balanced by the ratio $(\Delta M/\Delta m)$ of the mass widths at formation and now, so the limit on $\beta(M)$ scales as μ^{-1} . For $0.7 > \mu > 0.08$, the current number flux of photons from each PBH scales as $m^{-1} \propto \mu^{-1/3}$, so the effective limit on $\beta(M)$ scales as $\mu^{1/3}$. The observed γ -ray band enters the Wien part of the spectrum for $\mu > 0.7$, so the limit on $\beta(M)$ weakens exponentially for $M > 1.7 M_*$. (Although not mentioned in Ref. [7], one could in principle get a stronger limit in this mass regime from observations at energies lower than 70 MeV.) Hence the largest contribution to the Galactic background and the strongest constraint on $\beta(M)$ comes from PBHs with $M \approx 1.08 M_*$ and has the form indicated in Fig. 4.

Subsequently, the problem was studied in much greater detail by CKSY2 [142]. To go beyond the Lehoucq *et al.* analysis, we included several important effects. First, we distinguished between the initial mass $M = (1 + \mu) M_*$ and the current mass m , this being given by

$$m = \begin{cases} [(\mu + 1)^3 - 1 + (1 - \alpha^{-1}) q^3]^{1/3} M_* & (\mu \geq \mu_c) \\ (3\alpha\mu)^{1/3} (1 + \mu + \mu^2/3)^{1/3} M_* & (0 \leq \mu \leq \mu_c), \end{cases} \quad (34)$$

where

$$\mu_c \approx q^3/(3\alpha) = 0.005 (\alpha/4)^{-1} (q/0.4)^3 \quad (35)$$

is the value of μ corresponding to the mass M_c at which secondary emission eventually becomes important. Second, we distinguished between primary and secondary emission. The ratio of the energies at which the spectra peak is

$$\frac{\bar{E}^{\text{S}}}{\bar{E}^{\text{P}}} \approx (68 \text{ MeV}) / (600 m_{14}^{-1} \text{ MeV}) \approx 0.6 (m/M_*) , \quad (36)$$

while the flux ratio is

$$\left(\frac{d\dot{N}^{\text{S}}}{dE} \right)_{\bar{E}^{\text{S}}} / \left(\frac{d\dot{N}^{\text{P}}}{dE} \right)_{\bar{E}^{\text{P}}} \approx 1.4 \left(\frac{m}{M_*} \right)^{-1} e^{-\chi m/M_q} . \quad (37)$$

Third, we distinguished between initial mass function dn/dM and the current one,

$$\frac{dn}{dm} = \left[\frac{1}{\alpha} \left(\frac{m}{M_*} \right)^2 \left(\frac{dn}{dM} \right)_*, \left(\frac{m}{M_*} \right)^2 \left(\frac{dn}{dM} \right)_*, \left(\frac{dn}{dM} \right) \right] \quad \text{for } [m < M_q, M_q < m < M_*, m > M_*], \quad (38)$$

the main GRB contribution coming from the $dn/dm \propto m^2$ low mass tail.

Following Lehoucq *et al.*, we took the halo density profile to have the form

$$\rho_{\text{PBH}}(R) = \frac{f \rho_s}{(R/R_s)^\gamma [1 + (R/R_s)^\alpha]^{(\beta-\alpha)/\alpha}}, \quad (39)$$

with a set of best-fit parameters $\gamma = 1.24, \alpha = 1, \beta = 4 - \gamma = 2.86, R_s = 28.1 \text{ kpc}, \rho_s = 3.50 \times 10^{-3} M_\odot \text{ pc}^{-3}$. We described the directional dependence with the function

$$g(\mathbf{n}) = \frac{1}{r_{\text{gal}}} \int_0^{r_{\text{gal}}} dr \frac{\rho_{\text{PBH}}(R(\mathbf{n}, r))}{\bar{\rho}_{\text{PBH}}}, \quad (40)$$

with $r_{\text{gal}} = 100 \text{ kpc}$ being our distance from the edge of the halo. We then compared the predicted intensity with Fermi-LAT observations and inferred constraints on $\beta(M)$ and $n_{\text{PBH}}(M)$. We show the constraint for a monochromatic mass function in Fig. 8.

Note that the depth of the limit in Fig. 8 is sensitive to the width of the PBH mass function Δ and becomes arbitrarily small as $\Delta \rightarrow 0$. However, a very small value of Δ is almost certainly unphysical and the extragalactic and Galactic limits are comparable for $\Delta \sim 1$.

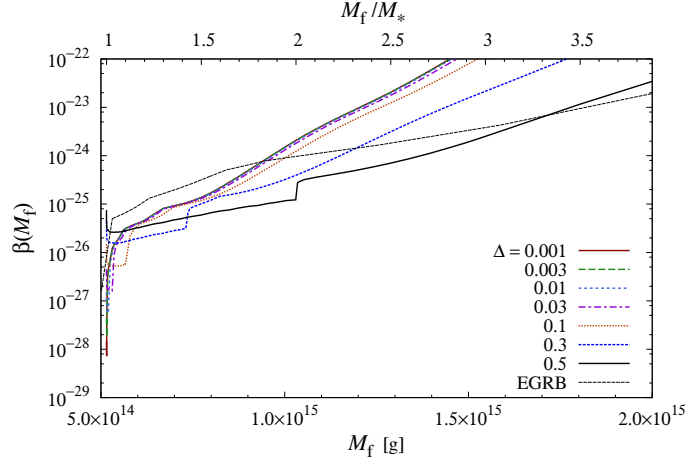


FIG. 8. Constraint for a monochromatic mass function from Ref. [142] where Δ specifies the width of the mass function.

3. Galactic positrons and antiprotons

The evaporation of PBHs with $M > 10^{17} \text{ g}$ is expected to inject sub-GeV electrons and positrons into the Galaxy. These particles are shielded by the solar magnetic field for Earth-bound detectors, but not for VOYAGER-1, which is now beyond the heliopause. Boudad and Cirelli [143] use its data to constrain the PBH dark matter fraction in the Galaxy and, as indicated in Fig. 4, find $f < 0.001$ for $M < 10^{16} \text{ g}$. Their limits are based on local Galactic measurements and thus complement those derived from cosmological observations.

Since the ratio of antiprotons to protons in cosmic rays is less than 10^{-4} over the energy range 100 MeV–10 GeV, whereas PBHs should produce them in equal numbers, PBHs could only contribute appreciably to the antiprotons [104, 144, 145]. It is usually assumed that the observed antiprotons are secondary particles, produced by spallation of the interstellar medium by primary cosmic rays. However, the spectrum of secondary antiprotons should show a steep cut-off at kinetic energies below 2 GeV, whereas the spectrum of PBH antiprotons should continue down to 0.2 GeV.

Also any primary antiproton fraction should tend to 0.5 at low energies. Both these features provide a distinctive signature of any PBH contribution.

The black hole temperature must be much larger than 1 GeV to generate antiprotons, so the local cosmic ray flux from PBHs should be dominated by the ones just entering their explosive phase at the present epoch. Such PBHs should be clustered inside our halo, so any charged particles emitted will have their flux enhanced relative to the extragalactic spectra by a factor ζ which depends upon the halo concentration factor and the time for which particles are trapped inside the halo by the Galactic magnetic field. This time is rather uncertain and also energy-dependent. At 100 MeV one expects roughly $\zeta \sim 10^3$ for electrons or positrons and $\zeta \sim 10^4$ for protons or antiprotons [135].

MacGibbon and Carr [128] originally calculated the PBH density required to explain the interstellar antiproton flux at 1 GeV and found a value somewhat larger than the density associated with the γ -ray limit. After the BESS balloon experiment measured the antiproton flux below 0.5 GeV [146], Maki *et al.* [147] tried to fit this in the PBH scenario by using Monte Carlo simulations of cosmic ray propagation. They found that the local PBH-produced antiproton flux is mainly due to PBHs exploding within a few kpc and used the observational data to infer a limit on the local PBH explosion rate of $\mathcal{R} < 0.017 \text{ pc}^{-3} \text{ yr}^{-1}$. A more recent attempt to fit the antiproton data came from Barrau *et al.* [148], who compared observations by BESS95 [146], BESS98 [149], CAPRICE [150] and AMS [151] with the spectrum from evaporating PBHs. According to their analysis, PBHs with $\beta'(M_*) \approx 5 \times 10^{-28}$ would be numerous enough to explain the observations. However, these results are based on the assumption that the PBHs have a spherically symmetric isothermal profile with a core radius of 3.5 kpc. A different clustering assumption would lead to a different constraint on $\beta'(M_*)$.

PBHs might also be detected by their antideuteron flux. Barrau *et al.* [152] argue that AMS and GAPS would be able to detect the antideuterons from PBH explosions if their local density were as large as $2.6 \times 10^{-34} \text{ g cm}^{-3}$ and $1.4 \times 10^{-35} \text{ g cm}^{-3}$, respectively. If a null result were maintained up to these levels, it would imply $\beta'(M_*) < 1.5 \times 10^{-26} (\zeta/10^4)^{-1}$ and $8.2 \times 10^{-28} (\zeta/10^4)^{-1}$, respectively. However, these are only potential and not actual limits.

More recent data come from the BESS Polar-I experiment, which flew over Antarctica in December 2004 [153]. The reported antiproton flux lies between that of BESS(95+97) and BESS(2000) and the \bar{p}/p ratio ($r \approx 10^{-5}$) is similar to that reported by BESS(95+97). Although the latter indicated an excess flux below 400 MeV, this was not found in the BESS Polar-I data. However, given the magnitude of the error bars, we might still expect a constraint on the local PBH number density similar to that discussed above, in which case the constraint on $\beta(M_*)$ becomes

$$\beta'(M_*) < 3.9 \times 10^{-25} \left(\frac{\zeta}{10^4} \right)^{-1}, \quad (41)$$

where we have used Eq. (6). For reasonable values of ζ , this is much weaker than the γ -ray background limit, but the value of ζ is anyway very uncertain and so this limit is not shown explicitly in Fig. 4.

4. Extragalactic antiprotons

Galactic antiprotons can constrain PBHs only in a very narrow range around $M \approx M_*$ since they diffusively propagate to the Earth on a time much shorter than the cosmic age. However, there will also be a spectrum of cosmic ray antiprotons from PBHs sufficiently light that they evaporated well before the epoch of galaxy formation ($\sim 1 \text{ Gyr}$). Although such pregalactic PBHs would not be clustered, the antiprotons they emitted could still be around today and may occasionally enter the Galaxy and be detectable at Earth, so we require that this does not happen frequently enough to exceed the observational limits. We assume that the maximum mass relevant for this constraint corresponds to the PBHs evaporating at galaxy formation:

$$M \lesssim \left(\frac{1 \text{ Gyr}}{t_0} \right)^{1/3} \left(\frac{f(M)}{f_*} \right)^{1/3} M_* \approx 2 \times 10^{14} \text{ g}. \quad (42)$$

This mass-scale is not necessarily relevant because even the antiprotons generated *inside* galaxies may escape on a cosmological timescale and become part of the extragalactic background. However, the leakage time depends on the size of the cosmic ray region, which is rather uncertain, and could well be comparable to t_0 . We therefore adopt the above upper mass limit. The minimum mass relevant for this constraint is determined as follows. The mean rate of $\bar{p}p$ annihilations in the cosmological background, where the target p 's are in hydrogen and helium nuclei, is

$$\Gamma_{\bar{p}p}(t) = \langle \sigma_{\bar{p}p} v_{\bar{p}} \rangle n_p(t) \approx 2 \times 10^{-22} \left(\frac{t}{t_0} \right)^{-2} \text{ s}^{-1}, \quad (43)$$

where we have used $\langle \sigma_{\bar{p}p} v_{\bar{p}} \rangle / c \approx 4 \times 10^{-26} \text{ cm}^2$ and $n_p(t_0) \approx 2 \times 10^{-7} \text{ cm}^{-3}$. The condition that an antiproton emitted by a PBH with lifetime τ survives until now is then

$$\int_{\tau}^{t_0} \Gamma_{\bar{p}p}(t') dt' \approx \left(\frac{t_0}{\tau} \right) \left(\frac{t_0}{5 \times 10^{21} \text{ s}} \right) \approx \frac{1.3 \text{ Myr}}{\tau} < 1. \quad (44)$$

Using Eq. (15), we infer that the extragalactic \bar{p} limit applies for

$$M \gtrsim \left(\frac{1.3 \text{ Myr}}{t_0} \right)^{1/3} \left(\frac{f(M)}{f_*} \right)^{1/3} M_* \approx 4 \times 10^{13} \text{ g}. \quad (45)$$

We have seen there is no primary emission of antiprotons and the analog of Eq. (19) implies that the current number density from secondary emission of PBHs with mass M is

$$n_{\bar{p}}(M, t_0) = \frac{n(\tau) \tau}{(1 + z(\tau))^3} \frac{d\dot{N}_{\bar{p}}}{d \ln E_{\bar{p}}}(E_{\bar{p}} = 100 \text{ MeV}) \approx 6 \times 10^{11} \beta'(M) \left(\frac{f(M)}{f_*} \right)^{-1} \left(\frac{M}{M_*} \right)^{1/2} \text{ cm}^{-3}. \quad (46)$$

Since the antiproton-to-proton ratio r is required to be less than 10^{-5} , one finds the upper bound

$$\beta'(M) \lesssim 3 \times 10^{-24} \left(\frac{r}{10^{-5}} \right) \left(\frac{f(M)}{f_*} \right) \left(\frac{M}{M_*} \right)^{-1/2} (4 \times 10^{13} \text{ g} \lesssim M \lesssim 2 \times 10^{14} \text{ g}). \quad (47)$$

This constraint is shown by the green line in Fig. 4. Although it is much weaker than the Galactic antiproton constraint, it is independent of the rather uncertain parameter ζ .

5. Annihilation-line radiation

Several authors have suggested that the 511 keV annihilation line radiation from the Galactic centre could result from the positrons emitted by the PBHs there [154–156], as first suggested by Okeke and Rees [9]. Most recently, DeRocco and Graham [157] have constrained 10^{16} – 10^{17} g PBHs using measurements of this line by SPI/INTEGRAL, excluding models in which they constitute all the dark matter. Laha [158] has also used SPI/INTEGRAL data and shown that - depending on their mass function and other astrophysical uncertainties - PBHs smaller than 10^{18} g could contribute to less than 1% of the dark matter. The constraint of DeRocco and Graham is indicated in Fig. 4. The annihilation-line constraints are particularly interesting if the PBHs are spinning [159]. In this case, they are typically weaker in the lower mass range and stronger in the higher mass range and they are generally stronger than those derived from the diffuse γ -ray measurements for M exceeding a few times 10^{16} g.

6. Emission of other particles

Neutrinos may either be emitted directly as black-body radiation (primaries) or they may result from the decay of emitted pions, leptons, neutrons and anti-neutrons (secondaries). As a result, their emission spectra are similar to those for photons up to a normalisation factor. The neutrino background can in principle constrain PBHs whose lifetime exceeds the time of neutrino decoupling ($\tau \gtrsim 1 \text{ s}$). This corresponds to a minimum mass of $M_{\text{min},\nu} \approx 10^9 \text{ g}$. However, the low-energy neutrinos which we have to use are poorly limited by observations. In Super-Kamiokande (SK), the null detection of relic $\bar{\nu}_e$'s implies $\Phi_{\bar{\nu}_e} \leq 1.2 \text{ cm}^{-2} \text{ s}^{-1}$ above the threshold $E_{\bar{\nu}_e 0} = 19.3 \text{ MeV}$ [160]. As seen in Fig. 9, this energy corresponds to the high-energy tail for light PBHs. The constraint associated with the relic neutrinos is shown by the green line in Fig. 4 and is much weaker than the BBN and photon background limits. Similar calculations have been made by Bugaev *et al.* [154, 155] and Dasgupta *et al.* [159]. However, they assume that the PBHs have a continuous mass function and they link their model with a particular inflationary scenario.

Lunardini and Perez-Gonzalez [161] show that the neutrino emission depends on whether they are Dirac or Majorana. In the Dirac case, PBHs radiate right-handed and left-handed neutrinos in equal amounts, thus increasing the effective number of neutrino species N_{eff} . They derive a new bound on $\beta'(M)$ for M in the range 4×10^7 – 10^9 g . Future measurements of N_{eff} may constrain the initial fraction for M as low as 1 g. If an excess in N_{eff} is found, PBHs with Dirac neutrinos could provide an explanation of it.

Evaporating PBH should produce any other particles predicted in theories beyond the Standard Model. The number of PBHs is therefore limited by both the abundance of stable massive particles [162] or the decay of long-lived ones

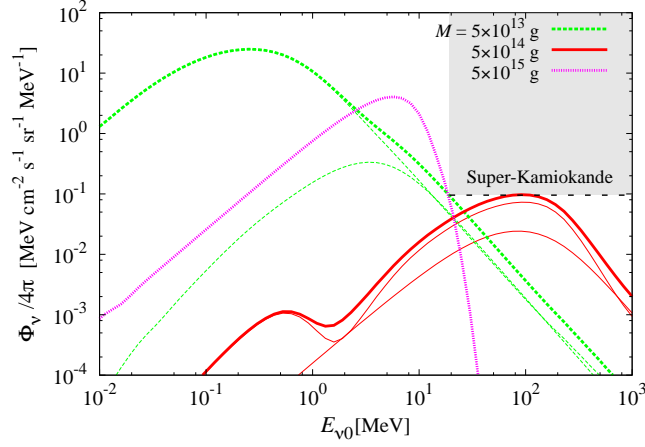


FIG. 9. An illustration of the maximum $\bar{\nu}_e$ flux allowed by the SK limit for three PBH masses, the shaded region being excluded. For $M \lesssim M_*$, the lower (upper) curves represent primary (secondary) components and the thick curves denote their sum. $M \gtrsim M_*$ holes emit primary neutrinos only.

[163]. In supersymmetry (SUSY) or supergravity (SUGRA), the lightest supersymmetric particle (LSP) is stable and becomes a candidate for the dark matter. If LSPs are produced by the evaporation of PBHs, in order not to exceed the observed CDM density at present, one obtains the upper bound [164]:

$$\beta'(M) \lesssim 10^{-18} \left(\frac{M}{10^{11} \text{ g}} \right)^{-1/2} \left(\frac{m_{\text{LSP}}}{100 \text{ GeV}} \right)^{-1} \quad (M < 10^{11} (m_{\text{LSP}}/100 \text{ GeV})^{-1} \text{ g}). \quad (48)$$

This constraint is shown in Fig. 4 but depends on the mass of the LSP and is therefore subject to considerable uncertainty [165, 166]. In addition, unstable particles such as the gravitino or neutralino might be produced by evaporating PBHs. The decay of these particles into lighter ones also affects BBN [116, 117] and this gives another constraint [163]:

$$\beta'(M) \lesssim 5 \times 10^{-19} \left(\frac{M}{10^9 \text{ g}} \right)^{-1/2} \left(\frac{Y_{\text{PBH}}}{10^{-14}} \right) \left(\frac{x_\phi}{0.006} \right)^{-1} \quad (M < 10^9 \text{ g}), \quad (49)$$

where Y_{PBH} is the PBH number density to entropy density ratio and x_ϕ is the fraction of the luminosity going into quasi-stable massive particles, both being normalised to reasonable values. This limit is not shown explicitly in Fig. 4 but it has a similar form to Eq. (48).

7. Reionisation and 21 cm signature

The Planck 2018 results give the optical depth as $\tau \sim 0.05$ [167] for CMB photons emitted from the last scattering surface and observations of the Gunn–Peterson troughs and a γ -ray burst around $z \sim 6$ imply that reionisation of the Universe occurred at $z \sim 6$ [130]. Thus PBHs cannot be so numerous that they lead to reionisation earlier than $z \sim 6$. In principle, this leads to a constraint on PBHs with

$$M \geq M_* \left(\frac{t_{\text{dec}}}{t_0} \right)^{1/3} \left(\frac{f(M)}{f_*} \right)^{1/3} \approx 2 \times 10^{13} \text{ g}. \quad (50)$$

On the other hand, Belotsky *et al.* have attributed the reionization of the pregalactic medium to evaporating PBHs [10, 168]. They show that PBHs with a monochromatic mass distribution around $5 \times 10^{16} \text{ g}$ could ensure this. They also argue that the reionization effect and contribution to the dark matter can be simultaneously enhanced with an extended mass distribution around the same mass.

An increase in the ionization of the intergalactic medium would also produce a 21 cm signature. Mack and Wesley [169] have shown that future observations of 21 cm radiation from high redshift neutral hydrogen could place important

constraints on PBHs in the mass range $5 \times 10^{13} \text{ g} < M < 10^{17} \text{ g}$. This is essentially due to the coincidence that photons emitted from PBHs during $30 < z < 300$ peak in the energy range in which the intergalactic medium has low optical depth. Any process which heats the intergalactic medium in this period will produce a signal but the ionising flux of photons, electrons and positrons from PBHs would generate a distinctive feature in the 21 cm brightness temperature. PBHs with $5 \times 10^{13} \text{ g} < M < 10^{14} \text{ g}$ evaporate in $30 < z < 90$ and would raise the 21 cm brightness temperature, thereby reducing the absorption seen against the CMB. PBHs with $M \sim 10^{14} \text{ g}$ would raise the spin temperature above the CMB, so that the 21 cm line appears in emission rather than absorption. PBHs with $10^{14} \text{ g} < M < 10^{17} \text{ g}$ would have a less pronounced effect. The latter limit is shown in Fig. 8 of their paper and can be expressed in the form

$$\beta'(M) < 3 \times 10^{-29} \left(\frac{M}{10^{14} \text{ g}} \right)^{7/2} \quad (M > 10^{14} \text{ g}). \quad (51)$$

It bottoms out at a mass of around 10^{14} g and is well below the photon background limit. The associated limits are not shown in Fig. 4.

Recently the Experiment to Detect the Global Epoch of Reionization Signature (EDGES) reported the detection of a 21 cm absorption signal stronger than astrophysical expectations. Clark *et al.* [170] study the impact of radiation from DM decay and PBHs on the 21 cm radiation temperature in the reionization epoch, and impose a constraint on the decaying dark matter and PBH energy injection in the intergalactic medium, which can heat up neutral hydrogen gas and weaken the 21 cm absorption signal. They require that the heating of the neutral hydrogen does not negate the 21 cm absorption signal. For $e\gamma\gamma$ final states they find strong 21 cm bounds that can be more stringent than the current extragalactic diffuse photon bounds.

D. PBH explosions

The extragalactic γ -ray background limit implies that the PBH explosion rate \mathcal{R} could be at most $10^{-6} \text{ pc}^{-3} \text{ yr}^{-1}$ if the PBHs are uniformly distributed or $10 \text{ pc}^{-3} \text{ yr}^{-1}$ if they are clustered inside galactic halos [6, 171]. The latter figure might be compared to the Lehoucq *et al.* Galactic γ -ray limit of $0.06 \text{ pc}^{-3} \text{ yr}^{-1}$ [7] and the Maki *et al.* antiproton limit of $0.02 \text{ pc}^{-3} \text{ yr}^{-1}$ [147]. We now compare these limits to the direct observational constraints on the explosion rate. These come both from γ -ray bursts and high-energy cosmic ray showers.

1. Gamma-ray bursts and photosphere effects

In the Standard Model of particle physics, where the number of elementary particle species never exceeds around 100, it has been appreciated for a long time that the likelihood of detecting the final explosive phase of PBH evaporations is very low [172]. However, the physics of the QCD phase transition is still uncertain and the prospects of detecting explosions would be improved in less conventional particle physics models. For example, in a Hagedorn-type picture [173], where the number of particle species exponentiates at the quark-hadron temperature, the upper limit on \mathcal{R} is reduced to $0.05 \text{ pc}^{-3} \text{ yr}^{-1}$ [174], which is comparable to the antiproton limit.

Even without the Hagedorn effect, something dramatic may occur at the QCD temperature since the number of species being emitted increases dramatically [175]. For this reason, Cline and colleagues have long argued that the formation of a fireball at the QCD temperature could explain some of the short period γ -ray bursts (i.e. those with duration less than 100 ms) [11, 176, 177]. In Ref. [178] they claim to find 42 BATSE candidates of this kind and the fact that their distribution matches the spiral arms suggests that they are Galactic. In Ref. [179] they claim that there is a class of short-period KONUS bursts which has a much harder spectrum than usual and identify these with exploding PBHs. More recently they have found a further 8 candidates in the Swift data [180]. Overall they claim that the BATSE, KONUS and Swift data correspond to a 4.5σ effect and that several events exhibit the time structure expected of PBH evaporations [181]. One distinctive feature of γ -ray bursts generated by PBH explosions would be a temporal delay between the high and low energy pulses, an effect which might be detectable by Fermi LAT [182].

It is clearly important to understand how likely PBHs are to resemble γ -ray bursts from a theoretical perspective. The usual assumption that there is no interaction between emitted particles [183] was refuted by Heckler [184], who claimed that QED interactions could produce an optically thick photosphere once the black hole temperature exceeds $T_{\text{BH}} = 45 \text{ GeV}$. He proposed that a similar effect may operate at an even lower temperature, $T_{\text{BH}} \approx 200 \text{ MeV}$, due to QCD effects [185]. Variants of these models and their astrophysical implications have been studied by various authors [186–188].

MacGibbon *et al.* [109] have identified a number of physical and geometrical effects which may invalidate these claims. First, the particles must be causally connected in order to interact and this means that the standard cross-sections are reduced (viz. the particles are created at a finite time and do not go back to the infinite past). Second, because of the Landau–Pomeranchuk–Migdal effect, a scattered particle requires a minimum distance to complete each bremsstrahlung interaction, with the consequence that there is unlikely to be more than one complete bremsstrahlung interaction per particle near the black hole. They conclude that the emitted particles do not interact sufficiently to form a QED photosphere and that the conditions for QCD photosphere formation could only be temporarily satisfied (if at all) when the black hole temperature is of order Λ_{QCD} . Even in this case, the strong damping of the Hawking production of QCD particles around this threshold may suffice to suppress it. In any case, they claim that no QCD photosphere persists once the black hole temperature climbs above Λ_{QCD} .

A rather different way of producing a γ -ray burst is to assume that the outgoing charged particles form a plasma due to turbulent magnetic field effects at sufficiently high temperatures [189]. However, MacGibbon *et al.* argue that this too is implausible. They conclude that the observational signatures of a cosmic or Galactic halo background of PBHs or an individual high-temperature black hole remain essentially those of the standard Hawking model, with little change to the detection probability. Nevertheless, perhaps the best strategy is to accept that our understanding of such effects is incomplete and focus on the empirical aspects of the γ -ray burst observations.

2. High energy cosmic rays showers

At much higher energies, several groups have looked for 1–100 TeV photons from PBH explosions using cosmic ray detectors. However, in this case, the constraints are also strongly dependent on the theoretical model [190]. In the Standard Model the upper limits on the explosion rate are $5 \times 10^8 \text{ pc}^{-3} \text{ yr}^{-1}$ from the CYGNUS array [191], $8 \times 10^6 \text{ pc}^{-3} \text{ yr}^{-1}$ from the Tibet array [192], $1 \times 10^6 \text{ pc}^{-3} \text{ yr}^{-1}$ from the Whipple Cerenkov telescope [193], and $8 \times 10^8 \text{ pc}^{-3} \text{ yr}^{-1}$ from the Andyrchy array [194]. These limits correct for the effects of burst duration and array “dead time.” Such limits are far weaker than the ones associated with observations at 100 MeV. They would be even weaker in the 45 GeV QED photosphere model advocated by Heckler, since there are then far fewer TeV particles [195]. For example, Bugaev *et al.* [196] have used Andyrchy data to obtain an upper limit of $1 \times 10^9 \text{ pc}^{-3} \text{ yr}^{-1}$ in the Daghigh–Kapusta model [187, 188, 197, 198] and $5 \times 10^9 \text{ pc}^{-3} \text{ yr}^{-1}$ in the Heckler model [184]. Because of the uncertainties, we do not show any of these limits in Fig. 4.

The most recent constraints on PBH explosions come observations of the High Altitude Water Cherenkov (HAWC) Observatory, which is sensitive to gamma-rays with energies of 300 GeV to 100 TeV. With its large instantaneous field-of-view of 2 steradians and a duty cycle over 95%, the observatory is well suited to perform an all-sky search for PBH bursts and Albert *et al.* [199] have obtained an upper limit on the local PBH burst rate density of $3400 \text{ pc}^{-3} \text{ yr}^{-1}$ at the 99% confidence level, far stronger than any existing electromagnetic limit.

E. Higgs instability

Evaporating PBHs can act as seeds for nucleating the decay of the metastable Higgs vacuum. The vacuum bubbles must percolate in order to completely destroy the false vacuum and the conditions for this were studied by Dai *et al.* [200]. This constrains the PBH mass spectrum for a particular Higgs potential or it constrains the Higgs potential if PBHs are detected. More recently Kohri and Matsui [201] have explored the consequences of a possible instability of the Higgs vacuum expectation value due to thermal fluctuations at the weak scale. They obtain an upper bound

$$\beta'(M) < 10^{-21} \left(\frac{M}{10^9 \text{ g}} \right)^{3/2} \quad (M < M_*). \quad (52)$$

Although this limit is very speculative, it extends the limits shown in Fig. 4 down to the Planck scale and it dominates the BBN limit below about 10^{10} g .

F. Planck mass relic constraints

If PBH evaporations leave stable Planck-mass relics, these might also contribute to the dark matter. This was first pointed out by MacGibbon [202] and has subsequently been explored in the context of inflationary scenarios by numerous authors [20, 53, 203–208]. If the relics have a mass κM_{Pl} and reheating occurs at a temperature T_{R} , then

the requirement that they have less than the critical density implies [53]

$$\beta'(M) < 8 \times 10^{-28} \kappa^{-1} \left(\frac{M}{M_{\text{Pl}}} \right)^{3/2} \quad (53)$$

for the mass range

$$\left(\frac{T_{\text{Pl}}}{T_{\text{R}}} \right)^2 < \frac{M}{M_{\text{Pl}}} < 10^{11} \kappa^{2/5}. \quad (54)$$

Note that we would now require the density to be less than $\Omega_{\text{CDM}} \approx 0.25$, which strengthens the original limit by a factor of 4. The lower mass limit arises because PBHs generated before reheating are diluted exponentially. The upper mass limit arises because PBHs larger than this dominate the total density before they evaporate, in which case the final cosmological baryon-to-photon ratio is determined by the baryon-asymmetry associated with their emission. This might be compared to lower limit imposed by the trans-Planckian censorship conjecture [209].

Alexander and Mészáros [210] have advocated an extended inflationary scenario in which evaporating PBHs naturally generate the dark matter, the entropy and the baryon asymmetry of the Universe. This triple coincidence applies providing inflation ends at $t \sim 10^{-23}$ s, so that the PBHs have an initial mass $M \sim 10^6$ g. This just corresponds to the upper limit indicated in Eq. (54), which explains one of the coincidences. The other coincidence involves the baryon-asymmetry generated in the evaporations. It should be stressed that the limit (53) still applies even if there is no inflationary period but then extends all the way down to the Planck mass.

It is usually assumed that such relics would be undetectable apart from their gravitational effects. However, Lehmann *et al.* [105] point out that they may carry electric charge, making them visible to terrestrial detectors. They evaluate constraints and detection prospects in detail and show that this scenario, if not already ruled out by monopole searches, can be explored within the next decade using existing or planned experimental equipment.

III. CONSTRAINTS ON NON-EVAPORATED PBHS

We next review the various constraints associated with PBHs which are too large to have evaporated completely by now, updating the equivalent discussion in Refs. [101, 102]. All the limits assume that PBHs cluster in the Galactic halo in the same way as other forms of CDM. In this section we also assume the PBHs have a monochromatic mass function, in the sense that they span a mass range of at most $\Delta M \sim M$. In this case, the fraction $f(M)$ of the halo in PBHs is related to $\beta'(M)$ by

$$f(M) \equiv \frac{\Omega_{\text{PBH}}(M)}{\Omega_{\text{CDM}}} \approx 3.79 \Omega_{\text{PBH}}(M) = 3.81 \times 10^8 \beta'(M) \left(\frac{M}{M_{\odot}} \right)^{-1/2}, \quad (55)$$

where we have taken $\Omega_{\text{CDM}} = 0.264$ from Ref. [211]. For an extended or multi-modal mass function, which we discuss later, one can define a total PBH contribution to the dark matter f_{PBH} by integrating over M and there is then a constraint $f_{\text{PBH}} < 1$. Our limits on $f(M)$ are summarised in Fig. 10, which is an updated version of Fig. 8 of Ref. [101]. The main constraints derive from (partial) PBH evaporations, gravitational lensing, numerous dynamical effects, PBH accretion and gravitational wave observations. Since Fig. 10 is complicated, the constraints for each of these categories are shown separately in subsequent figures. We note that there are several limits in most mass ranges.

Figure 10 only provides a rough guide for each constraint and a more precise discussion can be found in the original references. It must be stressed that the constraints have varying degrees of certainty and they all come with caveats. For some, the observations are well understood (e.g. the CMB and gravitational lensing data) but there are uncertainties in the black hole physics. For others, the observations themselves are not fully understood or depend upon additional astrophysical assumptions. Many of the constraints depend on physical parameters which are not indicated explicitly, and some of them depend on various cosmological and astrophysical assumptions. Note that some of the limits are extended into the $f > 1$ domain, although this is obviously unphysical. This is because each limit will shift downward as the observational data improve, so it is useful to know its form.

Similar figures can be found in numerous papers besides CKSY and CKS: see, for example, Table 1 of Josan *et al.* [100], Fig. 4 of Mack *et al.* [212], Fig. 9 of Ricotti *et al.* [14], Fig. 1 of Capela *et al.* [213], Fig. 1 of Clesse & García-Bellido [214] and Fig. 10 of Sasaki *et al.* [21]. However, we believe this is the most comprehensive treatment available to date (i.e. prior to 2020). We group the limits by type and discuss those within each type in order of increasing mass. Sometimes we express the limit in terms of an analytic function $f_{\text{max}}(M)$ over some mass range but this is not always possible.

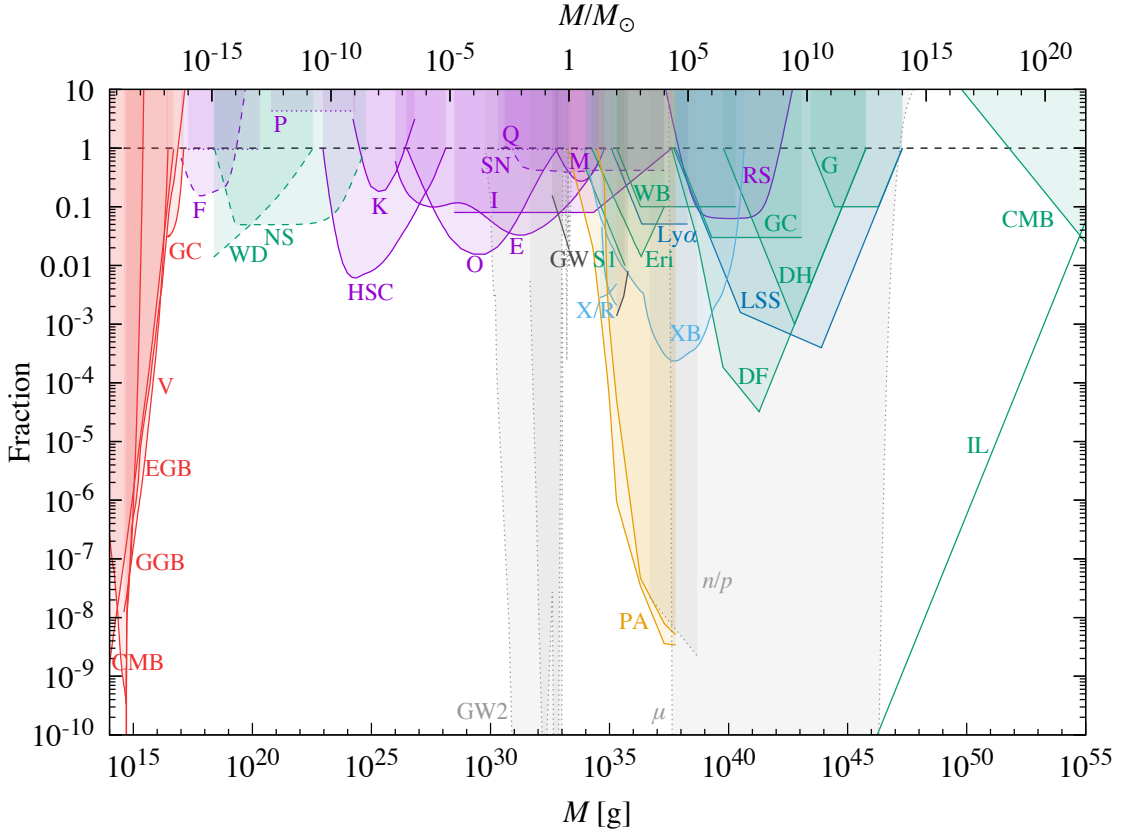


FIG. 10. Constraints on $f(M)$ from evaporation (red), lensing (magenta), dynamical effects (green), accretion (light blue), CMB distortions (orange), large-scale structure (dark blue) and background effects (grey). Evaporation limits come from the extragalactic gamma-ray background (EGB), the Galactic gamma-ray background (GGB) and Voyager e^\pm limits (V). Lensing effects come from femtolensing (F) and picolensing (P) of gamma-ray bursts, microlensing of stars in M31 by Subaru (HSC), in the Magellanic Clouds by MACHO (M) and EROS (E), in the local neighbourhood by Kepler (K), in the Galactic bulge by OGLE (O) and the Icarus event in a cluster of galaxies (I), microlensing of supernova (SN) and quasars (Q), and millilensing of compact radio sources (RS). Dynamical limits come from disruption of wide binaries (WB) and globular clusters (GC), heating of stars in the Galactic disk (DH), survival of star clusters in Eridanus II (Eri) and Segue 1 (S1), infalling of halo objects due to dynamical friction (DF), tidal disruption of galaxies (G), and the CMB dipole (CMB). Accretion limits come from X-ray and radio (X/R) observations, CMB anisotropies measured by Planck (PA) and gravitational waves from binary coalescences (GW). Background constraints come from CMB spectral distortion (μ), 2nd order gravitational waves (GW2) and the neutron-to-proton ratio (n/p). The incredulity limit (IL) corresponds to one hole per Hubble volume. Constraints shown by broken lines are insecure and probably wrong but included for historical completeness; those shown by a dotted line depend upon some additional assumptions.

A. Evaporation Constraints

For PBHs somewhat larger than M_* , one can use the γ -ray background to constrain the value of $f(M)$, this being equivalent to the constraint on $\beta(M)$ derived in Sec. II C 1. For $M > 2M_*$, one can neglect the change of mass altogether and the time-integrated spectrum dN^γ/dE of photons from each PBH is just obtained by multiplying the instantaneous spectrum $d\dot{N}^\gamma/dE$ by the age of the Universe t_0 . For PBHs of mass M , the discussion in the appendix of Ref. [101] gives

$$\frac{dN^\gamma}{dE} \propto \begin{cases} E^3 M^3 & (E < M^{-1}) \\ E^2 M^2 e^{-EM} & (E > M^{-1}), \end{cases} \quad (56)$$

where we put $\hbar = c = G = 1$. This peaks at $E \sim M^{-1}$ with a value independent of M . The number of background photons per unit energy per unit volume from all the PBHs is obtained by integrating over the mass function:

$$\mathcal{E}(E) = \int_{M_{\min}}^{M_{\max}} dM \frac{dn}{dM} \frac{dN^\gamma}{dE}(M, E), \quad (57)$$

where M_{\min} and M_{\max} specify the mass limits. For a monochromatic mass function, this gives

$$\mathcal{E}(E) \propto f(M) \times \begin{cases} E^3 M^2 & (E < M^{-1}) \\ E^2 M e^{-EM} & (E > M^{-1}) \end{cases} \quad (58)$$

and the associated intensity is

$$I(E) \equiv \frac{E \mathcal{E}(E)}{4\pi} \propto f(M) \times \begin{cases} E^4 M^2 & (E < M^{-1}) \\ E^3 M e^{-EM} & (E > M^{-1}) \end{cases} \quad (59)$$

with units $\text{s}^{-1} \text{sr}^{-1} \text{cm}^{-2}$. This peaks at $E \sim M^{-1}$ with a value $I^{\max}(M) \propto f(M) M^{-2}$. The observed extragalactic intensity is $I^{\text{obs}} \propto E^{-(1+\epsilon)} \propto M^{1+\epsilon}$ where ϵ lies between 0.1 (the value favoured in Ref. [141]) and 0.4 (the value favoured in Ref. [215]). Hence putting $I^{\max}(M) \leq I^{\text{obs}}(M)$ gives [101]

$$f(M) \lesssim 2 \times 10^{-8} \left(\frac{M}{M_*} \right)^{3+\epsilon} \quad (M > M_* = 5 \times 10^{14} \text{g}). \quad (60)$$

As expected, this is equivalent to condition (31), which is represented in Fig. 7 for $\epsilon = 0.2$. We have seen that the Galactic γ -ray background may give a stronger limit but this depends sensitively on the form of the mass function.

PBHs smaller than 10^{15}g have evaporated completely and therefore cannot contribute to the dark matter. The function $f(M)$ is not defined in this range, so the abundance is usually described in terms of the collapse fraction at formation, $\beta(M)$, as shown in Fig. 4. Nevertheless, one can still formally relate $\beta(M)$ to $f(M)$ using Eq. (55). The dominant constraints in Fig. 4 are therefore represented in Fig. 11, including the VOYAGER-I limits [143].

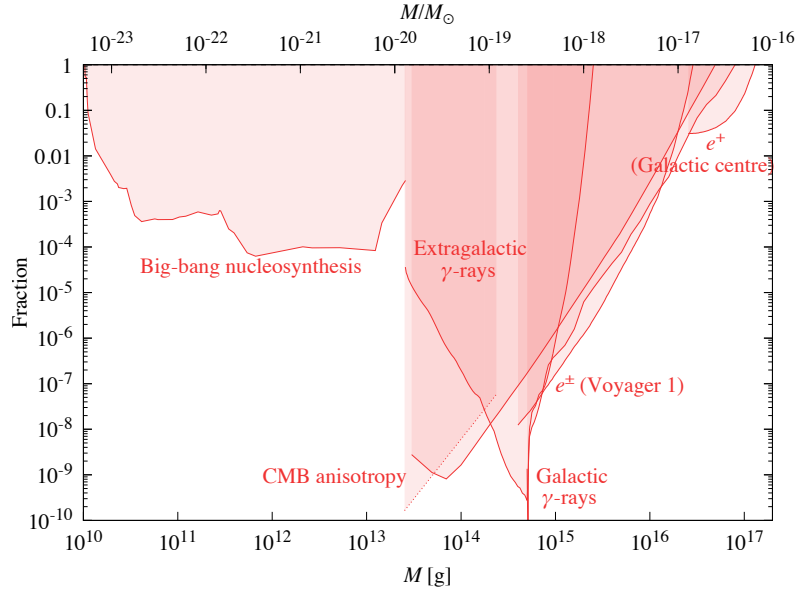


FIG. 11. Evaporative constraints on PBHs based on Fig. 4 and Eq. (55).

B. Lensing Constraints

The lensing constraints on $f(M)$ are summarised in Fig 12. These derive from a large number of papers and they come with different confidence levels. Where possible, we use the 95% CL constraint. Also one must distinguish

between limits based on positive detections and null detections. Claimed positive detections come from OGLE in the low mass range [216], MACHO and quasar microlensing [217] in the solar mass range and from Dong *et al.* [218] in the high mass range.

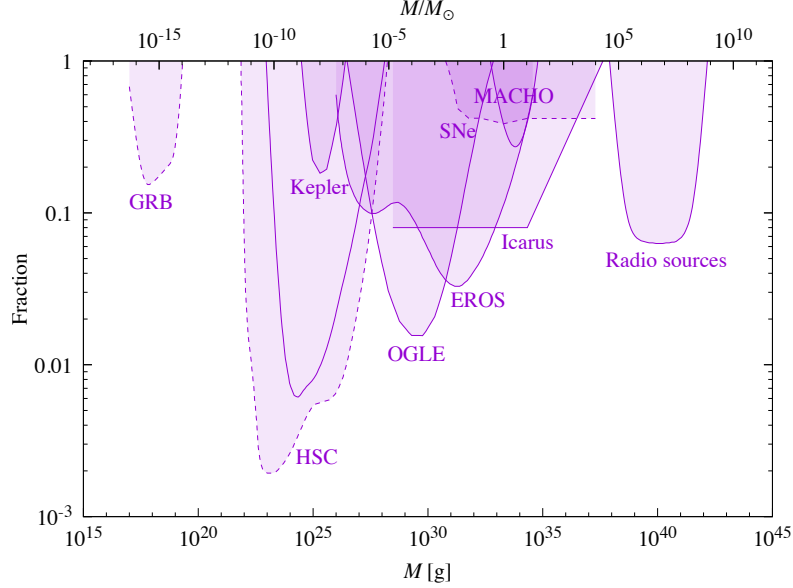


FIG. 12. Lensing constraints with the (disputed) GRB and SNe limits and the original HSC constraint shown by broken lines.

1. Femtolensing and picolensing

It has been argued that constraints on PBHs with very low M come from the femtolensing of γ -ray bursts. Assuming the bursts are at a redshift $z \sim 1$, early studies [219, 220] claimed to exclude $f = 1$ in the mass range 10^{-16} – $10^{-13} M_\odot$ and later work [221] gave a limit which can be approximated as

$$f(M) < 0.1 \quad (5 \times 10^{16} \text{ g} < M < 10^{19} \text{ g}), \quad (61)$$

as shown in Fig. 12. The femtolensers could either be PBHs or ultra-compact dark matter minihalos (e.g. made up of QCD axions). However, Katz *et al.* [222] have reviewed this argument, taking into account the extended nature of the source as well as wave optics effects, and argue that most GRBs are inappropriate for femtolensing searches due to their large sizes. This probably removes the femtolensing limit altogether. A small fraction, characterized by fast variability, might be small enough to be useful but many such bursts would be needed to achieve meaningful constraints. The femtolensing limits in Figs. 10 and 12 are shown with broken lines to reflect this uncertainty.

2. Microlensing of stars

Microlensing observations of stars in the Magellanic Clouds (LMC and SMC) probe the fraction of the Galactic halo in MACHOs over the mass range $10^{-7} M_\odot < M < 10 M_\odot$ [223]. The optical depth of the halo towards LMC and SMC, defined as the probability that any given star is amplified by at least 1.34 at a given time, is related to the fraction $f(M)$ by

$$\tau_L^{(\text{SMC})} = 1.4 \tau_L^{(\text{LMC})} = 6.6 \times 10^{-7} f(M) \quad (62)$$

for the S halo model [224]. Although the initial motivation for microlensing surveys was to search for brown dwarfs with $0.02 M_\odot < M < 0.08 M_\odot$, the possibility that the halo is dominated by these objects was soon ruled out by the MACHO experiment [225]. However, MACHO observed 17 events and claimed that these were consistent with compact objects of $M \sim 0.5 M_\odot$ contributing 20% of the halo mass [224]. This raised the possibility that some of the

dark matter could be PBHs formed at the QCD phase transition [60–62], although later studies suggested that the halo contribution of $M \sim 0.5 M_\odot$ PBHs could be at most 10% [226]. This limit is shown in Fig. 10.

The EROS collaboration monitored brighter stars in a wider solid angle and obtained fewer events than expected. They thus obtained more stringent constraints on f and argued that some of the MACHO events were due to self-lensing or halo clumpiness [227]. Specifically, they excluded $6 \times 10^{-8} M_\odot < M < 15 M_\odot$ objects from dominating the halo, although combining the MACHO and EROS results [228] extended the upper bound to $30 M_\odot$. These are shown in Fig. 10 and may be approximated as:

$$f(M) < \begin{cases} 1 & (6 \times 10^{-8} M_\odot < M < 30 M_\odot), \\ 0.1 & (10^{-6} M_\odot < M < 1 M_\odot), \\ 0.04 & (10^{-3} M_\odot < M < 0.1 M_\odot). \end{cases} \quad (63)$$

Similar limits were obtained by the POINT-AGAPE collaboration, which detected 6 microlensing events in a survey of the Andromeda galaxy [229].

There are also constraints from the OGLE experiment. The OGLE-II data [230–232] yielded somewhat weaker constraints but OGLE-III [233] and OGLE-IV [234] gave stronger results in the high mass range:

$$f(M) < \begin{cases} 0.2 & (0.4 M_\odot < M < 20 M_\odot), \\ 0.09 & (0.4 M_\odot < M < 1 M_\odot), \\ 0.06 & (0.1 M_\odot < M < 0.4 M_\odot). \end{cases} \quad (64)$$

Later (comparable) constraints combining EROS and OGLE data were presented in Ref. [235]. We do not include these limits in Fig. 10 because they depend on some unidentified detections being attributed to self-lensing. However, recently Niikura *et al.* [216] have used five year of observations of stars in the Galactic bulge by OGLE to constrain the PBH abundance of PBHs. The microlensing light-curves span a distribution of timescales over the range $t_E \approx [1, 300]$ days and can be well modeled as being due to brown dwarfs, main-sequence stars and white dwarfs or neutron stars. However, there are also six ultrashort events with $t_E \approx [0.1, 0.3]$ day. These might be attributed to free-floating planets but they could also be generated by planetary-mass PBHs with a dark matter fraction of around 1%. On the “null hypothesis” that the OGLE data contain no PBH event, there is a tight upper bound ($f < 0.1$) on the PBH abundance in the mass range $[10^{-5}, 10^{-2}] M_\odot$ and the full limit is shown in Fig. 10.

Wyrzykowski and Mandel [236] have used Gaia data on distances and proper motions of non-blended sources to improve the mass estimates in the annual parallax microlensing events found in 8 years of OGLE-III observations towards the Galactic Bulge. They identify 18 new events in that sample and the derived distribution of masses for the dark lenses is consistent with a continuous distribution of stellar remnant masses. However, they also find 8 candidates in the theoretically expected mass gap of $2\text{--}5 M_\odot$ between neutron stars and black holes. These might conceivably be PBHs [19], although they could also be stellar black holes if these receive natal kicks.

The interpretation of the MACHO, EROS and OGLE results is very sensitive to the properties of the Milky Way halo. All the above constraints assume a semi-isothermal density sphere but Calcino *et al.* [237] argue that this model is no longer consistent with data from the Milky Way rotation curve. They rederive the microlensing constraints with a new model and find that none of the old models sufficiently incorporate the uncertainties in the shape of the Milky Way halo. When this uncertainty is taken into account, the LMC microlensing constraints weaken for masses around $10 M_\odot$ but tighten at lower masses. Allowing for a wide PBH mass distribution and the effect of spatial clustering shifts the constraints towards smaller masses and may remove the microlensing constraint at $M \sim 1\text{--}10 M_\odot$ altogether for certain MACHO populations. Hawkins has argued that the recent low-mass Galactic halo models would relax the constraints and allow the halo to consist entirely of solar mass PBHs [238].

Recently Kepler data have improved the limits considerably in the low mass range [239, 240]:

$$f(M) < 0.3 \quad (2 \times 10^{-9} M_\odot < M < 10^{-7} M_\odot). \quad (65)$$

In a similar mass range, Niikura *et al.* [241] have carried out a dense-cadence 7-hour observation of M31 with the Subaru Hyper Suprime-Cam to search for microlensing of stars in M31 by PBHs lying in the halo regions of the Milky Way and M31. If light PBHs make up a significant fraction of DM, they expect to find many microlensing events for the PBH DM scenario. However, they identify only a single candidate event, which translates into the most stringent upper bounds on the abundance of PBHs in the mass range $10^{-10} M_\odot < M < 10^{-6} M_\odot$. Note that the black hole size becomes less than photon wavelength and the Einstein radius becomes smaller than the source size at the lower bound. However, Smyth *et al.* [242] point out that Niikura *et al.* underestimate this effect because they assume a source size of a solar radius, whereas the sources are likely to be larger than this. They find that the HSC constraints are weaker by up to almost three orders of magnitude in some cases, broadening the mass range in which PBHs can

provide all the dark matter by almost one order of magnitude. Sugiyama *et al.* [243] have also studied this effect and point out that, if a denser-cadence (10 sec) g-band monitoring of a sample of white dwarfs over a year were available, then one could probe the wave-optics effect on a microlensing light-curve and push the PBH constraint down to $10^{-11} M_\odot$.

Going beyond the local neighbourhood, the recent discovery of fast transient events in massive galaxy clusters, interpreted as highly magnified individual stars in giant arcs due to caustic crossing, opens up the possibility of using such microlensing events to constrain PBHs. Oguri *et al.* [244] find that the lens mass and source radius of the first event MACS J1149 are constrained, with the lens mass range being $0.1 M_\odot < M < 4 \times 10^3 M_\odot$. The derived lens properties are fully consistent with the interpretation of MACS J1149 LS1 as a microlensing event produced by a star that contributes to the intra-cluster light. They argue that compact dark matter models with high fractional mass densities for the mass range $10^{-5} M_\odot < M < 10^2 M_\odot$ are inconsistent with the observation of MACS J1149 because such models predict too low magnifications. This corresponds to the “Icarus” line in Fig. 10.

3. Microlensing of supernovae

PBHs cause most lines of sight to be demagnified relative to the mean, with a long tail of higher magnifications. Zumalacárregui and Seljak [245] have tested the PBH model using the lack of lensing signatures of type Ia supernovae (SNe), modelling the effects of large scale structure, allowing for a non-Gaussian model for the intrinsic SNe luminosity distribution and addressing potential systematic errors. Using current JLA SNe data, they derive a bound $f < 0.35$ at 95% confidence, ruling out PBHs comprising the totality of the dark matter at 5σ significance. The finite size of SNe limits the validity of the results to $M > 10^{-2} M_\odot$ but closes a previously open PBH mass range.

García-Bellido *et al.* [246] find several caveats in this analysis. (1) The constraints on the fraction of PBH dark matter depend on a very restrictive choice of priors for the cosmological parameters. (2) By considering more realistic physical sizes for the supernovae, they find that the effect on the lensing magnification distribution leads to significantly weaker constraints. (3) Considering a wide PBH mass spectrum (e.g. lognormal) further softens the constraints. They conclude that the bound on the fraction of PBH dark matter is $f < 1.09 (1.38)$ for the JLA (Union 2.1) catalogues, which is compatible with an all-PBH dark matter scenario in the LIGO band.

4. Quasar microlensing and millilensing

Early studies of the microlensing of quasars [247] seemed to exclude all the dark matter being in objects with $10^{-3} M_\odot < M < 60 M_\odot$. However, this limit does not apply in the Λ CDM picture and so is not shown in Fig. 10. At around the same time, Hawkins [217] claimed evidence for a critical density of jupiter-mass objects from observations of quasar microlensing and associated these with PBHs formed at the quark-hadron transition. However, his later analysis yielded a lower density (dark matter rather than critical) and a larger mass of around $1 M_\odot$ [248]. The status of this claim remains unclear [249], so the associated constraint is not included in Fig. 10. Studies of quasar microlensing by Mediavilla *et al.* initially found a limit [250]

$$f(M) < 1 \quad (10^{-3} M_\odot < M < 60 M_\odot) \quad (66)$$

but later found positive evidence for quasar microlensing, these indicating that 20% of the total mass is in compact objects in the mass range $0.05\text{--}0.45 M_\odot$ [251]. Although this might be compatible with a stellar component, Hawkins has argued that one requires PBHs to explain this [252]. It is difficult to express the result of Ref. [251] as a quantitative upper bound on the PBH mass fraction in this mass range, so we do not include it in Fig. 10.

In a higher mass range, Vedantham *et al.* [253] claim to have detected long-term radio variability – what they term Symmetric Achromatic Variability – in the light-curves of active galactic nuclei (AGN). They propose that this arises from gravitational millilensing of features in AGN jets moving relativistically through gravitational lensing caustics created by $10^3\text{--}10^6 M_\odot$ subhalo condensates or black holes located within intervening galaxies. The lower end of this mass range has been inaccessible with previous gravitational lensing techniques. This offers a new and powerful probe of cosmological matter distribution on these intermediate mass scales, as well as providing, for the first time, micro-arcsecond resolution of AGN, a factor of 30–100 greater than with ground-based VLBI.

Millilensing of compact radio sources [254] gives a limit which can be approximated as

$$f(M) < \begin{cases} (M/2 \times 10^4 M_\odot)^{-2} & (M < 10^5 M_\odot), \\ 0.06 & (10^5 M_\odot < M < 10^8 M_\odot), \\ (M/4 \times 10^8 M_\odot)^2 & (M > 10^8 M_\odot). \end{cases} \quad (67)$$

Though weaker than other constraints in this mass range, we include this limit in Fig. 10. Hezaveh *et al.* [255] have studied substructure in the matter density near galaxies using ALMA observations of the strong lensing system SDP.81. They find evidence for the presence of a $10^9 M_\odot$ subhalo near one of the images and derive constraints on the abundance of dark matter subhalos down to $M \sim 2 \times 10^7 M_\odot$ (the mass of the smallest detected satellites in the Local Group). There are hints of additional substructure but the results are consistent with the Λ CDM prediction. Although they do not explicitly constrain PBHs, their results require $f < 0.04$ for $10^7 < M/M_\odot < 10^9$.

5. Microlensing of Mira variables, pulsars and fast radio bursts

Finally, we list a number of lensing effects which have been discussed in the literature and may eventually constrain the PBH dark matter fraction. However, these are not shown in Fig. 10 because they are only potential limits. Karami *et al.* [256] discuss the detection of microlensing of Mira variables with VLBI. These stars are sufficiently bright and compact to permit direct imaging using long baseline interferometers such as the Very Long Baseline Array (VLBA). Microlensing by Galactic black holes is relatively common and features in the associated images are sufficiently well resolved to fully reconstruct the lens properties, enabling the measurement of mass, distance, and tangential velocity of the lensing object to a precision better than 15%. Future radio microlensing surveys conducted with upcoming radio telescopes combined with modest improvements in the VLBA could increase the rate of Galactic black hole events to roughly 10 yr^{-1} , sufficient to double the number of known stellar mass black holes in a couple years and permitting the construction of distribution functions of stellar mass black holes.

Other interesting constraints come from pulsar timing. Schutz and Liu [257] claim the non-detection of the third order Shapiro time delay as PBHs move around the Galactic halo will soon constrain those with mass in the range $1\text{--}10^3 M_\odot$. Indeed, observations with the Square Kilometer Array (SKA) potentially preclude PBHs having more than 1–10% of the dark matter. However, the limit flattens off below $f \sim 10^{-2}$, so this does not exclude supermassive seeds. Munoz *et al.* [258] have pointed out that similar limits could come from the lensing of fast radio bursts. The potential constraint in this case bottoms out at a mass of around $10 M_\odot$ with a value $f \sim 0.01$.

Dror *et al.* [259] have studied the sensitivity of pulsar timing arrays (PTAs) to single transiting PBHs. They find that the SKA can exclude PBHs providing all the dark matter over the mass range from $10 M_\odot$ to well above $100 M_\odot$ and less than 1% over significant parts of this range. The PTAs can potentially probe a substantially lower density of such objects because of the large effective radius over which they can be observed.

Due to a combination of wave and finite source size effects, the traditional microlensing of stars does not probe the mass range $10\text{--}100 M_\odot$. However, Bai *et al.* [260] point out that X-ray pulsars with higher photon energies and smaller sizes are good sources for microlensing in this mass window. Among existing X-ray pulsars, the most promising is SMC X-1 because of its apparent brightness and large distance. Their analysis of existing data from the RXTE telescope suggests that 100% of dark matter in PBHs is close to being excluded. Future observations of this source by X-ray telescopes with larger effective areas could close this the last mass dark matter window.

C. Dynamical Constraints

A variety of dynamical constraints come into play at higher mass scales and many of them involve the destruction of various astronomical objects by the passage of nearby PBHs. As shown by Carr and Sakellariadou [261], if the PBHs have density ρ and velocity dispersion V , while the objects have mass M_c , radius R_c , velocity dispersion V_c and survival time t_L , then the constraint has the general form:

$$f(M) < \begin{cases} M_c V / (G M \rho t_L R_c) & (M < M_c (V/V_c)) \\ M_c / (\rho V_c t_L R_c^2) & (M_c (V/V_c) < M < M_c (V/V_c)^3) \\ M V_c^2 / (\rho R_c^2 V^3 t_L) \exp[(M/M_c) (V_c/V)^3] & (M > M_c (V/V_c)^3) \end{cases} \quad (68)$$

The three limits correspond to disruption by multiple encounters, one-off encounters and non-impulsive encounters, respectively, and we assume $V > V_c$. The fraction is thus constrained over the mass range

$$\frac{M_c V}{G \rho_{\text{DM}} t_L R_c} < M < M_c \left(\frac{V}{V_c} \right)^3, \quad (69)$$

where ρ_{DM} is the dark matter density. The mass limits correspond to the values of M for which one would have $f = 1$, so PBHs could provide *all* the dark matter only if M is below the lower limit or above the higher limit. Note that various numerical factors are omitted in these expressions.

These limits apply providing there is at least one PBH within the relevant environment, be that a galactic halo, a cluster of galaxies or the Universe itself. Reference [261] terms this the “incredulity limit” and for an environment of mass M_E , it corresponds to the condition

$$f(M) > f_{\text{IL}} \equiv (M/M_E), \quad (70)$$

where M_E is around $3 \times 10^{12} M_\odot$ for halos, $10^{14} M_\odot$ for clusters and $10^{22} M_\odot$ for the Universe. However, this is only relevant if the exponential upper cut-off in (68) lies to the right of the incredulity limit and this applies only for $M_E V_c^2 < \rho_{\text{DM}} t_L R_C^2 V^3$. This determines which of the limits in Fig. 10 are cut off at the right.

These dynamical limits are summarised in Fig. 13. Each of them is subject to certain provisos but it is interesting that they all correspond to an upper limit on the mass of the objects which dominate the halo in the range $500\text{--}2 \times 10^4 M_\odot$. This is particularly relevant for constraining models in which the dark matter is postulated to comprise IMBHs. Apart from the galaxy heating arguments of Refs. [262, 263], it must be stressed that none of these dynamical effects gives *positive* evidence for MACHOs. Furthermore, none of them requires the MACHOs to be PBHs. For example, Raidal *et al.* have suggested that large primordial curvature fluctuations could collapse into horizonless exotic compact objects (ECOs) instead of PBHs [110]. The dark objects might also be clusters of smaller objects [264, 265] or Ultra-Compact Mini-Halos (UCMHs) [266]. This is pertinent in light of the claim by Dokuchaev *et al.* [85] and Chisholm [267] that PBHs could form in tight clusters, giving a local overdensity well in excess of that provided by the halo concentration alone. It is also important to note that the UCMH constraints on the density perturbations may be stronger than the PBH limits in the higher-mass range [266].

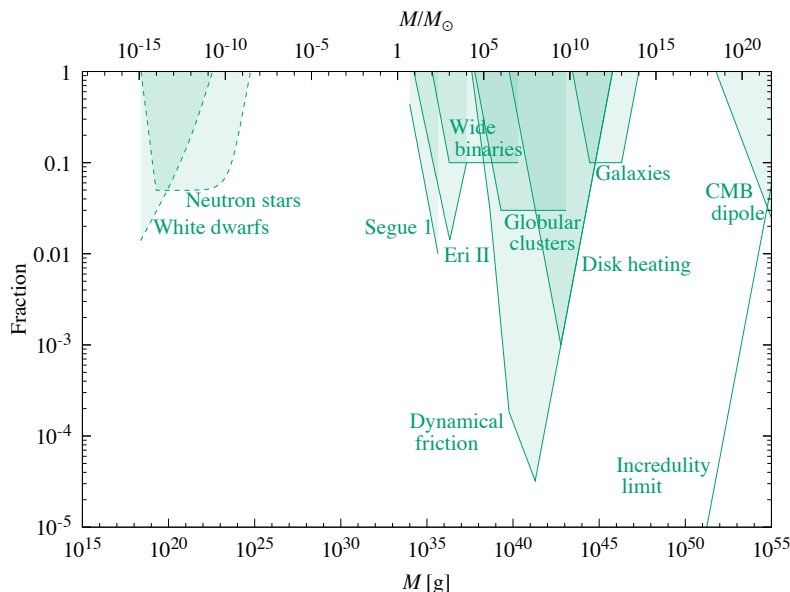


FIG. 13. Dynamical constraints.

1. Collisions

The effects of PBH collisions on astronomical objects—including the Earth [268]—have been a subject of long-standing interest, although we do not show these constraints in Fig. 10. For example, Zhilyaev [269] has suggested that collisions with stars could produce γ -ray bursts and Khriplovich *et al.* [270] have examined whether terrestrial collisions could be detected acoustically. Gravitational-wave observatories in space might detect the dynamical effects of PBHs. Luo *et al.* [271] have proposed a mechanism to search for PBH transits through or near the Earth by studying the associated seismic waves in Earth’s interior. There are two unique signatures: the wave arrives almost simultaneously everywhere on Earth’s surface and the excitation of unusual spheroidal modes with a characteristic frequency-spacing. The seismic energy deposited by a 10^{15} g PBH is comparable to a 4th magnitude earthquake but the time between collisions is very long (10^7 yr) even if the PBHs provide all of dark matter. Encounters with larger (Earth-threatening) PBHs are even rarer but the rate at which non-colliding close encounters could be detected by

seismic activity is two orders of magnitude larger. Another possibility is that LISA could detect PBHs in the mass range 10^{14} – 10^{20} g by measuring the gravitational impulse induced by any nearby passing one [272, 273].

2. Neutron stars and white dwarfs

Roncadelli *et al.* [274] have suggested that halo PBHs could be captured and swallowed by stars in the Galactic disc. The stars would eventually be accreted by the holes, producing radiation and a population of subsolar black holes which could only be of primordial origin. Every disc star should contain such a black hole if the dark matter were in PBHs smaller than 3×10^{26} g and the following analytic argument [101] gives the form of the constraint. Since the time-scale on which a star captures a PBH scales as $\tau_{\text{cap}} \propto M f(M)^{-1}$, requiring this to exceed the age of the Galactic disc implies

$$f < (M/3 \times 10^{26} \text{ g}), \quad (71)$$

which corresponds to a *lower* limit on the mass of objects providing the dark matter. A similar analysis of the collisions of PBHs with main-sequence stars, red-giant cores, white dwarfs and neutron stars by Abramowicz *et al.* [275] suggests that collisions are too rare for $M > 10^{20}$ g. However, in a related argument, Capela *et al.* have constrained PBHs as dark matter candidates by considering their capture by white dwarfs [276] and neutron stars [213]. The survival of these objects implies a limit which can be approximated as

$$f(M) < \frac{M}{4.7 \times 10^{24} \text{ g}} \left(1 - \exp \left[-\frac{M}{2.9 \times 10^{23} \text{ g}} \right] \right)^{-1} \quad (2.5 \times 10^{18} \text{ g} < M < 10^{25} \text{ g}). \quad (72)$$

This is similar to Eq. (71) at the high-mass end and the flattening at intermediate masses can be understood from Eq. (68). There is also a lower cut-off at 2×10^{18} g because PBHs lighter than this will not have time to consume the neutron stars during the age of the Universe. This argument assumes that there is dark matter at the centers of globular clusters and is sensitive to the dark matter density there (taken to be 10^4 GeV cm^{-3}). Pani and Loeb [277] have argued that this excludes PBHs from providing the dark matter throughout the sublunar window. However, all these limits have been disputed [278, 279] because the dark matter density is limited to much lower values than assumed above for particular globular clusters [280, 281].

Graham *et al.* [282] argue that PBHs can trigger white dwarf (WD) explosions. Their transit through a WD causes localized heating through dynamical friction and this can initiate runaway thermonuclear fusion, causing the WD to explode as a supernova. The shape of the observed WD distribution rules out PBHs with masses 10^{19} – 10^{20} g providing the local dark matter. Those as large as 10^{24} g will be excluded if recent observations of a WD population near the galactic center are confirmed. Those in the range 10^{20} – 10^{22} g are also constrained by the observed supernova rate. These bounds can be further strengthened through measurements of WD binaries in gravitational wave observatories. This raises the intriguing possibility that a class of supernova may be triggered through rare events induced by dark matter rather than the conventional mechanism of accreting white dwarfs that explode upon reaching the Chandrasekhar mass. However, Montero-Camacho *et al.* argue that this argument is inapplicable [283].

Fuller *et al.* [284] show that some or all of the inventory of r-process nucleosynthesis can be produced in interactions of PBHs with neutron stars if those with masses 10^{-14} – $10^{-8} M_{\odot}$ make up a few percent or more of the dark matter. A PBH captured by a NS sinks to the center and consumes it from the inside. When this occurs in a rotating millisecond NS, the resulting spin-up ejects ~ 0.1 – $0.5 M_{\odot}$ of relatively cold neutron-rich material. This can also produce a kilonova-type afterglow and a fast radio burst but not significant gravitational radiation or neutrinos, allowing such events to be differentiated from compact object mergers detectable by gravitational wave observatories. The PBH-NS destruction scenario is consistent with pulsar and NS statistics, the dark matter content and spatial distributions in the Galaxy and Ultra Faint Dwarfs (UFD), as well as with the r-process content and evolution histories in these sites. Ejected matter is heated by beta decay, which leads to emission of positrons in an amount consistent with the observed 511 keV line from the Galactic Center.

Abramowicz and Bejger [285] argue that collisions of neutron stars with PBHs of 10^{23} g may explain the phenomenology of fast radio bursts (FRB), in particular their millisecond durations and large luminosities. Contrary to the usual explanation for FRBs, no large magnetic fields are needed in their model.

3. Wide binaries

Binary star systems with wide separation are vulnerable to disruption from encounters with PBHs or any other type of MACHO [286, 287]. Observations of wide binaries in the Galaxy therefore constrain the abundance of halo PBHs.

By comparing the result of simulations with observations, Yoo *et al.* [288] ruled out MACHOs with $M > 43 M_\odot$ from providing most of the halo mass. However, Quinn *et al.* [289] later performed a more careful analysis of the radial velocities of these binaries and found that one of the widest-separation ones is spurious. The resulting constraint became

$$f(M) < \begin{cases} (M/500 M_\odot)^{-1} & (500 M_\odot < M \lesssim 10^3 M_\odot), \\ 0.4 & (10^3 M_\odot \lesssim M < 10^8 M_\odot). \end{cases} \quad (73)$$

It flattens off above $10^3 M_\odot$ because the encounters are non-impulsive there. Although not shown in Fig. 10, more recent studies by Monroy-Rodriguez and Allen reduced the lower mass limit from $500 M_\odot$ to $21\text{--}78 M_\odot$ or even $7\text{--}12 M_\odot$ [290]. The narrow window between the microlensing lower bound and the wide-binary upper bound is therefore shrinking and may even have been eliminated altogether.

4. Disruption of globular clusters and dwarf galaxies

An argument similar to the binary disruption one shows that the survival of globular clusters against tidal disruption by passing PBHs gives a limit (not shown in Fig. 10)

$$f(M) < \begin{cases} (M/3 \times 10^4 M_\odot)^{-1} & (3 \times 10^4 M_\odot < M < 10^6 M_\odot), \\ 0.03 & (10^6 M_\odot < M < 10^{11} M_\odot), \end{cases} \quad (74)$$

although this depends sensitively on the mass and the radius of the cluster. The limit flattens off above $10^6 M_\odot$ because the encounter becomes non-impulsive (cf. the binary case). The upper limit of $3 \times 10^4 M_\odot$ on the mass of objects dominating the halo is consistent with the numerical calculations of Moore [291].

In a related limit, Brandt [292] claims that a mass above $5 M_\odot$ is excluded by the fact that a star cluster near the centre of the dwarf galaxy Eridanus II has not been disrupted by halo objects. His constraint can be written as

$$f(M) \lesssim \begin{cases} (M/3.7 M_\odot)^{-1}/[1.1 - 0.1 \ln(M/M_\odot)] & (M < 10^3 M_\odot), \\ (M/10^6 M_\odot) & (M > 10^3 M_\odot), \end{cases} \quad (75)$$

where the density and velocity dispersion of the dark matter at the centre of the galaxy are taken to be $0.1 M_\odot \text{pc}^{-3}$ and 5 km s^{-1} , respectively, and the age of the star cluster is taken to be 3 Gyr. The second expression in Eq. (75) was not included in Ref. [292] but corresponds to having one black hole for the dwarf galaxy.

Koushiappas and Loeb [293] have studied the effects of black holes on the dynamical evolution of stars in dwarf galaxies. They find that mass segregation leads to a depletion of stars in the center of such galaxies and the appearance of a ring in the projected stellar surface density profile. Using Segue 1 as an example they show that current observations of the projected surface stellar density rule out at the 99.9% confidence level more than 4% of the dark matter being PBHs of few tens of solar masses.

Zhu *et al.* [294] have explored this scenario in more detail, using a combination of dynamical simulations and Bayesian inference methods. The joint evolution of stars and PBH dark matter is followed with a Fokker–Planck code for different dark matter parameters. They then use a Markov chain Monte Carlo approach to constrain the PBH properties with observations of ultra-faint galaxies. They find that two-body relaxation between the stars and PBHs drives up the stellar core size and increases the central stellar velocity dispersion. Using the observed half-light radius and velocity dispersion of stars in the compact ultra-faint dwarf galaxies as joint constraints, they infer that these dwarfs may have a cored dark matter halo with the central density in the range of $1\text{--}2 M_\odot \text{pc}^{-3}$, and that the PBHs may have a mass range of $2\text{--}14 M_\odot$ if they constitute all or a substantial fraction of the dark matter.

Boldrini *et al.* [295] use an N-body code to show that PBH dark matter can induce a cusp-to-core transition in low-mass dwarf galaxies via dynamical friction by dark matter particles at $1 M_\odot$ mass resolution acting on PBHs in the mass range $25\text{--}100 M_\odot$. This requires a lower limit $f < 0.01$ on the total dwarf galaxy dark matter content. The transition time-scale is between 1 and 8 Gyr and depends on M , $f(M)$ and the radius of the initial density profile of the PBH distribution.

Stegmann *et al.* [296] have improved these limits by considering the largest observational sample of UFDGs and by allowing the PBHs to have a lognormal mass distribution. The analysis of the half-light radii and velocity dispersions resulting from their simulations leads to three findings excluding PBHs with $\mathcal{O}(1\text{--}100) M_\odot$ from constituting all of the DM: (i) a critical sub-sample of UFDGs only allows $\mathcal{O}(1) M_\odot$ PBHs; (ii) for any PBH mass, there is an UFDG in their sample that disfavors it; (iii) for a majority of UFDGs, dynamical heating by PBHs would be too efficient to match the observed stellar half-light radii.

5. Disc heating

Other dynamical limits come into play at higher mass scales. Halo objects will overheat the stars in the Galactic disc unless one has [261]

$$f(M) < \begin{cases} (M/3 \times 10^6 M_\odot)^{-1} & (M < 3 \times 10^9 M_\odot), \\ (M/M_{\text{halo}}) & (M > 3 \times 10^9 M_\odot), \end{cases} \quad (76)$$

where the lower expression is the incredulity limit. The upper limit of $3 \times 10^6 M_\odot$ agrees with the more precise calculations by Lacey and Ostriker [262], although they argued that black holes with $2 \times 10^6 M_\odot$ could *explain* some features of disc heating. Constraint (76) bottoms out at $M \sim 3 \times 10^9 M_\odot$ with a value $f \sim 10^{-3}$. Evidence for a similar effect may come from the claim of Totani [263] that elliptical galaxies are puffed up by dark halo objects of $10^5 M_\odot$, although this limit is not shown in Fig. 10.

6. Tidal streams

Tidal streams in the Milky Way are sensitive probes of the population of low-mass dark-matter subhalos predicted by CDM simulations. This was originally considered for subhalos in the form of thermal relics [297] but the argument can also be applied to constrain massive PBHs. Bovy *et al.* [298] have developed a method for calculating the perturbed distribution function of a stream segment, computing the perturbed stream density for subhalo distributions down to $10^5 M_\odot$. They apply this to formalism to data for the Pal 5 stream and make a rigorous determination for 10 dark-matter subhalos with masses in the range $10^{6.5-10^9} M_\odot$ within 20 kpc of the Galactic center. If one applies this argument to PBHs, their limit corresponds to $f(r < 20 \text{ kpc}) < 0.002$, assuming that the Pal 5 stream is 5 Gyr old.

7. Dynamical friction effect on halo objects

Another limit in this mass range arises because halo objects will be dragged into the nucleus of our own Galaxy by the dynamical friction of the spheroid stars and halo objects themselves (if they have an extended mass function), this leading to excessive nuclear mass unless [261]

$$f(M) < \begin{cases} (M/2 \times 10^4 M_\odot)^{-10/7} (r_c/2 \text{ kpc})^2 & (M < 5 \times 10^5 M_\odot), \\ (M/4 \times 10^4 M_\odot)^{-2} (r_c/2 \text{ kpc})^2 & (5 \times 10^5 M_\odot \ll M < 2 \times 10^6 (r_c/2 \text{ kpc}) M_\odot), \\ (M/0.1 M_\odot)^{-1/2} & (2 \times 10^6 (r_c/2 \text{ kpc}) M_\odot < M < 10^7 M_\odot), \\ (M/M_{\text{halo}}) & (M > 10^7 M_\odot). \end{cases} \quad (77)$$

The last expression is the incredulity limit and first three correspond to the drag being dominated by spheroid stars (low M), halo objects (high M) and some combination of the two (intermediate M). This limit is sensitive to the halo core radius r_c . The limit bottoms out at $M \sim 10^7 M_\odot$ with a value $f \sim 10^{-5}$. Also there is a caveat here in that holes drifting into the nucleus might be ejected by the slingshot mechanism if there is already a binary black hole there [299]. This possibility was explored by Xu and Ostriker [300], who obtained an upper limit of $3 \times 10^6 M_\odot$.

8. Disruption and tidal distortion of galaxies in clusters

A similar argument to that used for globular clusters shows that the survival of galaxies in clusters against tidal disruption by giant cluster PBHs gives a limit

$$f(M) < \begin{cases} (M/7 \times 10^9 M_\odot)^{-1} & (7 \times 10^9 M_\odot < M < 10^{11} M_\odot), \\ 0.05 & (10^{11} M_\odot < M < 10^{13} M_\odot), \end{cases} \quad (78)$$

although this depends sensitively on the mass and the radius of the cluster. Note that Van den Bergh [301] concluded from the lack of observed tidal distortions of galaxies that the missing mass could not be in the form of compact object in the mass range $10^{10-10^{13}} M_\odot$. Carr and Hawking [23] claimed that the upper limit could be removed because the lower number of high mass objects would be balanced by their inducing tidal distortions in a larger volume of space but the incredulity limit still applies.

9. Intergalactic PBHs

If there were a population of huge intergalactic PBHs with density parameter $\Omega_D(M)$, each galaxy would have a peculiar velocity due to its gravitational interaction with the nearest one [302]. If the objects were smoothly distributed, the typical distance between them would be

$$d \approx 30 \Omega_D(M)^{-1/3} (M/10^{16} M_\odot)^{1/3} h^{-2/3} \text{Mpc}. \quad (79)$$

This would also be the expected distance of the nearest black hole to the Milky Way. Over the age of the universe, this should induce a peculiar velocity

$$V_{\text{pec}} \approx G M f(\Omega_0) t_0/d^2, \quad (80)$$

where $\Omega_0 \approx 0.3$ is the total density parameter and $f(\Omega_0) \approx \Omega_0^{0.6}$. Since the CMB dipole anisotropy shows that the peculiar velocity of our Galaxy is only 400 km s^{-1} , one infers

$$\Omega_D < (M/5 \times 10^{15} M_\odot)^{-1/2} (t_0/10^{10} \text{yr})^{-3/2} \Omega_0^{-0.9} h^{-2} \quad (81)$$

and this is shown in Figs. 10 and 13. This scenario is interesting only if there is at least one such object within the observable universe and this corresponds to the lower limit

$$\Omega_D(M) > 3 \times 10^{-8} (M/10^{16} M_\odot) (t_0/10^{10} \text{yr})^{-3} h^{-2}, \quad (82)$$

where we have taken the horizon scale to be $d \approx 3ct_0 \approx 10h^{-1} \text{Gpc}$. This intersects Eq. (81) at $M = 8 \times 10^{20} (t_0/10^{10} \text{yr}) M_\odot$, so this corresponds to the largest possible intergalactic dark object within the visible universe.

D. Cosmic Structure Constraints

PBHs larger than $10^2 M_\odot$ cannot provide dark matter but Carr and Silk [303] point out that such PBHs could generate cosmic structures through the ‘seed’ or ‘Poisson’ effect even if f is small. The seed effect was first pointed out by Hoyle and Narlikar [304] and subsequently studied in Refs. [268, 305]. The Poisson effect was first pointed out by Mészáros [306] and subsequently studied in Refs. [307–309]. This raises the issue of the maximum mass of a PBH and whether 10^6 – $10^{10} M_\odot$ black holes in galactic nuclei could be primordial. It is sometimes argued that BBN implies that PBHs can only form before 1 s, corresponding to a limit $M < 10^5 M_\odot$. However, the fraction of universe in PBHs at that time is only $10^{-6} (t/\text{s})^{1/2}$, so the effect on BBN should be tiny. As discussed later, the most important constraint in this mass range comes from the limit on the CMB μ distortion.

If a region of mass \mathcal{M} contains PBHs of mass M , the initial fluctuation is

$$\delta_i \approx \begin{cases} M/\mathcal{M} & (\text{seed}) \\ (f M/\mathcal{M})^{1/2} & (\text{Poisson}). \end{cases} \quad (83)$$

If $f = 1$, the Poisson effect dominates for all \mathcal{M} ; if $f \ll 1$, the seed effect dominates for $\mathcal{M} < M/f$. In either case, the fluctuation grows as z^{-1} from the redshift of CDM domination ($z_{\text{eq}} \approx 4000$), so the mass binding at redshift z_B is

$$\mathcal{M} \approx \begin{cases} 4000 M z_B^{-1} & (\text{seed}) \\ 10^7 f M z_B^{-2} & (\text{Poisson}). \end{cases} \quad (84)$$

If PBHs provide the dark matter ($f = 1$), the above dynamical limits require $M < 10^3 M_\odot$ and so the Poisson effect could only bind a scale $\mathcal{M} < 10^{11} z_B^{-2} M_\odot$, which is necessarily subgalactic. This assumes the PBHs have a monochromatic mass function. If it is extended, the situation is more complicated [303] because the mass of the effective seed for a region may depend on the mass of that region \mathcal{M} .

Even if PBHs do not play a role in generating cosmic structures, one can still place interesting upper limits on the fraction of dark matter in them by requiring that various types of structure do not form too early. Carr and Silk find the constraints associated with the first bound clouds, dwarf galaxies, Milky-Way-type galaxies and clusters of galaxies, these being shown in Fig. 14 and discussed below. There is also a Poisson constraint associated with observations of the Lyman- α forest, which we discuss first since it was misrepresented on our earlier work.

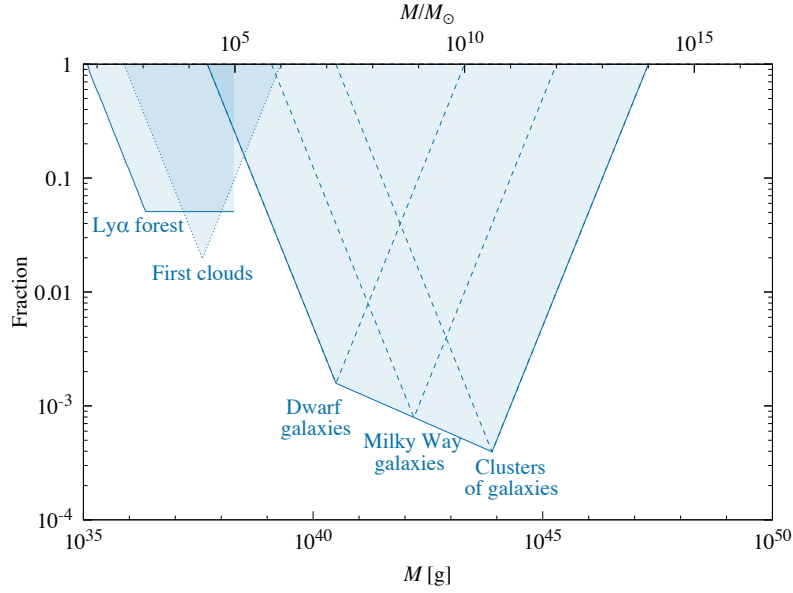


FIG. 14. Large-scale structure constraints from Refs. [303] and [310].

1. Lyman- α systems

Afshordi *et al.* [13] used observations of the Lyman- α forest to obtain an upper limit of about $10^4 M_\odot$ on the mass of PBHs which provide the dark matter. CKSY extended this result to the case in which the PBHs provide a fraction $f(M)$ of the dark matter and the Lyman- α forest is associated with a single mass $M_{\text{Ly}\alpha} \sim 10^{10} M_\odot$. Since the Poisson fluctuation in the number of PBHs on this mass scale grows between $z_{\text{eq}} \approx 4000$ and the redshift up to which the Lyman- α forest is observed ($z_{\text{Ly}\alpha} \approx 4$), corresponding to a growth factor of $z_{\text{eq}}/z_{\text{Ly}\alpha} \approx 10^3$, CKSY claim that the forest will form earlier than observed unless $f(M) < (M/10^4 M_\odot)^{-1}$. However, there was some confusion here because the Afshordi *et al.* limit is independent of the nature of the Lyman- α objects themselves; it just uses their power spectrum as a tracer of the density fluctuations. Furthermore most Lyman- α clouds are much smaller than $10^{10} M_\odot$. So the CKSY limit just corresponds to the requirement that $10^{10} M_\odot$ objects (i.e. dwarf galaxies) must not bind too early, as discussed below.

Murgia *et al.* [310] have recently improved the Lyman- α limit, using a grid of hydrodynamic simulations to explore different values of astrophysical parameters. They obtain a marginalized (2σ) upper limit of the form $f(M) < (M/60 M_\odot)^{-1}$, when a Gaussian prior on the reionization redshift is imposed, and this limit is shown in Fig. 14. The bound weakens to $f(M) < (M/170 M_\odot)^{-1}$ when a conservative flat prior is assumed. Both limits are significantly stronger than the original Afshordi *et al.* one and are included in Fig. 14. They also analyse non-monochromatic PBH mass distributions, ruling out large regions of the parameter space for extended mass functions.

2. Galaxies and clusters of galaxies

Galaxies clearly span a range of masses and form over a range of redshifts. However, if we apply the above argument to Milky-Way-type galaxies, assuming these have a typical mass of $10^{12} M_\odot$ and must not bind before a redshift $z_B \sim 3$, we obtain

$$f(M) < \begin{cases} (M/10^6 M_\odot)^{-1} & (10^6 M_\odot < M \lesssim 10^9 M_\odot) \\ M/10^{12} M_\odot & (10^9 M_\odot \lesssim M < 10^{12} M_\odot) \end{cases} \quad (85)$$

This limit is shown in Fig. 14 and bottoms out at $M \sim 10^9 M_\odot$ with a value $f \sim 0.001$. The first expression can be obtained by putting $\mathcal{M} \sim 10^{12} M_\odot$ and $z_B \sim 3$ in Eq. (84). The second expression corresponds to having just one PBH per galaxy (the incredulity limit) and is also the line above which the seed effect dominates the Poisson effect ($f < M/\mathcal{M}$). Indeed, since the initial seed fluctuation is M/\mathcal{M} , the seed mass required for a Milky-Way-type

galaxy to bind at $z \approx 3$ is immediately seen to be $10^9 M_\odot$. There is no constraint on PBHs below this line because the fraction of the Universe going into galaxies would be small, with most of the baryons presumably going into the intergalactic medium. Therefore the seed effect does not modify the form of the limit shown in Fig. 14.

If we apply the same argument to dwarf galaxies, assuming these have a mass of $10^{10} M_\odot$ and must not bind before $z_B \sim 10$, we obtain

$$f(M) < \begin{cases} (M/10^5 M_\odot)^{-1} & (10^5 M_\odot < M \lesssim 10^7 M_\odot) \\ M/10^{10} M_\odot & (10^7 M_\odot \lesssim M < 10^{10} M_\odot), \end{cases} \quad (86)$$

this bottoming out at $M \sim 10^7 M_\odot$ with a value $f \sim 0.001$. On the other hand, if we apply the argument to clusters of galaxies, assuming these have a mass of $10^{14} M_\odot$ and must not bind before $z_B \sim 1$, we obtain

$$f(M) < \begin{cases} (M/10^7 M_\odot)^{-1} & (10^7 M_\odot < M \lesssim 3 \times 10^{10} M_\odot) \\ M/10^{14} M_\odot & (3 \times 10^{10} M_\odot \lesssim M < 10^{14} M_\odot), \end{cases} \quad (87)$$

this bottoming out at $M \sim 3 \times 10^{10} M_\odot$ with a value $f \sim 0.0003$. Clearly all these limits are very approximate and the division into different types of bound structure is simplistic. Nevertheless, the above analysis at least yields a set of qualitative constraints. In practice, one should combine all the limits shown in Fig. 14 to obtain the boundary indicated by the bold line.

3. First baryonic clouds

The first bound clouds would be expected to have a mass of $10^6 M_\odot$ in the CDM picture. We cannot apply the above argument to these directly because there is no observational constraint on their formation redshift. However, these clouds would form at $z_B \sim 100$ in the CDM picture, so we can still derive a limit corresponding to the requirement that the standard picture is not perturbed. In this case, Eq. (85) is replaced by

$$f(M) < \begin{cases} (M/10^3 M_\odot)^{-1} & (10^3 M_\odot < M \lesssim 10^4 M_\odot) \\ M/10^6 M_\odot & (10^4 M_\odot \lesssim M < 10^6 M_\odot), \end{cases} \quad (88)$$

this bottoming out at $M \sim 3 \times 10^4 M_\odot$ with a value $f \sim 0.03$. This constraint is shown in Fig. 14. Recently, Kashlinksy has been prompted by the LIGO/Virgo observations to consider the effects of the Poisson fluctuations induced by a dark-matter population of $30 M_\odot$ black holes [311]. This can be seen as a special case of the general analysis presented above. However, he adds an interesting new feature to the scenario by suggesting that the black holes might also lead to the cosmic infrared background (CIB) fluctuations detected by the *Spitzer/Akari* satellites [312, 313]. This is because the associated Poisson fluctuations would allow more abundant early collapsed halos than in the standard scenario. It has long been appreciated that the CIB and its fluctuations would be a crucial test of any scenario in which the dark matter comprises the black-hole remnants of Population III stars [314], but in this case the PBHs are merely triggering high-redshift star formation and not generating the CIB directly.

A similar effect can allow clusters of large PBHs to evolve into the supermassive black holes thought to reside in galactic nuclei [305, 315, 316]; if one replaces $M_{\text{Ly}\alpha}$ with $10^8 M_\odot$ and $z_{\text{Ly}\alpha}$ with 10 in the above analysis, one reduces the limiting mass in Eq. (85) to $600 M_\odot$. This naturally explains the observed $M_{\text{SMBH}}/M_{\text{bulge}}$ relation and the mass function of galaxies. We do not attempt to derive constraints on the PBH scenario from the CIB observations, since many other astrophysical parameters are involved.

4. Clusters of PBHs

Clesse and García-Bellido stress that PBHs could be spatially clustered into sub-haloes if they are part of a larger-scale overdense region [214]. Indeed, this idea goes back to the early work of Dokuchaev *et al.* [85] and Chisholm [267]. They infer that the lensing constraints in the mass range required to explain the LIGO/Virgo detections can be relaxed and this also has important implications for the efficacy of PBH merging in the early Universe. However, this argument depends on details of small-scale structure formation which are not fully understood. For example, Bringmann *et al.* [317] claim that the PBH constraints become even stronger if there is large initial clustering.

Ali-Haïmoud [318] has studied the initial clustering of PBHs formed from the gravitational collapse of large density fluctuations and does not find small-scale clustering beyond that expected from Poisson effects. He also derives an

analytic expression for the two-point correlation function of large-threshold fluctuations, generalizing previous results to arbitrary separation. While Poisson shot noise tends to dominate in a radiation-dominated era, strong clustering is not realized [319]. Desjacques and Riotto [320] have also discussed the issue of PBH spatial clustering and its impact on the large-scale power spectrum. Even if a Poissonian self-pair term is always present in the zero-lag correlation, this does not necessarily imply that PBHs are Poisson distributed. While the initial PBH clustering depends on the detailed shape of the small-scale power spectrum, this is not relevant for the PBH masses still allowed by observations.

Young and Byrnes [321] consider the impact of local non-Gaussianity on the initial PBH clustering and mass function due to mode coupling between long and short wavelength modes. They show that even a small amount of non-Gaussianity results in a significant enhancement of clustering and merging, shifting the mass function to higher masses. However, as the clustering becomes strong, the local PBH number density becomes large, leading to a large theoretical uncertainty in the merger rate. Suyama and Yokoyama [322] have also studied this problem, using a functional integration approach. They find that PBH clustering on super-Hubble scales can never be induced if the initial primordial fluctuations are Gaussian but that it could be enhanced by the local-type trispectrum of the primordial curvature perturbations. Matsubara *et al.* have considered the clustering of PBHs if they form in an early matter-dominated epoch from non-Gaussian fluctuations [323]. Clustering is less significant in this case but can still be much larger than Poisson shot noise.

E. Accretion and μ -distortion constraints

There are a large number of constraints associated with the accretion of PBHs and these are summarised in Fig. 15. However, it should be stressed that these limits depend on a large number of astrophysical parameters and qualitative features such as whether one has disc or spherical accretion. Also most studies assume Bondi accretion, even though there is little evidence for this. Therefore these limits may be less secure than the dynamical ones.

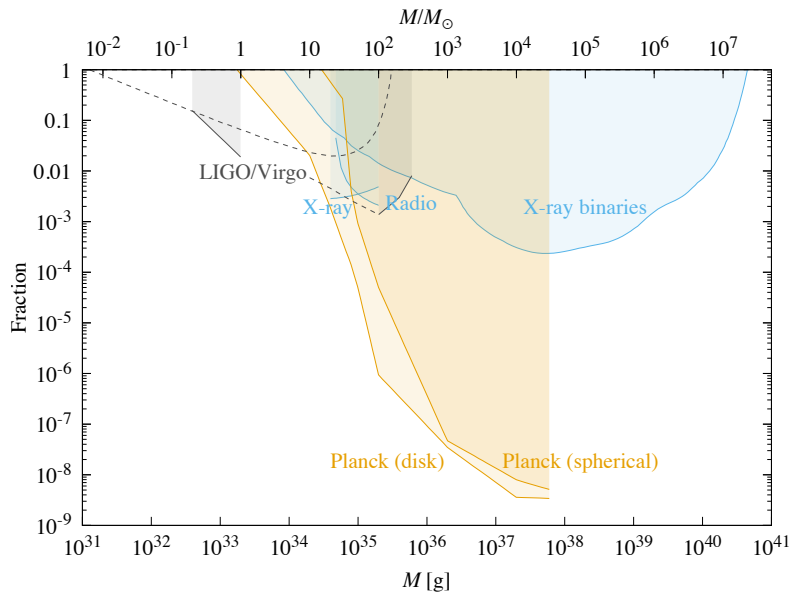


FIG. 15. Accretion (cyan and yellow) and gravitational wave (grey) constraints from LIGO [324–326] (broken if potential).

1. Accretion during radiation-dominated era

There are good reasons for believing that PBHs cannot grow very much during the radiation-dominated era. Although a simple Bondi-type argument suggests that they could grow as fast as the horizon [1], this does not account for the background cosmological expansion and a fully relativistic calculation shows that such self-similar growth is impossible [23, 327, 328]. Consequently there is very little growth during the radiation era. The only exception might be if the Universe were dominated by a “dark energy” fluid with $p < -\rho/3$, as in the quintessence

scenario, since self-similar black-hole solutions do exist in this situation [329–331]. This may support the claim of Bean and Magueijo [12] that intermediate-mass PBHs might accrete quintessence efficiently enough to evolve into the supermassive black holes (SMBHs) in galactic nuclei.

2. Limit from ionisation and thermal history

Even if PBHs cannot accrete appreciably in the radiation-dominated era, they might still do so in the period after decoupling and the Bondi-type analysis *should* then apply. The associated accretion and emission of radiation could have a profound effect on the thermal history of the Universe, as first analysed by Carr [332]. This possibility was investigated in more detail by Ricotti *et al.* [14], who studied the effects of such accreting PBHs on the ionisation and temperature evolution of the Universe. The emitted X-rays would produce measurable anisotropies and spectral distortions in the CMB. Using WMAP data to constrain the first, they obtained the limit

$$f(M) < \begin{cases} (M/30 M_\odot)^{-2} & (30 M_\odot < M \lesssim 10^4 M_\odot), \\ 10^{-5} & (10^4 M_\odot \lesssim M < 10^{11} M_\odot), \\ M/M_{\ell=100} & (M > 10^{11} M_\odot), \end{cases} \quad (89)$$

where the last expression is not included in Ref. [14] but corresponds to having one PBH on the scale associated with the CMB anisotropies; for $\ell = 100$ modes, this is $M_{\ell=100} \approx 10^{16} M_\odot$. Using FIRAS data to constrain the second, they obtained the limit

$$f(M) < \begin{cases} (M/1 M_\odot)^{-2} & (1 M_\odot < M \lesssim 10^3 M_\odot), \\ 0.015 & (10^3 M_\odot \lesssim M < 10^{14} M_\odot), \\ M/M_{\ell=100} & (M > 10^{14} M_\odot). \end{cases} \quad (90)$$

Although this appears to exclude $f = 1$ down to masses as low as $1 M_\odot$, this limit is very model-dependent and also depends on the duty-cycle parameter.

Recently this problem has been reconsidered by three groups, who argue that the limits are weaker than indicated in Ref. [14]. Ali-Haïmoud and Kamionkowski [333] calculate the accretion on the assumption that it is suppressed by Compton drag and Compton cooling from CMB photons, allowing for the PBH velocity relative to the background gas. They find the spectral distortions are too small to be detected, while the anisotropy constraints have a similar form to Eq. (89) but only exclude $f = 1$ above $10^2 M_\odot$. Horowitz [334] performs a similar analysis and gets an upper limit of $30 M_\odot$. However, neither of these analyses includes the super-Eddington flattening above some mass. Aloni *et al.* [335] also calculate the effect of PBH accretion on the ionization history but do not give explicit constraints on the dark matter fraction. Although all these analyses exclude PBHs comprising the dark matter above some critical mass, they do not exclude the small fraction required to seed galaxies. The fraction of the mass in SMBHs in galactic nuclei today is $\Omega_{\text{smbh}}/\Omega_{\text{dm}} \sim 2 \times 10^{-5}$, whereas limit (89) bottoms out at $f(M) < 10^{-5}$.

Chen *et al.* [336] use Planck data to constrain the PBH dark matter contribution in two different reionization models and improve the upper limit (89) on the abundance of PBHs from WMAP by two orders of magnitude. Their new limits imply that the event rates of mergers of PBH binaries ($\text{Gpc}^{-3} \text{yr}^{-1}$) are less than 0.002 for $M = 30 M_\odot$, 5 for $M = 2 M_\odot$ and 2000 for $M = 30 M_\odot$ at 95% confidence level. They infer that GW150914 is very unlikely to have been produced by the merger of a PBH binary.

Poulin *et al.* [337] argue that the spherical accretion approximation breaks down and that an accretion disk should form. Even under conservative accretion assumptions, their constraints exclude a monochromatic distribution of PBHs with masses above $2 M_\odot$ as the dominant form of DM. The bound on the median PBH mass gets more stringent if a broad (lognormal) mass function is considered. In addition, Serpico *et al.* [338] study disk and/or spherical accretion onto a PBH plus halo system, this being strongly constrained by the latest observations of CMB polarization [167, 211].

Gaggero *et al.* [339] model the accretion of gas onto a population of massive PBHs in the Milky Way and compare the predicted radio and X-ray emission with observational data. With conservative assumptions about the accretion process, they use the VLA radio catalog at 1.4 GHz and the Chandra X-ray catalog to exclude $O(10) M_\odot$ PBHs from providing all of the dark matter at the 5σ level. They argue that more sensitive future radio and X-ray surveys could identify a PBH population using this method. Similar arguments have been made by Mansharnden *et al.* [340].

PBH interactions with the interstellar medium should result in significant X-ray flux, thereby contributing to the observed number density of compact X-ray objects in galaxies. For example, Mack *et al.* [212] and Kawaguchi *et al.* [341] considered the growth of large PBHs through the capture of dark-matter halos and suggested that their accretion could give rise to ultra-luminous X-ray sources. More recently, Inoue and Kusenko [342] use existing X-ray

data to constrain the PBH number density in the mass range from a few to $2 \times 10^7 M_\odot$, although the density needed to account for the black holes detected by LIGO/Virgo is marginally allowed. Their limit is shown in Fig. 15.

Ewall-Wice *et al.* [343] estimate the 21 cm radio background from accretion onto the first IMBHs between $z = 30$ and $z = 16$. Combining plausible scenarios for black hole formation and growth with empirical correlations between luminosity and radio emission observed in low-redshift active galactic nuclei, they find that Pop III black hole remnants are able to produce a 21 cm background. In particular, this could explain the surprisingly large amplitude of the 21 cm absorption feature recently reported by the EDGES collaboration. These black holes also produce significant X-ray emission and contribute to the 0.5–2 keV soft X-ray background at a level consistent with existing constraints. The same black holes will overproduce radiation in the optical band unless they are either heavily obscured or their radioloud fraction is higher than in the local universe. Hektor *et al.* [344] have also used the EDGES results to place bounds on the energy injection from the accretion of $O(1 - 100) M_\odot$ PBHs. By requiring that the temperature of the gas at $z \sim 17$ does not exceed the EDGES value, they infer $f < 1 - 10^{-2}$ for $O(10) M_\odot$ PBHs.

Mena *et al.* [345] demonstrate that observations of the 21 cm transition in neutral hydrogen during the epoch of reionization will provide stringent constraints on solar mass PBHs. There are three distinct effects: (i) the modification to the primordial power spectrum (and thus the halo mass function) induced by Poisson noise, (ii) a uniform heating and ionization of the intergalactic medium via X-rays produced during accretion, and (iii) a local modification to the temperature and density of the ambient medium surrounding isolated PBHs. Using a 4-parameter astrophysical model, they show that experiments like SKA and HERA could potentially improve upon existing constraints by more than an order of magnitude.

Eroshenko [346] shows that the accumulation of dark matter particles near the PBHs immediately after their formation in the radiation era should give rise to density spikes. This would generate bright γ -ray sources due to the annihilation of dark-matter particles in orbit around the PBHs. Comparison of the calculated signal from particle annihilation with the Fermi-LAT data [347] constrains Ω_{PBH} for $M > 10^{-8} M_\odot$ to values between 1 and 10^{-8} . These constraints are several orders of magnitude more stringent than other ones but they are not included in Fig. 15 since they depend on the assumption that the dark matter is dominated by WIMPs. Nakama *et al.* [348] also point out that compact minihalos of the dark matter are likely to form abundantly in the early Universe, with their formation redshift and abundance depending on the primordial non-Gaussianity, and these may be detected via future pulsar observations. Bertone *et al.* [349] show that the successful detection of one or more PBHs by radio searches with the SKA and gravitational waves with LIGO/Virgo and the Einstein Telescope would set extraordinarily stringent constraints on virtually all weak-scale extensions of the Standard Model with stable relics, including those predicting a WIMP abundance much smaller than that of DM.

Abe *et al.* [350] have investigated the Sunyaev–Zel’dovich (SZ) effect on the CMB caused by the emission of UV and X-ray photons by accreting PBHs. These photons can ionize and heat the intergalactic medium (IGM) around the PBH. They compute the profiles for the ionization fraction and temperature around each PBH and then evaluate the Compton y -parameter created by the IGM gas. They find the SZ temperature anisotropy has a flat angular power spectrum up to the scale of the ionized region ($l \leq 2000$) and could dominate the primordial temperature spectrum below the Silk scale.

3. μ distortion

If PBHs form from the high- σ tail of Gaussian density fluctuations, as in the simplest scenario [24], then another interesting limit comes from the dissipation of those density fluctuations by Silk damping at a much later time. This merely decreases the baryon-to-photon ratio for $t < 7 \times 10^6$ s, leading to a weak BBN limit. However, it leads to a μ distortion in the CMB spectrum [351] for $7 \times 10^6 \text{ s} < t < 3 \times 10^9 \text{ s}$, leading to an upper limit $\delta(M) < \sqrt{\mu} \sim 10^{-2}$ over the mass range $10^3 < M/M_\odot < 10^{12}$. This limit was first given in Ref. [352], based on a result in Ref. [353], but the limit on μ is now much stronger. There is also a y distortion for $3 \times 10^9 \text{ s} < t < 3 \times 10^{12} \text{ s}$ (the time of decoupling). In principle, observational limits on the μ distortions can be translated into upper limits on the PBH abundance.

This argument gives a very strong constraint on $f(M)$ in the range $10^4 < M/M_\odot < 10^{12}$ [354]. However, the assumption that the fluctuations are Gaussian may be incorrect. For example, Nakama *et al.* [355] have proposed a “patch” model, in which the relationship between the background inhomogeneities and the overdensity in the tiny fraction of the volume which collapses to PBHs is modified. The μ distortion constraint could thus be much weaker. One therefore needs to consider the dependence of this limit on the possible non-Gaussianity of primordial fluctuations. A phenomenological description of such non-Gaussianity was introduced in Ref. [355] and involves a parameter p , such that – for a fixed PBH formation probability – the dispersion of the primordial fluctuations becomes smaller as p is reduced, thereby reducing the μ distortion.

Recently, Nakama *et al.* [356] have calculated the μ -distortion constraints on $f(M)$, using both the current FIRAS limit and the projected upper limit from PIXIE [357]. However, one must be careful in the interpretation of M here.

The diffusion mass is given by

$$M_D \sim \sqrt{M_\tau M_H} \sim \begin{cases} 10^{10} (t/t_{\text{eq}})^{7/4} M_\odot & (t < t_{\text{eq}}) \\ 10^{13} (t/t_{\text{dec}})^{11/6} M_\odot & (t_{\text{eq}} < t < t_{\text{dec}}), \end{cases} \quad (91)$$

where M_H is the horizon mass and M_τ is the mass of unit optical depth to Thomson scattering. The PBH also has the horizon mass at formation but – unlike the radiation mass – it is not subsequently reduced by redshift effects, so the PBH and diffusion masses on a given scale are related by

$$M \sim \begin{cases} 10^2 (M_D/M_\odot)^{6/7} M_\odot & (t < t_{\text{eq}}) \\ 10 (M_D/M_\odot)^{10/11} M_\odot & (t_{\text{eq}} < t < t_{\text{dec}}). \end{cases} \quad (92)$$

For a non-Gaussian probability distribution,

$$P(\zeta) = \frac{1}{2\sqrt{2}\tilde{\sigma}\Gamma(1+1/p)} \exp\left[-\left(\frac{|\zeta|}{\sqrt{2}\tilde{\sigma}}\right)^p\right], \quad (93)$$

which becomes Gaussian for $p = 2$, the collapse fraction is

$$\beta = \int_{\zeta_c}^{\infty} P(\zeta) d\zeta = \frac{\Gamma(1/p, 2^{-p/2}(\zeta_c/\tilde{\sigma})^p)}{2p\Gamma(1+1/p)}, \quad (94)$$

where ζ_c is the threshold for PBH formation and $\Gamma(a, z)$ is the incomplete gamma function. The μ distortion is

$$\mu \simeq 2.2\sigma^2 \left[\exp\left(-\frac{\hat{k}_*}{5400}\right) - \exp\left(-\left[\frac{\hat{k}_*}{31.6}\right]^2\right) \right], \quad (95)$$

where \hat{k}_* is the wave-number in units of Mpc^{-1} , this peaking at $k = 80 \text{ Mpc}^{-1}$ or $3 \times 10^9 M_\odot$. This is required to be less than 9×10^{-5} from FIRAS and 10^{-9} from HYPERPIXIE. Equations (94) and (95) and the relation

$$k \simeq 7.5 \times 10^5 \gamma^{1/2} \text{Mpc}^{-1} \left(\frac{g_*}{10.75}\right)^{-1/12} \left(\frac{M}{30 M_\odot}\right)^{-1/2}, \quad (96)$$

where the parameters γ and g_* are defined in Sec. IC, then lead to constraints on $\beta(M)$ and $f(M)$.

This limit is shown in Fig. 16, and this corresponds to which indicates that the PBH density is severely constrained in the range $10^5 M_\odot < M < 10^{11} M_\odot$, with the mass range around $10^9 M_\odot$ being most restricted. We need huge non-Gaussianity if such massive PBHs are to evade the μ distortion constraints. It would therefore be more plausible to invoke PBHs with initial masses below $10^5 M_\odot$ which undergo substantial accretion between the μ -distortion era and the time of matter-radiation equality. In particular, PBHs with $10^6 < M/M_\odot < 10^{10}$ and $f \sim 10^{-4}$, such as are required for quasars, require either $p < 0.5$ or an accretion factor of $(M/10^5 M_\odot)^{-1}$.

F. Gravitational Wave Constraints

In recent years interest in PBHs has intensified because of the detection of gravitational waves from coalescing black hole binaries by LIGO/Virgo [15–18] and the possibility that these might be of primordial origin. Even if this is not the case, the observations place important constraints on the number density of PBHs. Indeed, such constraints date back to well before the LIGO/Virgo observations. Although it is unclear whether the black holes associated with the LIGO events are of primordial or stellar origin, it is important to stress that the constraints are based on a clear detection rather than a null result.

1. Gravitational wave background

A population of massive PBHs would be expected to generate a gravitational wave background (GWB) [358]. This would be especially interesting if there were a population of binary black holes, coalescing at the present epoch due to gravitational-radiation losses. This was first discussed by Bond and Carr [359] in the context of Population III black

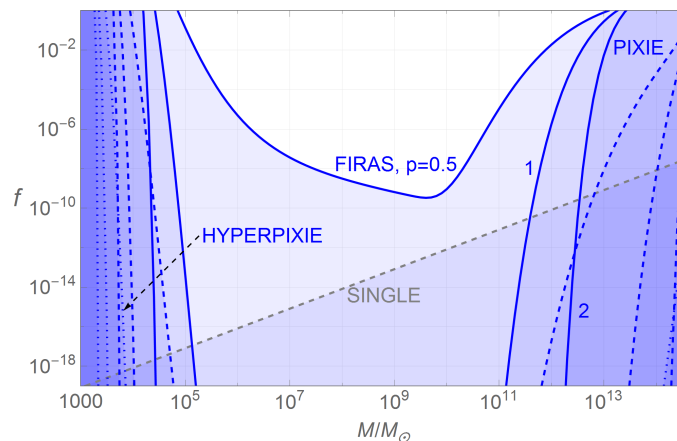


FIG. 16. μ constraints from Ref. [356].

holes and later in Refs. [360, 361] in the context of PBHs. However, the precise formation epoch of the holes is not crucial since the coalescence occurs much later. In either case, the black holes would be expected to cluster inside galactic halos (along with other forms of dark matter) and so the detection of the gravitational waves would provide a probe of the halo distribution [362]. Indeed, the LIGO data had already placed weak constraints on such scenarios over decade ago [363].

The non-observation of a gravitational wave background gives potential constraints on the fraction of dark matter in PBHs, which are stronger than any other current constraint in the PBH mass range $0.5\text{--}30 M_\odot$. Raidal *et al.* [324] show that the predicted GWB can be observed by the upcoming LIGO/Virgo runs, and non-observation would indicate that the observed events are not of primordial origin. These limits are shown in Fig. 15. Bartolo *et al.* [364] calculate the anisotropies and non-Gaussianity of a stochastic GWB deriving from both their formation time and propagation effects. They conclude that a large anisotropy and non-Gaussianity would imply that PBHs do not provide all the dark matter. The non-Gaussianity required to avoid μ limit would result in more mergers [321] and therefore increase the GRB (Shi, private communication).

Wang *et al.* [365] point out that some PBHs may accumulate at the center of a galaxy and follow a prograde or retrograde orbit due to the gravity of a central massive black hole. If the PBH mass is $\mathcal{O}(1) M_\odot$ or smaller, the incoherent superposition of all the extreme-mass-ratio inspirals in the Universe can generate a background of gravitational waves detectable by LISA.

2. PBHs and the LIGO/Virgo events

Using slightly different approaches, Refs. [366] and [214] derive merger rates for particular PBH populations and find them to be compatible with the range $9\text{--}240 \text{ Gpc}^{-3} \text{ yr}^{-1}$ obtained by the LIGO/Virgo analysis. However, according to Ref. [367], the PBH merger rates would be highly suppressed by tidal forces, in which case the LIGO/Virgo results would allow only a small fraction of the dark matter to be in PBHs. This conclusion is also drawn in Ref. [368], which points out that the lower limit on the merger rate may be in tension with the CMB spectral distortion constraints [14] for objects in the IMBH range. On the other hand, the accretion and merging of smaller PBHs after decoupling might still provide the observed events without violating the CMB constraints [214].

Raidal *et al.* [324] have studied the production of PBH binaries and the resulting merger rate, accounting for an extended PBH mass function and the possibility of a clustered spatial distribution. They show that it is possible to satisfy all present constraints on the PBH abundance for a lognormal mass function. In more recent work [369] they have studied how the abundance of $0.1\text{--}10^3 M_\odot$ PBHs can be tested by gravitational wave observations of the merger rate of PBH binaries formed in the early universe. They first derive very conservative analytical merger rates for a general mass function. They then study the formation and evolution of PBH binaries before recombination with N-body simulations and find that the analytical merger rate estimate fails when PBHs comprise all dark matter, as most initial binaries are disrupted by the surrounding PBHs. This is expected due to the formation of compact N-body systems at matter-radiation equality. However, if PBHs make up just 10% of the dark matter, the analytic estimates become more reliable. In that case, the constraint from the observed LIGO merger rate is strongest in the mass range $2\text{--}160 M_\odot$ and the present BH-BH merger rate is larger than $\mathcal{O}(10) \text{ Gpc}^{-3} \text{ yr}^{-1}$.

Ali-Haïmoud *et al.* [325] compute the probability distribution of orbital parameters for PBH binaries formed in the early Universe, accounting for tidal torquing by other PBHs and the halo field and dynamical friction by unbound standard DM particles. Their analytic estimates indicate that these effects are much weaker than previously calculated but possibly large enough to affect the eccentricity of typical PBH binaries. They also calculate the PBH-binary merger rate resulting from gravitational capture in present-day halos. If binaries formed in the early Universe survive until the present time, as suggested by their analytic estimates, they should dominate the total PBH merger rate. Moreover, the merger rate would be orders of magnitude larger than LIGO's current upper limits if PBHs make a significant fraction of the dark matter, implying $f(M) < 0.01$ for $10\text{--}300 M_\odot$ PBHs. These limits are shown in Fig. 15.

Advanced LIGO/Virgo searches for compact binary systems with component masses in the range $0.2\text{--}1.0 M_\odot$ find no viable gravitational wave candidates, which constrains monochromatic non-spinning PBHs in this range [370]. Neither black holes nor neutron stars are expected to form below $1 M_\odot$ through normal stellar evolution but they infer $f < 0.3$ for $M < 0.2 M_\odot$ and $f < 0.05$ for $M < 1 M_\odot$ for a particular PBH binary formation scenario. A similar search of data obtained during the second LIGO/Virgo run [326] found no viable candidates with a component in the range $0.2\text{--}1.0 M_\odot$. This constrained the binary merger rate of $0.2 M_\odot$ binaries to be less than $3.7 \times 10^5 \text{ Gpc}^{-3} \text{ yr}^{-1}$ and that of $1.0 M_\odot$ binaries to be less than $5.2 \times 10^3 \text{ Gpc}^{-3} \text{ yr}^{-1}$, corresponding to at most 16% or 2% of the dark matter, respectively. This is shown in Figs. 10 and 15. Future sensitivities for the merger rates of PBHs much smaller than $\mathcal{O}(1) M_\odot$ are studied in Refs. [326, 371].

Several authors have considered the PBH merger rate as a function of the binary mass ratio [19]. In particular, Gow *et al.* [372] consider both the current and design sensitivity of LIGO for five different PBH mass functions, showing that the empirical preference for nearly equal-mass binaries in current data can be consistent with a PBH hypothesis once observational selection effects are taken into account. Although current data allow some PBH mass distributions, future data may exclude the possibility that all BH mergers have a primordial origin.

Diego [373] has constrained PBHs of $5\text{--}50 M_\odot$ from the gravitational lensing of gravitational waves at the LIGO frequency. He finds that at the typical magnifications expected for observed GW events, the fraction of dark matter in PBHs can be constrained at the percent level. Similarly, if a small percentage of the dark matter is in the form of microlenses of $\mathcal{O}(10) M_\odot$, at sufficiently large magnification factors all gravitational waves will show interference effects.

3. Constraints from second order tensor perturbations

A different type of gravitational-wave constraint on $f(M)$, first pointed out by Saito and Yokoyama [374, 375], arises because of the second-order tensor perturbations generated by the scalar perturbations which produce the PBHs. The associated frequency was originally given as $10^{-8} (M/10^3 M_\odot) \text{ Hz}$ but this estimate contained a numerical error and was later reduced by a factor of 10^3 [374, 375]. The limit on $f(M)$ just relates to the amplitude of the density fluctuations at the horizon epoch and is of order 10^{-52} . This effect has subsequently been studied by other authors [376–378] and limits from LIGO/Virgo and the Big Bang Observer (BBO) could potentially cover the mass range down to 10^{20} g . Conversely, one can use PBH limits to constrain a background of primordial gravitational waves [379, 380]. These limits apply only if the PBHs are generated by super-Hubble scale Gaussian fluctuations, like the ones created during inflation, in the radiation-dominated universe. (See Refs. [381–383] for their formation in a matter-dominated Universe.) Although this is questionable in the context of the large-amplitude fluctuations relevant to PBH formation, the studies in Refs. [44, 384, 385] show that non-Gaussian effects are not expected to be large. These constraints are summarised in Fig. 17.

One of the mass ranges in which PBHs could provide the dark matter is around $10^{-12} M_\odot$. If these PBHs are due to enhanced scalar perturbations produced during inflation, their formation is inevitably accompanied by the generation of non-Gaussian gravitational waves with frequency peaked in the mHz range (the maximum sensitivity of LISA). Bartolo *et al.* [386, 387] show that LISA will be able to detect not only the GW power spectrum but also the non-Gaussian 3-point GW correlator, thus allowing this scenario to be thoroughly tested. A similar point has been made by Cai *et al.* [388], who study GWs induced by non-Gaussian curvature perturbations and find this can exceed the Gaussian part. A multi-peak structure in Ω_{GW} would be a smoking gun of primordial non-Gaussianity. If PBHs with masses of $10^{20}\text{--}10^{22} \text{ g}$ are the dark matter, the corresponding GWs will be detectable by LISA, irrespective of the value of f_{NL} . A general infrared behavior of the power spectrum of a stochastic GWB can also be expected: for a wide class of perturbations giving rise to PBHs, $\Omega_{\text{GW}} \propto k^3$ for a wide peak and $\Omega_{\text{GW}} \propto k^2$ for a narrow peak [389].

Chen *et al.* [390] have obtained PBH limits by searching for induced gravitational waves in the 11-year data set of the North American Nanohertz Observatory for Gravitational waves (NANOGrav). No statistically significant detection was made, excluding PBHs in the mass range $0.002\text{--}0.4 M_\odot$ from comprising more than a millionth of the dark matter. Cai *et al.* [391] argue that the tension with PTA constraints can be relieved if the perturbations are locally non-Gaussian with $f_{\text{NL}} \gtrsim \mathcal{O}(10)$ but the induced GWs could still be detectable by SKA within a decade.

The robustness of the LIGO/Virgo bounds on PBH of $\mathcal{O}(10) M_\odot$ depends on the accuracy with which the formation of PBH binaries in the early Universe can be described. Ballesteros *et al.* [319] revisit the standard estimate of the merger rate, focusing on a couple of key ingredients: the spatial distribution of nearest neighbours and the initial clustering of PBHs associated to a given primordial power spectrum. Overall, they confirm the robustness of the results presented in the literature in the case of a narrow mass function (which constrain the PBH fraction of dark matter to be $f \sim 0.001\text{--}0.01$). Any initial clustering of PBHs might tighten the current constraint but only for very broad mass functions, corresponding to wide bumps in the primordial power spectra extending at least over a couple of decades in k .

Korol *et al.* [392] have investigated the formation of binaries through Newtonian gravitational interactions in small clusters of 30 PBHs in the absence of initial binaries. The binaries act as heat sources for the cluster, increasing its velocity dispersion and inhibiting mergers through gravitational-wave two-body captures. They conclude that the rate of PBH mergers rates are at least an order of magnitude smaller than previously suggested, so that gravitational-wave observations cannot constrain the PBH contribution to the dark matter.

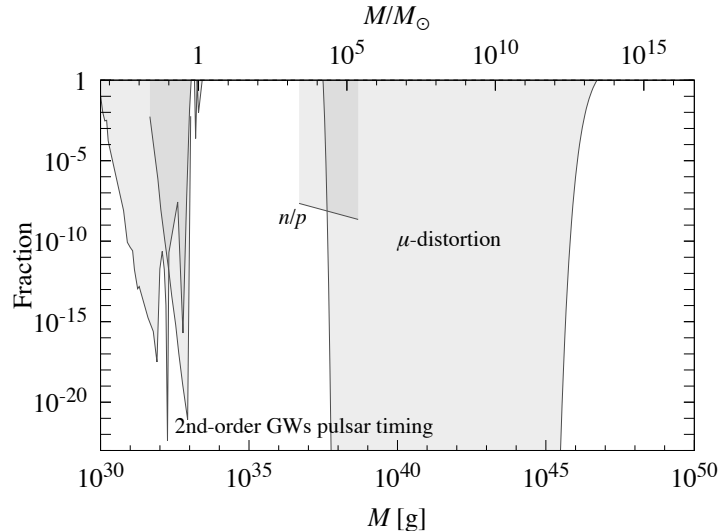


FIG. 17. Constraints on the PBH dark matter fraction from observations of various kinds of background radiation: second-order gravitational waves, acoustic reheating, the CMB μ distortion and the n/p ratio.

IV. CONSTRAINTS FOR MONOCHROMATIC AND EXTENDED PBH MASS FUNCTIONS

Our master diagram of all the $\beta'(M)$ constraints for a monochromatic PBH mass function is shown in Fig. 18. For each mass range, this gives the strongest limit shown in Fig. 4 for evaporating PBHs and Fig. 10 for non-evaporating ones, where we have used relation (55) in the latter case to convert from $f(M)$ to $\beta'(M)$.

This implies various constraints on models of the early Universe. In particular, it impose a limit on the power spectrum of the primordial inhomogeneities, as indicated in Fig. 19, and thereby constraints on the scalar spectral index and its running [393]. Possible modifications of this method can be found in Refs. [394, 395] for peak statistics, Ref.[396] for choices of the window function and Refs. [31, 394, 397] for non-linear relations between curvature and density perturbations and some extensions of peak theory [398, 399]. We note that Fig. 19 does not include the constraints shown in Fig. 17 because these do not *derive* from PBH limits. For example, the μ -distortion limit constrains both the power spectrum and the PBH density but the latter is not used to constrain μ .

Various other people have studied these power-spectrum constraints. Kalaja *et al.* [395] have used results from numerical relativity simulations and peak theory to study PBH formation for a range of perturbation shapes, including non-linearities, perturbation profile and a careful treatment of smoothing and filtering scales. Sato-Polito *et al.* [400] incorporate uncertainties in the critical overdensity for collapse and considerations of ellipsoidal collapse. These results provide the most stringent PBH limits on the primordial curvature power spectrum on small scales and cover a range of scales not probed by other cosmological observables.

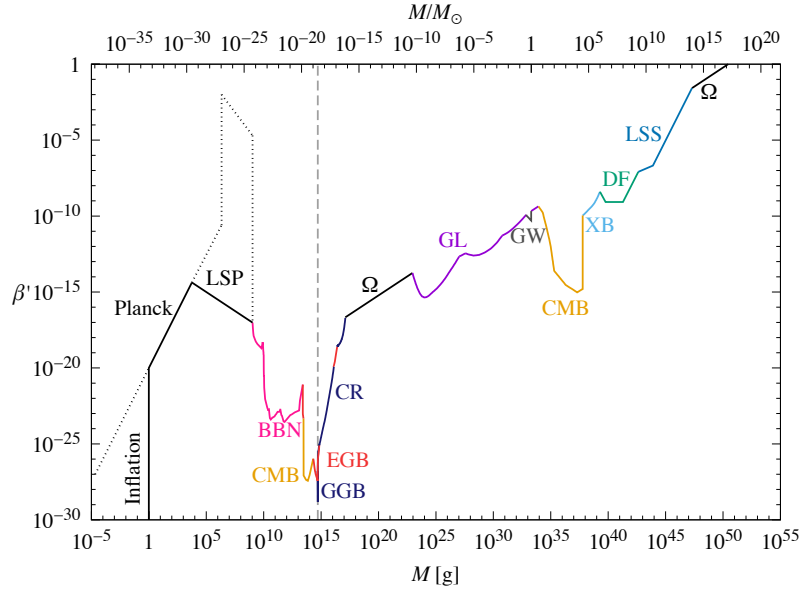


FIG. 18. Combined constraints on $\beta(M)$ for a monochromatic PBH mass function. For each mass range, this gives the strongest limit for either evaporating and non-evaporating PBHs. No PBHs form to the left of the ‘inflation’ line, so this is a theoretical rather than observational constraint.

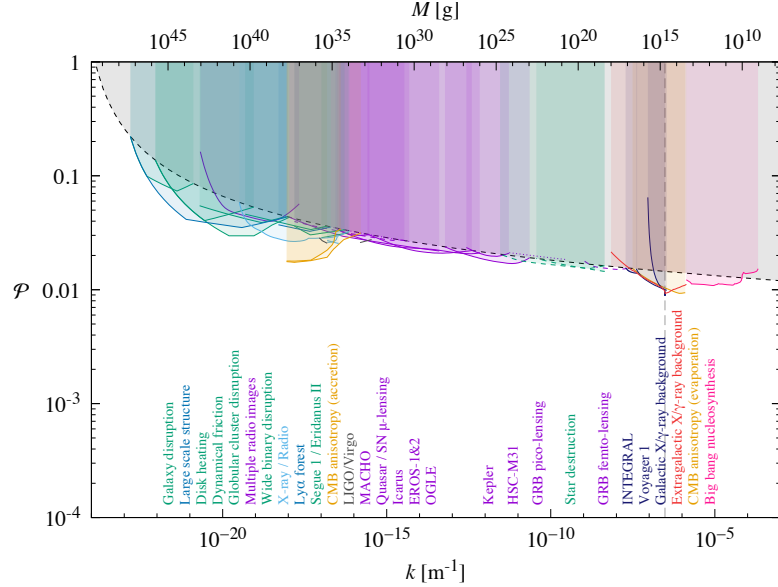


FIG. 19. Constraints on power spectrum $\mathcal{P}(k)$ implied by Fig. 10 for Gaussian fluctuations.

The constraints shown in Fig. 18 assume that the PBH mass function is quasi-monochromatic (i.e. with a width $\Delta M \sim M$). This is unrealistic and in most scenarios one would expect the mass function to be extended. In the context of the dark-matter problem, this is a two-edged sword [102]. On the one hand, it means that the *total* PBH density may suffice to explain the dark matter, even if the density in any particular mass band is small and within the observational bounds discussed in Sec. III. On the other hand, even if PBHs can provide all the dark matter at some mass scale without violating the constraints there, the extended mass function may still violate the constraints at some other scale. This problem is particularly pertinent if the mass function extends over many decades. For example, Hasegawa *et al.* [401] have proposed a scenario in the minimally supersymmetric standard model which generates

both intermediate-mass PBHs to explain the LIGO detections and lunar-mass PBHs to explain the dark matter. The first are generated by baryon number perturbations induced by a special type of Affleck–Dine mechanism, while the second comprise non-topological solitons (Q-balls).

A detailed assessment of this problem requires a knowledge of the expected PBH mass fraction, $f_{\text{exp}}(M)$, and the maximum fraction allowed by the constraint, $f_{\text{max}}(M)$. However, the procedure is non-trivial even when these functions are known. In particular, one cannot just plot $f_{\text{exp}}(M)$ for a given model in Fig. 10 and infer that the model is allowed because it does not intersect $f_{\text{max}}(M)$, even though this procedure is sometimes used in the literature.

If the PBHs span an extended range of masses, the differential mass function is usually written as dn/dM where dn is the number density of PBHs in the mass range $(M, M + dM)$. One approach is to define the continuous function

$$n(M) \equiv M \frac{dn}{dM} = \frac{dn}{d \ln M}, \quad (97)$$

which can be interpreted as the number density of PBHs in the mass range $(M, 2M)$. One can then define the mass density and dark matter fraction in the same mass range as

$$\rho(M) \equiv M^2 \frac{dn}{dM}, \quad f(M) \equiv \frac{\rho(M)}{\rho_{\text{CDM}}}, \quad (98)$$

where $\Omega_{\text{CDM}} \approx 0.27$ is the cold dark matter density in units of the critical density. Alternatively, one can define $n(M)$, $\rho(M)$ and $f(M)$ as integrated values for PBHs with mass larger or smaller than M . However, these are only simply related to the first functions for a power law spectrum.

In Ref. [102], Carr *et al.* assumed that a general constraint can be treated as a sequence of flat constraints by breaking it up into narrow mass bins. They then studied the possible dark matter windows in some detail. However, this was quite a complicated procedure and it attracted some criticism from Green [402]. A more elegant methodology - similar to the one adopted by Green - was taken by Carr *et al.* in Ref. [403] and we adopt this in the present discussion. In this, one introduces the function

$$\psi(M) \propto M \frac{dn}{dM}, \quad (99)$$

normalised so that the *total* fraction of the DM in PBHs is

$$f_{\text{PBH}} \equiv \frac{\Omega_{\text{PBH}}}{\Omega_{\text{CDM}}} = \int_{M_{\text{min}}}^{M_{\text{max}}} dM \psi(M). \quad (100)$$

Note that $\psi(M)$ is the distribution function of $\log M$ and has units $[\text{mass}]^{-1}$. The lower cut-off in the mass integral necessarily exceeds $M_* \approx 4 \times 10^{14} \text{ g}$, the mass of the PBHs evaporating at the present epoch [101].

A. PBH mass function

Reference [403] considers three types of mass function, which we summarise briefly here.

1. A lognormal mass function of the form:

$$\psi(M) = \frac{f_{\text{PBH}}}{\sqrt{2\pi} \sigma M} \exp\left(-\frac{\log^2(M/M_c)}{2\sigma^2}\right), \quad (101)$$

where M_c is the mass at which the function $M\psi(M)$ peaks and σ is the width of the spectrum. This is often a good approximation if the PBHs result from a smooth symmetric peak in the inflationary power spectrum. It was first suggested in Ref. [91] and then demonstrated numerically in Ref. [402] and analytically in Ref. [404] for the case in which the slow-roll approximation holds. For a given value of f_{PBH} , the mass function is therefore described by two parameters. Note that the lognormal mass function used in Refs. [334, 402, 405] omits the M^{-1} term in Eq. (101), in which case the function $M\psi(M)$ peaks at $e^{\sigma^2} M_c$ rather than M_c . The form (101) is more useful for our purposes because $M\psi(M)$ relates to the DM fraction in PBHs of mass M .

2. A power-law mass function of the form

$$\psi(M) \propto M^{\gamma-1} \quad (M_{\text{min}} < M < M_{\text{max}}). \quad (102)$$

For $\gamma \neq 0$, either the lower or upper cut-off can be neglected if $M_{\min} \ll M_{\max}$, so this scenario is effectively described by two parameters. Only in the $\gamma = 0$ case are both cut-offs important. For example, a mass function of this form arises naturally if the PBHs form from scale-invariant density fluctuations or from the collapse of cosmic strings. In both cases, $\gamma = -2w/(1+w)$, where w specifies the equation of state, $p = w\rho c^2$, when the PBHs form [24]. In a non-inflationary universe, $w \in (-1/3, 1)$ and so the range of the mass function exponent is $\gamma \in (-1, 1)$. Equation (102) is not applicable for $w \in (-1, -1/3)$, corresponding to $\gamma \in (1, \infty)$, because PBHs do not form during such an inflationary phase but only *after* it as a result of inflation-generated density fluctuations.

3. A critical collapse mass function [56, 57, 142, 406]:

$$\psi(M) \propto M^{2.85} \exp(-(M/M_f)^{2.85}), \quad (103)$$

where the exponent 2.85 assumes radiation-domination. This may apply generically if the PBHs form from density fluctuations with a δ -function power spectrum. In this case, the mass spectrum extends down to arbitrarily low masses but there is an exponential upper cut-off at a mass-scale M_f which corresponds roughly to the horizon mass at the collapse epoch. In this case, the mass function is described by a single parameter. However, if the density fluctuations are themselves extended, as expected in the inflationary scenario, then Eq. (103) must be modified [102]. Indeed, the lognormal distribution may then be appropriate, so two parameters may be required in the more realistic critical collapse situation.

4. Special consideration is required in the $w = 0$ (matter-dominated) case [49, 407], because both cut-offs in (102) can be relevant. For example, this may arise due to some form of phase transition in which the mass is channeled into non-relativistic particles [49, 50] or due to slow reheating after inflation [53]. Since one expects $\gamma = 0$ in this case, $\rho(m)$ should increase logarithmically with m . However, the analysis breaks down in this case because the Jeans length is much smaller than the particle horizon, so collapse is prevented by deviations from spherical symmetry rather than pressure and the probability of PBH formation becomes

$$\beta(m) \approx 0.02 \delta_H(m)^5. \quad (104)$$

The factor $\delta_H(M)^5$ was first derived in Refs. [49, 50] and is in agreement with the more recent analysis of Ref. [408]. In addition, a finite spin is produced during collapse in a matter-dominated period which can exponentially suppress PBH production for smaller density perturbation [409], so we need to consider this in the present context [410]. $\beta(M)$ is small for $\delta_H(M) \ll 1$ but much larger than the exponentially suppressed fraction in the radiation-dominated case. If the matter-dominated phase extends from t_1 to t_2 , PBH formation is enhanced over the mass range

$$m_{\min} \sim M_H(t_1) < m < m_{\max} \sim M_H(t_2) \delta_H(m_{\max})^{3/2}. \quad (105)$$

The lower limit is the horizon mass at the start of matter-dominance and the upper limit is the horizon mass at the epoch when the region which binds at the end of matter-dominance enter the horizon. For nearly scale-invariant primordial fluctuations, $\beta(m)$ is constant and $f(m)$ is logarithmic. Thus, for a given value of f_{PBH} , the mass function is determined by the values of t_1 and t_2 [411].

To compare with the lognormal case, we describe the mass function in the first three cases by the mean and variance of the $\log M$ distribution:

$$\log M_c \equiv \langle \log M \rangle_\psi, \quad \sigma^2 \equiv \langle \log^2 M \rangle_\psi - \langle \log M \rangle_\psi^2, \quad (106)$$

where

$$\langle X \rangle_\psi \equiv f_{\text{PBH}}^{-1} \int dM \psi(M) X(M). \quad (107)$$

For a power-law distribution these are

$$M_c = M_{\text{cut}} e^{-\frac{1}{\gamma}}, \quad \sigma = \frac{1}{|\gamma|}, \quad (108)$$

where $M_{\text{cut}} \equiv \max(M_{\min}, M_*)$ if $\gamma < 0$ or M_{\max} if $\gamma > 0$. For the critical-collapse distribution, the exponential cut-off is very sharp, so the mass function is well approximated by a power-law distribution with $\gamma = 3.85$ and $M_{\max} \approx M_f$. As it is relatively narrow, Eq. (108) implying $\sigma = 0.26$, even the monochromatic mass function provides a good fit.

Since critical collapse should be a fairly generic feature of PBH formation, $\sigma = 0.26$ will usually provide a lower limit to the width of the mass function. Critical collapse may not be relevant in the cosmic string or matter-dominated ($w = 0$) scenarios but Ref. [403] does not discuss these anyway.

It should be stressed that two parameters should always suffice to describe the PBH mass function *locally* (i.e. close to a peak) since this just corresponds to the first two terms in a Taylor expansion. However, in principle the mass function could be more complicated than this. For example, depending on the form of the inflationary potential, it could have several distinct peaks. Indeed, with a sufficiently contrived form, these peaks could be tuned to match all the constraint windows.

B. Constraints for extended PBH mass function

Reference [403] introduces a general method for dealing with extended mass functions. For this purpose, consider an astrophysical observable $A[\psi(M)]$ depending on the PBH abundance (e.g. the number of microlensing events of given duration in a given time interval). It can generally be expanded as

$$A[\psi(M)] = A_0 + \int dM \psi(M) K_1(M) + \int dM_1 dM_2 \psi(M_1) \psi(M_2) K_2(M_1, M_2) + \dots, \quad (109)$$

where A_0 is the background contribution and the functions K_j depend on the details of the underlying physics and the nature of the observation. If PBHs with different mass contribute independently to the observable, only the first two terms in Eq. (109) need to be considered. Explicit expressions are given for lensing and survival of stars in Ref. [402], for evaporation in Ref. [102] and for neutron star capture and accretion in Ref. [405].

If a measurement puts an upper bound on the observable,

$$A[\psi(M)] \leq A_{\text{exp}}, \quad (110)$$

then for a monochromatic mass function with $M = M_c$ we have

$$\psi_{\text{mon}}(M) \equiv f_{\text{PBH}}(M_c) \delta(M - M_c). \quad (111)$$

The maximum allowed fraction of dark matter in the PBHs is then

$$f_{\text{PBH}}(M_c) \leq \frac{A_{\text{exp}} - A_0}{K_1(M_c)} \equiv f_{\text{max}}(M_c). \quad (112)$$

Combining Eqs. (109)–(112) then yields

$$\int dM \frac{\psi(M)}{f_{\text{max}}(M)} \leq 1. \quad (113)$$

Once f_{max} is known, it is possible to apply Eq. (113) for an arbitrary mass function $\psi(M)$ to obtain the constraints equivalent to those for a monochromatic mass function. We first integrate Eq. (113) over the mass range (M_1, M_2) for which the constraint applies, assuming a particular function $\psi(M; f_{\text{PBH}}, M_c, \sigma)$. Once we have specified M_1 and M_2 , this constrains f_{PBH} as a function of M_c and σ .

The procedure must be implemented separately for each observable. Different constraints can be combined by using the relation

$$\sum_{j=1}^N \left(\int dM \frac{\psi(M)}{f_{\text{max},j}(M)} \right)^2 \leq 1, \quad (114)$$

where $f_{\text{max},j}(M)$ correspond to the different bounds for a monochromatic mass function, as defined by Eq. (112). Most of the constraints shown in Fig. 20 rely on a single observable. For lensing this is the number of lensing events [221, 227, 228, 241], for neutron star capture it is the age of neutron stars [213], and for white dwarfs and wide binaries it is their abundance [282, 290].

The constraints on the allowed fraction of PBH dark matter are shown in Fig. 20, the constraint for a monochromatic mass function being shown in the upper left panel. The last three panels in Fig. 20 are then derived by assuming $\sigma = 2$ for the lognormal mass function (upper right panel) and $\gamma = \pm 1$ for the power law mass function (lower panels). The important qualitative point is that the form of Fig. 20 in the non-monochromatic case is itself dependent on the PBH mass function. One cannot just compare a predicted extended mass function with the monochromatic form of the

constraints, as some authors have done. In displaying the constraints, one also needs to select values of the parameters which describe the mass function. In both the lognormal and power-law cases, we have taken these to be σ and M_c . For the critical collapse model, there is only one parameter (M_f) but this model is practically indistinguishable from the monochromatic one because only a small fraction of the PBH density is associated with the low-mass tail. So this case is not shown explicitly.

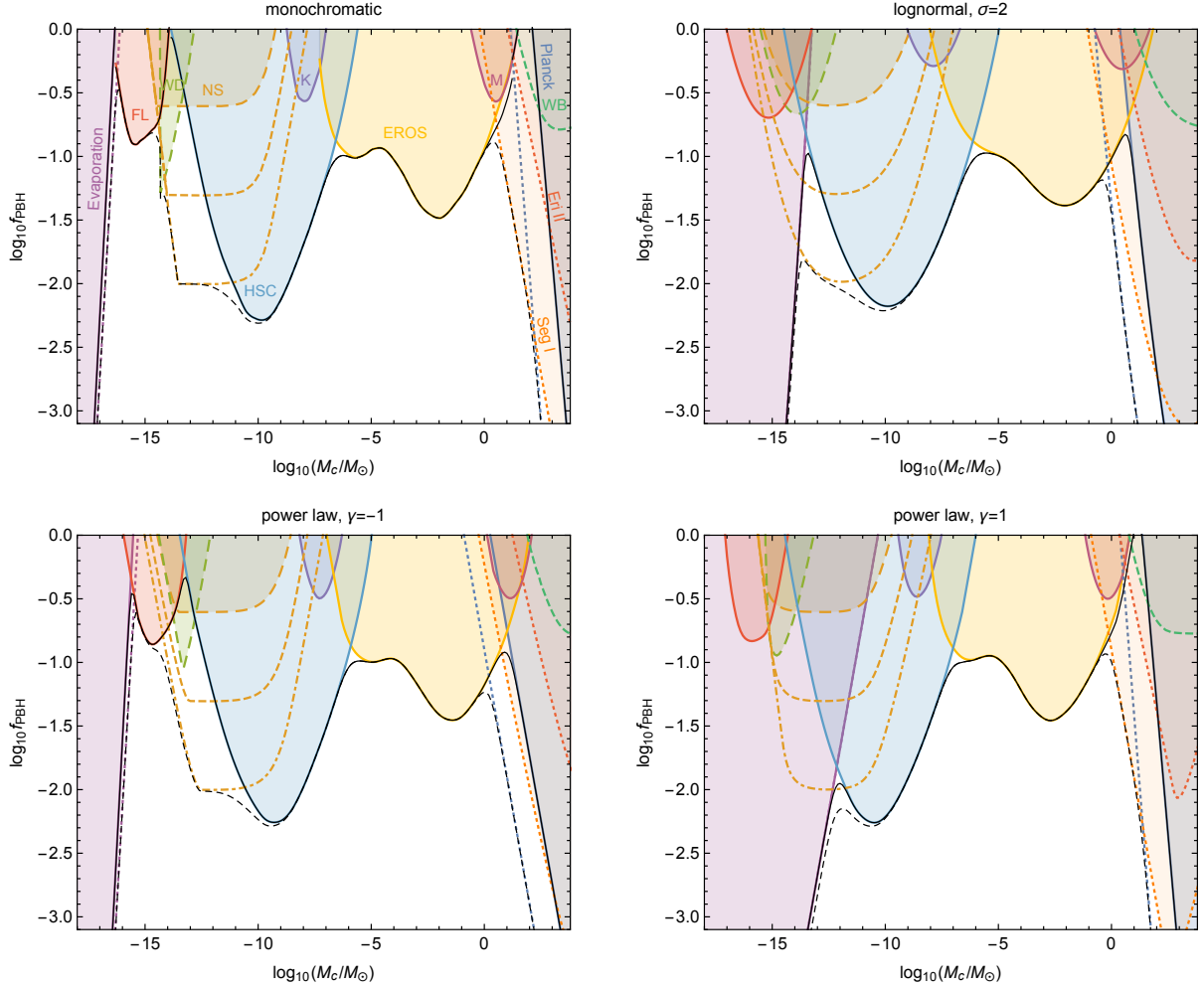


FIG. 20. *Upper left panel:* Constraints from different observations on the fraction of PBH DM, $f_{\text{PBH}} \equiv \Omega_{\text{PBH}}/\Omega_{\text{DM}}$, as a function of the PBH mass M_c , assuming a monochromatic mass function. The purple region on the left is excluded by evaporations [101], the red region by femtolensing of gamma-ray bursts (FL) [221], the brown region by neutron star capture (NS) for different values of the dark matter density in the cores of globular clusters [213], the green region by white dwarf explosions (WD) [282], the blue, violet, yellow and purple regions by the microlensing results from Subaru (HSC) [241], Kepler (K) [240], EROS [227] and MACHO (M) [228], respectively. The dark blue, orange, red and green regions on the right are excluded by Planck data [333], survival of stars in Segue I (Seg I) [293] and Eridanus II (Eri II) [292], and the distribution of wide binaries (WB) [290], respectively. The black dashed and solid lines show, respectively, the combined constraint with and without the constraints depicted by the colored dashed lines. *Other panels:* Same as the upper left panel but for a lognormal PBH mass function with $\sigma = 2$ (upper right) and for a power-law PBH mass function with $\gamma = -1$ (lower left) and $\gamma = 1$ (lower right).

The main results of this analysis are presented in Fig. 21, which shows constraints on the maximum allowed fraction of PBH dark matter, f_{max} , in the (M_c, σ) plane for lognormal and power-law PBH mass functions. In the upper right panel all the constraints shown in Fig. 20 are considered, using the most restrictive forms for the evaporation, accretion and neutron star constraints, as depicted by the dotted lines. In the other panels only the constraints corresponding to the solid lines are taken into account. The constraints have been combined using Eq. (114). The black lines in Fig. 20 correspond to constant σ slices in Fig. 21. The regions where 10%, 20%, 50% and 100% of DM can consist of PBHs are indicated in Fig. 21 by the dotted, dot-dashed, dashed and solid lines, respectively, while less

than 0.1% of the DM can be in PBHs in the white region.

The shape of the constraints in Fig. 21 makes it clear that the allowed mass range for fixed f_{PBH} decreases with increasing width σ , thus ruling out the possibility of evading the constraints by simply extending the mass function. Moreover, Fig. 21 gives an upper bound $\sigma \lesssim 1$ if all dark matter is in the form of PBHs. This implies $|\gamma| \gtrsim 1$, which effectively rules out PBH dark matter from the collapse of cosmic strings or scale-invariant density fluctuations. This agrees with the conclusions of Refs. [334, 402, 405]. Reference [405] performs a more comprehensive analysis, covering the mass range 10^{-18} – $10^4 M_\odot$, but their study does not include the recent HSC constraint [241] and they calculate the Planck constraint as in Ref. [336], which is unnecessarily stringent.

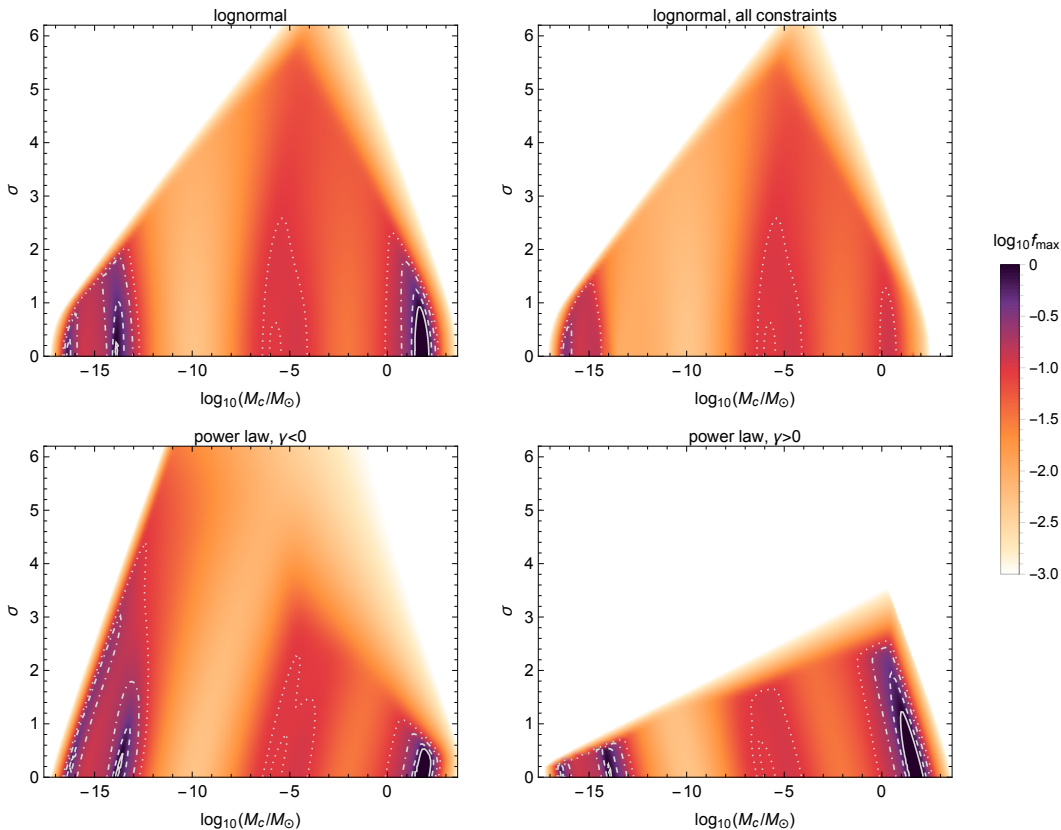


FIG. 21. *Upper panels:* Combined observational constraints on M_c and σ for a lognormal PBH mass function. The color coding shows the maximum allowed fraction of PBH dark matter. In the white region $\log_{10} f_{\text{max}} < -3$, while the solid, dashed, dot-dashed and dotted contours correspond to $f_{\text{max}} = 1$, $f_{\text{max}} = 0.5$, $f_{\text{max}} = 0.2$ and $f_{\text{max}} = 0.1$, respectively. In the left panel only the constraints depicted by the solid lines in Fig. 20 are included, whereas the right panel includes all the constraints. *Lower panels:* Same as the upper left panel but for a power-law mass function with $\gamma < 0$ (left) and $\gamma > 0$ (right).

V. CONCLUSION

Although this review has focused on the constraints on PBHs, our motivation has not been to exclude their existence, so the large number of constraints discussed should not merely be regarded as “nails in the coffin” of the PBH scenario. We will therefore conclude by emphasizing the positive aspects of the constraints.

First, each constraint could in principle provide *evidence* for PBHs. Indeed, historically some of them have already been thought to do so. For example, microlensing of stars in the LMC once suggested that PBHs with $M \sim 1 M_\odot$ could provide the dark matter; later observations seemed to exclude this but the source of the extra events remains unclear, so there could still be some PBHs. There were also claims to have detected PBHs with $M \sim 10^{-3} M_\odot$ from microlensing of quasars. At one stage it was argued that PBHs with $M \sim 10^6 M_\odot$ could generate the observed heating of the Galactic disc, although this now seems unlikely. It was once proposed that accretion by PBHs with $M \sim 10^2 M_\odot$ could generate the extragalactic X-ray background. More recently, it has been claimed that exploding

PBHs with $M \sim 10^{15}$ g could explain some short-period gamma-ray bursts or that PBHs with $M \sim 10 M_\odot$ could provide the black hole coalescences observed by LIGO. None of these claims may represent the mainstream view – and some have now definitely been rejected – but future observations, involving more sensitive searches for some of the effects reviewed here, might do so.

Second, much attention has focussed on whether PBHs could provide the dark matter but they could still have important cosmological consequences even if the dark matter fraction is small. For example, they could still explain the LIGO observations without providing the dark matter and supermassive PBHs could seed large-scale cosmic structure even for f as low as 10^{-5} . Indeed, if PBHs have an extended mass function, they could in principle play all three roles – providing dark matter, LIGO coalescences and seeds for cosmic structure. For comparison, on the particle physics side, neutrinos are no longer regarded as viable dark matter candidates, but they still play a vital role in both astrophysics and particle physics.

It should be stressed that PBHs can be interesting even if f is small. Indeed, PBHs have been invoked for three astrophysical purposes: (1) to provide the dark matter; (2) to explain the black hole coalescences observed by LIGO; (3) to seed large-scale cosmic structures. These proposals are essentially independent if the PBHs have a monochromatic mass function and only the first requires $f \sim 1$. In this context, it has been clear for a long time that there are three options: (A) black holes in the intermediate mass range $10 M_\odot < M < 10^3 M_\odot$ between the microlensing and wide binary limits; (B) black holes in the sublunar mass range 10^{20} g $< M < 10^{24}$ g between the (contentious) femtolensing limit and the HSC microlensing limit; (C) black holes in the asteroid mass range 10^{16} g $< M < 10^{17}$ g between the γ -ray background and (contentious) femtolensing limits. There is also a fourth window: (D) Planck-mass relics of Hawking evaporation in the range around $M \sim 10^{-5}$ g. (A) is topical because of the LIGO results. (B) was originally excluded by the neutron star and white dwarf limits but these are no longer reliable. (C) is perhaps implausible because the constraint at M_* is so strong, although this possibility was stressed in Ref. [101]. (D) is essentially untestable because the relics are too small (10^{-33} cm) to be detected non-gravitationally.

Third, even if none of the effects reviewed in this paper provides evidence for PBHs, their non-detection over various mass ranges still provides important constraints on the early Universe. In particular, the limits on $\beta(M)$ can be used to constrain the various PBH formation scenarios: for example, models involving inflation, an early matter-dominated phase and the collapse of cosmic strings or domain walls. Most importantly, they restrict the form of the primordial inhomogeneities (whatever their source) and their possible non-Gaussianity. Although we have not discussed them here, the limits could also constrain more exotic models of the early Universe, such as those involving a variable gravitational constant or a different number of spatial dimensions. In the latter context, we note that the existence of extra dimensions which are large compared to the Planck length could permit the formation of black holes in accelerators (e.g. in the TeV quantum gravity scenario). Even though such black holes are not themselves primordial, the existence of the extra dimensions in the early Universe could have important implications for PBH formation.

Finally we stress that all the constraints shown in Fig. 10 come with caveats. Few of them are completely secure, either because of uncertainties in the observations or because of flexibility in the models. Some limits can be relaxed in various ways (e.g. by invoking PBH clustering for the lensing constraints or non-Gaussian fluctuations for the μ distortion constraints). Indeed, while we have tried to cover all the literature for historical completeness, we have also stressed when constraints are no longer believed. Ideally, one should associate a confidence level with each constraint but that would require a much longer discussion and could not easily be represented in our constraint figures. We have therefore compromised by showing more controversial constraints as broken lines.

ACKNOWLEDGMENTS

For many years of fruitful PBH collaboration we thank Laila Alabidi, Dick Bond, Francesca Calore, Sebastien Clesse, Juan García-Bellido, Jaume Garriga, Jonathan Gilbert, Tomohiro Harada, Stephen Hawking, Kimitake Hayasaki, Sanjay Jhingan, Takafumi Kokubu, Florian Kuhnel, Koutarou Kyutoku, Matt Lake, Jim Lidsey, Hideki Maeda, Jane MacGibbon, Tomohiro Matsuda, Hiroki Matsui, Jonas Mureika, Shigehiro Nagataki, Tomohiro Nakama, Ken-ichi Nakao, Piero Nicolini, Vivian Poulin, Marti Raidal, Martin Rees, Mari Sakellariadou, Ryo Saito, Marit Sandstad, Katsuhiko Sato, Pasquale Serpico, Joe Silk, Teruaki Suyama, Keitaro Takahashi, Tommi Tenkanen, Takahiro Terada, Ville Vaskonen, Hardi Veermäe and Chul-Moon Yoo. For useful input we also thank Anne Green, Carlos Hidalgo, Maxim Khlopov, Alex Kusenkov, Karim Malik, Takahiko Matsubara, Shi Pi and Sasha Polnarev. B.J.C. thanks the Research Center for the Early Universe (RESCEU), University of Tokyo, for hospitality received during this work. The work of K.K. is supported in part by JSPS KAKENHI grant No. JP17H01131 (KK) and MEXT KAKENHI Grant Nos. JP15H05889, 18H04594 (KK). Y.S. is supported in part by JSPS KAKENHI Grant Number 16K17675.

J.Y. is supported in part by JSPS KAKENHI, Grant JP15H02082 and Grant on Innovative Areas JP15H05888.

-
- [1] Y. B. Zel'dovich and I. D. Novikov, *Sov. Astron.* **10**, 602 (1967).
 - [2] S. W. Hawking, *Nature* **248**, 30 (1974).
 - [3] P. A. R. Ade *et al.* (Planck), *Astron. Astrophys.* **594**, A13 (2016), arXiv:1502.01589 [astro-ph.CO].
 - [4] G. F. Chapline, *Nature* **253**, 251 (1975).
 - [5] R. H. Cyburt, B. D. Fields, and K. A. Olive, *Phys. Lett.* **B567**, 227 (2003), arXiv:astro-ph/0302431 [astro-ph].
 - [6] D. N. Page and S. W. Hawking, *Astrophys. J.* **206**, 1 (1976).
 - [7] R. Lehoucq, M. Cassé, J.-M. Casandjian, and I. Grenier, *Astron. Astrophys.* **502**, 37 (2009), arXiv:0906.1648 [astro-ph.HE].
 - [8] A. Barrau, *Astropart. Phys.* **12**, 269 (2000), arXiv:astro-ph/9907347 [astro-ph].
 - [9] P. N. Okele and M. J. Rees, *Astron. Astrophys.* **81**, 263 (1980).
 - [10] K. M. Belotsky and A. A. Kirillov, *J. Cosmol. Astropart. Phys.* **1501**, 041 (2015), arXiv:1409.8601 [astro-ph.CO].
 - [11] D. B. Cline, D. A. Sanders, and W. Hong, *Astrophys. J.* **486**, 169 (1997).
 - [12] R. Bean and J. Magueijo, *Phys. Rev.* **D66**, 063505 (2002), arXiv:astro-ph/0204486.
 - [13] N. Afshordi, P. McDonald, and D. N. Spergel, *Astrophys. J. Lett.* **594**, L71 (2003), arXiv:astro-ph/0302035.
 - [14] M. Ricotti, J. P. Ostriker, and K. J. Mack, *Astrophys. J.* **680**, 829 (2008), arXiv:0709.0524 [astro-ph].
 - [15] B. P. Abbott *et al.* (Virgo, LIGO Scientific), *Phys. Rev. Lett.* **116**, 061102 (2016), arXiv:1602.03837 [gr-qc].
 - [16] B. P. Abbott *et al.* (Virgo, LIGO Scientific), *Phys. Rev. Lett.* **116**, 241103 (2016), arXiv:1606.04855 [gr-qc].
 - [17] B. P. Abbott *et al.* (Virgo, LIGO Scientific), (2016), arXiv:1602.03842 [astro-ph.HE].
 - [18] B. P. Abbott *et al.* (LIGO Scientific, Virgo), (2018), arXiv:1811.12907 [astro-ph.HE].
 - [19] B. Carr, S. Clesse, J. García-Bellido, and F. Kuhnel, (2019), arXiv:1906.08217 [astro-ph.CO].
 - [20] A. Barrau, D. Blais, G. Boudoul, and D. Polarski, *Annalen Phys.* **13**, 115 (2004), arXiv:astro-ph/0303330.
 - [21] M. Sasaki, T. Suyama, T. Tanaka, and S. Yokoyama, *Class. Quant. Grav.* **35**, 063001 (2018), arXiv:1801.05235 [astro-ph.CO].
 - [22] S. Hawking, *Mon. Not. Roy. Astron. Soc.* **152**, 75 (1971).
 - [23] B. J. Carr and S. W. Hawking, *Mon. Not. Roy. Astron. Soc.* **168**, 399 (1974).
 - [24] B. J. Carr, *Astrophys. J.* **201**, 1 (1975).
 - [25] D. K. Nadezhin, I. D. Novikov, and A. G. Polnarev, *Sov. Astron.* **22**, 129 (1978).
 - [26] G. V. Bicknell and R. N. Henriksen, *Astrophys. J.* **232**, 670 (1979).
 - [27] I. Musco, J. C. Miller, and L. Rezzolla, *Class. Quant. Grav.* **22**, 1405 (2005), arXiv:gr-qc/0412063.
 - [28] I. Musco, J. C. Miller, and A. G. Polnarev, *Class. Quant. Grav.* **26**, 235001 (2009), arXiv:0811.1452 [gr-qc].
 - [29] T. Harada, C.-M. Yoo, and K. Kohri, *Phys. Rev.* **D88**, 084051 (2013), [Erratum: *Phys. Rev.* D89, no.2, 029903(2014)], arXiv:1309.4201 [astro-ph.CO].
 - [30] I. Musco, *Phys. Rev.* **D100**, 123524 (2019), arXiv:1809.02127 [gr-qc].
 - [31] C. Germani and I. Musco, *Phys. Rev. Lett.* **122**, 141302 (2019), arXiv:1805.04087 [astro-ph.CO].
 - [32] M. Shibata and M. Sasaki, *Phys. Rev.* **D60**, 084002 (1999), arXiv:gr-qc/9905064.
 - [33] T. Harada, C.-M. Yoo, T. Nakama, and Y. Koga, *Phys. Rev.* **D91**, 084057 (2015), arXiv:1503.03934 [gr-qc].
 - [34] A. Escriv, C. Germani, and R. K. Sheth, (2019), arXiv:1907.13311 [gr-qc].
 - [35] T. Nakama, T. Harada, A. G. Polnarev, and J. Yokoyama, *JCAP* **1401**, 037 (2014), arXiv:1310.3007 [gr-qc].
 - [36] P. Ivanov, P. Naselsky, and I. Novikov, *Phys. Rev.* **D50**, 7173 (1994).
 - [37] J. Yokoyama, *Astron. Astrophys.* **318**, 673 (1997), arXiv:astro-ph/9509027 [astro-ph].
 - [38] J. García-Bellido, A. D. Linde, and D. Wands, *Phys. Rev.* **D54**, 6040 (1996), arXiv:astro-ph/9605094.
 - [39] J. Yokoyama, *Phys. Rev.* **D58**, 083510 (1998), arXiv:astro-ph/9802357 [astro-ph].
 - [40] J. Yokoyama, *Phys. Rept.* **307**, 133 (1998).
 - [41] M. Kawasaki and T. Yanagida, *Phys. Rev.* **D59**, 043512 (1999), arXiv:hep-ph/9807544.
 - [42] T. Kanazawa, M. Kawasaki, and T. Yanagida, *Phys. Lett.* **B482**, 174 (2000), arXiv:hep-ph/0002236 [hep-ph].
 - [43] S. Chongchitnan and G. Efstathiou, *JCAP* **0701**, 011 (2007), arXiv:astro-ph/0611818 [astro-ph].
 - [44] R. Saito, J. Yokoyama, and R. Nagata, *J. Cosmol. Astropart. Phys.* **0806**, 024 (2008), arXiv:0804.3470 [astro-ph].
 - [45] L. Alabidi and K. Kohri, *Phys. Rev.* **D80**, 063511 (2009), arXiv:0906.1398 [astro-ph.CO].
 - [46] K. Kohri, C.-M. Lin, and T. Matsuda, *Phys. Rev.* **D87**, 103527 (2013), arXiv:1211.2371 [hep-ph].
 - [47] K. Kohri, D. H. Lyth, and A. Melchiorri, *JCAP* **0804**, 038 (2008), arXiv:0711.5006 [hep-ph].
 - [48] H. Motohashi and W. Hu, *Phys. Rev.* **D96**, 063503 (2017), arXiv:1706.06784 [astro-ph.CO].
 - [49] M. Y. Khlopov and A. G. Polnarev, *Phys. Lett.* **B97**, 383 (1980).
 - [50] A. G. Polnarev and M. Y. Khlopov, *Sov. Astron.* **25**, 406 (1981).
 - [51] A. G. Polnarev and M. Y. Khlopov, *Sov. Astron.* **26**, 391 (1982).
 - [52] M. Y. Khlopov, B. A. Malomed, and Y. B. Zel'dovich, *Mon. Not. Roy. Astron. Soc.* **215**, 575 (1985).
 - [53] B. J. Carr, J. H. Gilbert, and J. E. Lidsey, *Phys. Rev.* **D50**, 4853 (1994), arXiv:astro-ph/9405027.
 - [54] T. Kokubu, K. Kyutoku, K. Kohri, and T. Harada, (2018), arXiv:1810.03490 [astro-ph.CO].
 - [55] J. C. Niemeyer and K. Jedamzik, *Phys. Rev. Lett.* **80**, 5481 (1998), arXiv:astro-ph/9709072.

- [56] J. C. Niemeyer and K. Jedamzik, Phys. Rev. **D59**, 124013 (1999), arXiv:astro-ph/9901292.
- [57] J. Yokoyama, Phys. Rev. **D58**, 107502 (1998), arXiv:gr-qc/9804041.
- [58] A. M. Green and A. R. Liddle, Phys. Rev. **D60**, 063509 (1999), arXiv:astro-ph/9901268.
- [59] G. D. Kribs, A. K. Leibovich, and I. Z. Rothstein, Phys. Rev. **D60**, 103510 (1999), arXiv:astro-ph/9904021.
- [60] K. Jedamzik, Phys. Rev. **D55**, R5871 (1997), arXiv:astro-ph/9605152.
- [61] P. Widerin and C. Schmid, (1998), arXiv:astro-ph/9808142.
- [62] K. Jedamzik and J. C. Niemeyer, Phys. Rev. **D59**, 124014 (1999), arXiv:astro-ph/9901293.
- [63] C. T. Byrnes, M. Hindmarsh, S. Young, and M. R. S. Hawkins, J. Cosmol. Astropart. Phys. **8**, 041 (2018), arXiv:1801.06138.
- [64] S. W. Hawking, Phys. Lett. **B231**, 237 (1989).
- [65] A. Polnarev and R. Zembowicz, Phys. Rev. **D43**, 1106 (1991).
- [66] R. N. Hansen, M. Christensen, and A. L. Larsen, Int. J. Mod. Phys. **A15**, 4433 (2000), arXiv:gr-qc/9902048.
- [67] C. J. Hogan, Phys. Lett. **B143**, 87 (1984).
- [68] M. Nagasawa, Gen. Rel. Grav. **37**, 1635 (2005).
- [69] H. Honma and H. Minakata, (1991).
- [70] T. Matsuda, J. High Energy Phys. **04**, 017 (2006), arXiv:hep-ph/0509062.
- [71] M. Lake, S. Thomas, and J. Ward, J. High Energy Phys. **12**, 033 (2009), arXiv:0906.3695 [hep-ph].
- [72] M. Crawford and D. N. Schramm, Nature **298**, 538 (1982).
- [73] S. W. Hawking, I. G. Moss, and J. M. Stewart, Phys. Rev. **D26**, 2681 (1982).
- [74] H. Kodama, M. Sasaki, and K. Sato, Prog. Theor. Phys. **68**, 1979 (1982).
- [75] D. La and P. J. Steinhardt, Phys. Lett. **B220**, 375 (1989).
- [76] I. G. Moss, Phys. Rev. **D50**, 676 (1994).
- [77] R. V. Konoplich, S. G. Rubin, A. S. Sakharov, and M. Y. Khlopov, Astronomy Letters **24**, 413 (1998).
- [78] R. V. Konoplich, S. G. Rubin, A. S. Sakharov, and M. Y. Khlopov, Phys. Atom. Nucl. **62**, 1593 (1999).
- [79] E. Cotner and A. Kusenko, Phys. Rev. Lett. **119**, 031103 (2017), arXiv:1612.02529 [astro-ph.CO].
- [80] E. Cotner and A. Kusenko, Phys. Rev. **D96**, 103002 (2017), arXiv:1706.09003 [astro-ph.CO].
- [81] E. Cotner, A. Kusenko, and V. Takhistov, Phys. Rev. **D98**, 083513 (2018), arXiv:1801.03321 [astro-ph.CO].
- [82] E. Cotner, A. Kusenko, M. Sasaki, and V. Takhistov, JCAP **1910**, 077 (2019), arXiv:1907.10613 [astro-ph.CO].
- [83] S. G. Rubin, M. Y. Khlopov, and A. S. Sakharov, Grav. Cosmol. **S6**, 51 (2000), arXiv:hep-ph/0005271.
- [84] S. G. Rubin, A. S. Sakharov, and M. Y. Khlopov, J. Exp. Theor. Phys. **91**, 921 (2001), arXiv:hep-ph/0106187.
- [85] V. Dokuchaev, Y. Eroshenko, and S. Rubin, Grav. Cosmol. **11**, 99 (2005), arXiv:astro-ph/0412418.
- [86] M. Y. Khlopov, R. V. Konoplich, S. G. Rubin, and A. S. Sakharov, Grav. Cosmol. **6**, 153 (2000).
- [87] J. Garriga, A. Vilenkin, and J. Zhang, J. Cosmol. Astropart. Phys. **1602**, 064 (2016), arXiv:1512.01819 [hep-th].
- [88] H. Deng, J. Garriga, and A. Vilenkin, JCAP **1704**, 050 (2017), arXiv:1612.03753 [gr-qc].
- [89] H. Deng and A. Vilenkin, JCAP **1712**, 044 (2017), arXiv:1710.02865 [gr-qc].
- [90] J. Liu, Z.-K. Guo, and R.-G. Cai, (2019), arXiv:1908.02662 [astro-ph.CO].
- [91] A. Dolgov and J. Silk, Phys. Rev. **D47**, 4244 (1993).
- [92] M. Kopp, S. Hofmann, and J. Weller, Phys. Rev. D **83**, 124025 (2011), arXiv:1012.4369 [astro-ph.CO].
- [93] T. Harada and B. J. Carr, Phys. Rev. **D71**, 104009 (2005), arXiv:astro-ph/0412134.
- [94] Y. Akrami *et al.* (Planck), (2018), arXiv:1807.06211 [astro-ph.CO].
- [95] Y. Sendouda, S. Nagataki, and K. Sato, J. Cosmol. Astropart. Phys. **0606**, 003 (2006), arXiv:astro-ph/0603509.
- [96] J. D. Barrow, Phys. Rev. **D46**, R3227 (1992).
- [97] J. D. Barrow and B. J. Carr, Phys. Rev. **D54**, 3920 (1996).
- [98] T. Harada, C. Goymer, and B. J. Carr, Phys. Rev. **D66**, 104023 (2002), arXiv:astro-ph/0112563.
- [99] I. D. Novikov, A. G. Polnarev, A. A. Starobinsky, and Y. B. Zeldovich, Astron. Astrophys. **80**, 104 (1979).
- [100] A. S. Josan, A. M. Green, and K. A. Malik, Phys. Rev. **D79**, 103520 (2009), arXiv:0903.3184 [astro-ph.CO].
- [101] B. J. Carr, K. Kohri, Y. Sendouda, and J. Yokoyama, Phys. Rev. **D81**, 104019 (2010), arXiv:0912.5297 [astro-ph.CO].
- [102] B. Carr, F. Kühnel, and M. Sandstad, Phys. Rev. **D94**, 083504 (2016), arXiv:1607.06077 [astro-ph.CO].
- [103] S. W. Hawking, Commun. Math. Phys. **43**, 199 (1975), erratum-ibid.46:206-206,1976.
- [104] B. J. Carr, Astrophys. J. **206**, 8 (1976).
- [105] B. V. Lehmann, C. Johnson, S. Profumo, and T. Schwemberger, (2019), 10.1088/1475-7516/2019/10/046, [JCAP1910,no.10,046(2019)], arXiv:1906.06348 [hep-ph].
- [106] D. N. Page, Phys. Rev. **D13**, 198 (1976).
- [107] J. H. MacGibbon, Phys. Rev. **D44**, 376 (1991).
- [108] J. H. MacGibbon and B. R. Webber, Phys. Rev. **D41**, 3052 (1990).
- [109] J. H. MacGibbon, B. J. Carr, and D. N. Page, Phys. Rev. **D78**, 064043 (2008), arXiv:0709.2380 [astro-ph].
- [110] M. Raidal, S. Solodukhin, V. Vaskonen, and H. Veermäe, Phys. Rev. **D97**, 123520 (2018), arXiv:1802.07728 [astro-ph.CO].
- [111] B. V. Vainer and P. D. Naselskii, Astron. Zh. **55**, 231 (1978), [Sov. Astron. **22**, 138 (1978).].
- [112] S. Miyama and K. Sato, Prog. Theor. Phys. **59**, 1012 (1978).
- [113] Y. B. Zel'dovich, A. A. Starobinskii, M. I. Khlopov, and V. M. Chechetkin, Pisma Astron. Zh. **3**, 208 (1977), [Sov. Astron. Lett. **3**, 110 (1977).].
- [114] D. Lindley, Mon. Not. Roy. Astron. Soc. **193**, 593 (1980).
- [115] K. Kohri and J. Yokoyama, Phys. Rev. **D61**, 023501 (1999), arXiv:astro-ph/9908160.
- [116] M. Kawasaki, K. Kohri, and T. Moroi, Phys. Rev. **D71**, 083502 (2005), arXiv:astro-ph/0408426.

- [117] M. Kawasaki, K. Kohri, and T. Moroi, Phys. Lett. **B625**, 7 (2005), arXiv:astro-ph/0402490.
- [118] S. K. Acharya and R. Khatri, (2020), arXiv:2002.00898 [astro-ph.CO].
- [119] A. Coc, *Proceedings, 14th International Symposium on Nuclei in the Cosmos (NIC-XIV): Niigata, Japan, June 19-24, 2016*, JPS Conf. Proc. **14**, 010102 (2017).
- [120] A. Coc, M. Pospelov, J.-P. Uzan, and E. Vangioni, Phys. Rev. **D90**, 085018 (2014), arXiv:1405.1718 [hep-ph].
- [121] A. Goudelis, M. Pospelov, and J. Pradler, Phys. Rev. Lett. **116**, 211303 (2016), arXiv:1510.08858 [hep-ph].
- [122] W. Hu and J. Silk, Phys. Rev. Lett. **70**, 2661 (1993).
- [123] H. Tashiro and N. Sugiyama, Phys. Rev. **D78**, 023004 (2008), arXiv:0801.3172 [astro-ph].
- [124] R. A. Sunyaev and J. Chluba, Astron. Nachr. **330**, 657 (2009), arXiv:0908.0435 [astro-ph.CO].
- [125] J. Chluba, Mon. Not. Roy. Astron. Soc. **402**, 1195 (2010), arXiv:0910.3663 [astro-ph.CO].
- [126] T. R. Slatyer, N. Padmanabhan, and D. P. Finkbeiner, Phys. Rev. **D80**, 043526 (2009), arXiv:0906.1197 [astro-ph.CO].
- [127] L. Zhang, X. Chen, M. Kamionkowski, Z.-g. Si, and Z. Zheng, Phys. Rev. **D76**, 061301(R) (2007), arXiv:0704.2444 [astro-ph].
- [128] J. H. MacGibbon and B. J. Carr, Astrophys. J. **371**, 447 (1991).
- [129] X.-L. Chen and M. Kamionkowski, Phys. Rev. **D70**, 043502 (2004), arXiv:astro-ph/0310473 [astro-ph].
- [130] X.-H. Fan, C. L. Carilli, and B. G. Keating, Ann. Rev. Astron. Astrophys. **44**, 415 (2006), arXiv:astro-ph/0602375.
- [131] V. Poulin, J. Lesgourgues, and P. D. Serpico, JCAP **1703**, 043 (2017), arXiv:1610.10051 [astro-ph.CO].
- [132] P. Stöcker, M. Krämer, J. Lesgourgues, and V. Poulin, (2018), arXiv:1801.01871 [astro-ph.CO].
- [133] M. Lucca, N. Schneberg, D. C. Hooper, J. Lesgourgues, and J. Chluba, (2019), arXiv:1910.04619 [astro-ph.CO].
- [134] H. Poulter, Y. Ali-Haïmoud, J. Hamann, M. White, and A. G. Williams, (2019), arXiv:1907.06485 [astro-ph.CO].
- [135] B. J. Carr and J. H. MacGibbon, Phys. Rept. **307**, 141 (1998).
- [136] A. Barrau, G. Boudoul, and L. Derome, in *Proceedings, 28th International Cosmic Ray Conference (ICRC 2003): Tsukuba, Japan, July 31-August 7, 2003* (2003) pp. 1697–1699, arXiv:astro-ph/0304528 [astro-ph].
- [137] G. Ballesteros, J. Coronado-Blázquez, and D. Gaggero, (2019), arXiv:1906.10113 [astro-ph.CO].
- [138] A. Arbey, J. Auffinger, and J. Silk, (2019), arXiv:1906.04750 [astro-ph.CO].
- [139] H. Fukuda and K. Nakayama, (2019), arXiv:1910.06308 [hep-ph].
- [140] E. L. Wright, Astrophys. J. **459**, 487 (1996), astro-ph/9509074.
- [141] P. Sreekumar *et al.* (EGRET), Astrophys. J. **494**, 523 (1998), arXiv:astro-ph/9709257.
- [142] B. J. Carr, K. Kohri, Y. Sendouda, and J. Yokoyama, Phys. Rev. **D94**, 044029 (2016), arXiv:1604.05349 [astro-ph.CO].
- [143] M. Boudaud and M. Cirelli, Phys. Rev. Lett. **122**, 041104 (2019), arXiv:1807.03075 [astro-ph.HE].
- [144] M. S. Turner, Nature **297**, 379 (1982).
- [145] P. Kiraly, J. Szabelski, J. Wdowczyk, and A. W. Wolfendale, Nature **293**, 120 (1981).
- [146] K. Yoshimura *et al.* (BESS), Phys. Rev. Lett. **75**, 3792 (1995).
- [147] K. Maki, T. Mitsui, and S. Orito, Phys. Rev. Lett. **76**, 3474 (1996), arXiv:astro-ph/9601025.
- [148] A. Barrau, D. Blais, G. Boudoul, and D. Polarski, Phys. Lett. **B551**, 218 (2003), arXiv:astro-ph/0210149.
- [149] S. Orito *et al.* (BESS), Phys. Rev. Lett. **84**, 1078 (2000), arXiv:astro-ph/9906426.
- [150] M. Boezio *et al.* (WiZard/CAPRICE), Astrophys. J. **561**, 787 (2001), arXiv:astro-ph/0103513.
- [151] A. Jacholkowska (AMS), Nucl. Phys. Proc. Suppl. **165**, 324 (2007).
- [152] A. Barrau *et al.*, Astron. Astrophys. **398**, 403 (2003), arXiv:astro-ph/0207395.
- [153] K. Abe *et al.* (BESS), Phys. Lett. **B670**, 103 (2008), arXiv:0805.1754 [astro-ph].
- [154] E. V. Bugaev and K. V. Konishchev, Phys. Rev. **D66**, 084004 (2002), arXiv:astro-ph/0206082.
- [155] E. Bugaev and P. Klimai, Phys. Rev. **D79**, 103511 (2009), arXiv:0812.4247 [astro-ph].
- [156] C. Bambi, A. D. Dolgov, and A. A. Petrov, Phys. Lett. **B670**, 174 (2008), [Erratum: Phys. Lett. **B681**, 504 (2009)], arXiv:0801.2786 [astro-ph].
- [157] W. DeRocco and P. W. Graham, (2019), arXiv:1906.07740 [astro-ph.CO].
- [158] R. Laha, (2019), arXiv:1906.09994 [astro-ph.HE].
- [159] B. Dasgupta, R. Laha, and A. Ray, (2019), arXiv:1912.01014 [hep-ph].
- [160] M. Malek *et al.* (Super-Kamiokande), Phys. Rev. Lett. **90**, 061101 (2003), arXiv:hep-ex/0209028.
- [161] C. Lunardini and Y. F. Perez Gonzalez, (2019), arXiv:1910.07864 [hep-ph].
- [162] A. M. Green, Phys. Rev. **D60**, 063516 (1999), arXiv:astro-ph/9903484.
- [163] M. Y. Khlopov, A. Barrau, and J. Grain, Class. Quant. Grav. **23**, 1875 (2006), arXiv:astro-ph/0406621.
- [164] M. Lemoine, Phys. Lett. **B481**, 333 (2000), arXiv:hep-ph/0001238.
- [165] K. Kohri, T. Moroi, and A. Yotsuyanagi, Phys. Rev. **D73**, 123511 (2006), arXiv:hep-ph/0507245.
- [166] M. Kawasaki, K. Kohri, T. Moroi, and A. Yotsuyanagi, Phys. Rev. **D78**, 065011 (2008), arXiv:0804.3745 [hep-ph].
- [167] N. Aghanim *et al.* (Planck), (2019), arXiv:1907.12875 [astro-ph.CO].
- [168] K. M. Belotsky, A. A. Kirillov, N. O. Nazarova, and S. G. Rubin, Int. J. Mod. Phys. **D26**, 1750102 (2017), arXiv:1702.06338 [astro-ph.CO].
- [169] K. J. Mack and D. H. Wesley, (2008), arXiv:0805.1531v2 [astro-ph].
- [170] S. Clark, B. Dutta, Y. Gao, Y.-Z. Ma, and L. E. Strigari, Phys. Rev. **D98**, 043006 (2018), arXiv:1803.09390 [astro-ph.HE].
- [171] N. A. Porter and T. C. Weekes, Nature **277**, 199 (1979).
- [172] D. V. Semikoz, Astrophys. J. **436**, 254 (1994).
- [173] B. Carter, G. W. Gibbons, D. N. C. Lin, and M. J. Perry, Astron. Astrophys. **52**, 427 (1976).
- [174] C. E. Fichtel *et al.*, Astrophys. J. **434**, 557 (1994).
- [175] F. Halzen, E. Zas, J. H. MacGibbon, and T. C. Weekes, Nature **353**, 807 (1991).

- [176] D. B. Cline and W. Hong, *Astrophys. J.* **401**, L57 (1992).
- [177] D. B. Cline and W. Hong, *Astropart. Phys.* **5**, 175 (1996).
- [178] D. B. Cline, C. Matthey, and S. Otwinowski, *Astropart. Phys.* **18**, 531 (2003), arXiv:astro-ph/0110276.
- [179] D. B. Cline, B. Czerny, C. Matthey, A. Janiuk, and S. Otwinowski, *Astrophys. J.* **633**, L73 (2005), arXiv:astro-ph/0510309.
- [180] D. B. Cline, C. Matthey, S. Otwinowski, B. Czerny, and A. Janiuk, *AIP Conf. Proc.* **921**, 280 (2007), arXiv:astro-ph/0608158.
- [181] D. B. Cline and S. Otwinowski, (2009), arXiv:0908.1352 [astro-ph.CO].
- [182] T. N. Ukwatta *et al.*, *AIP Conf. Proc.* **1133**, 440 (2009), arXiv:0901.0542 [astro-ph.HE].
- [183] J. Oliensis and C. T. Hill, *Phys. Lett.* **B143**, 92 (1984).
- [184] A. F. Heckler, *Phys. Rev.* **D55**, 480 (1997), arXiv:astro-ph/9601029.
- [185] A. F. Heckler, *Phys. Rev. Lett.* **78**, 3430 (1997), arXiv:astro-ph/9702027.
- [186] J. M. Cline, M. Mostoslavsky, and G. Servant, *Phys. Rev.* **D59**, 063009 (1999), arXiv:hep-ph/9810439.
- [187] J. I. Kapusta, *Phys. Rev. Lett.* **86**, 1670 (2001), arXiv:astro-ph/0008222.
- [188] R. G. Daghigh and J. I. Kapusta, *Phys. Rev.* **D73**, 124024 (2006), arXiv:astro-ph/0604439.
- [189] A. A. Belyanin, V. V. Kocharovskiy, and V. V. Kocharovskiy, *Mon. Not. Roy. Astron. Soc.* **283**, 626 (1996).
- [190] E. Bugaev, P. Klimai, and V. Petkov, in *Proceedings, 30th International Cosmic Ray Conference (ICRC 2007): Merida, Yucatan, Mexico, July 3-11, 2007*, Vol. 3 (2007) pp. 1123–1126, [3,1123(2007)], arXiv:0706.3778 [astro-ph].
- [191] D. E. Alexandreas *et al.*, *Phys. Rev. Lett.* **71**, 2524 (1993).
- [192] M. Amenomori *et al.* (Tibet AS γ), *Astron. Astrophys.* **311**, 919 (1996).
- [193] E. T. Linton *et al.*, *J. Cosmol. Astropart. Phys.* **0601**, 013 (2006).
- [194] V. B. Petkov *et al.*, *Astron. Lett.* **34**, 509 (2008), [*Pisma Astron. Zh.* **34**, 563 (2008)], arXiv:0808.3093 [astro-ph].
- [195] V. B. Petkov, E. V. Bugaev, P. A. Klimai, and D. V. Smirnov, *J. Exp. Theor. Phys. Lett.* **87**, 1 (2008), arXiv:0803.2313 [astro-ph].
- [196] E. V. Bugaev *et al.*, (2009), arXiv:0906.3182 [astro-ph.CO].
- [197] R. G. Daghigh and J. I. Kapusta, *Phys. Rev.* **D65**, 064028 (2002), arXiv:gr-qc/0109090.
- [198] R. G. Daghigh and J. I. Kapusta, *Phys. Rev.* **D67**, 044006 (2003), arXiv:astro-ph/0211579.
- [199] A. Albert *et al.* (HAWC), (2019), arXiv:1911.04356 [astro-ph.HE].
- [200] D.-C. Dai, R. Gregory, and D. Stojkovic, (2019), arXiv:1909.00773 [hep-ph].
- [201] K. Kohri and H. Matsui, (2017), arXiv:1708.02138 [hep-ph].
- [202] J. H. MacGibbon, *Nature* **329**, 308 (1987).
- [203] J. D. Barrow, E. J. Copeland, and A. R. Liddle, *Phys. Rev.* **D46**, 645 (1992).
- [204] A. M. Green and A. R. Liddle, *Phys. Rev.* **D56**, 6166 (1997), arXiv:astro-ph/9704251.
- [205] S. Alexeyev, A. Barrau, G. Boudoul, O. Khovanskaya, and M. Sazhin, *Class. Quant. Grav.* **19**, 4431 (2002), arXiv:gr-qc/0201069.
- [206] P. Chen and R. J. Adler, *Nucl. Phys. Proc. Suppl.* **124**, 103 (2003), arXiv:gr-qc/0205106.
- [207] P. Chen, *New Astron. Rev.* **49**, 233 (2005), arXiv:astro-ph/0406514.
- [208] K. Nozari and S. H. Mehdipour, *Mod. Phys. Lett.* **A20**, 2937 (2005), arXiv:0809.3144 [gr-qc].
- [209] R.-G. Cai and S.-J. Wang, (2019), arXiv:1910.07981 [astro-ph.CO].
- [210] S. Alexander and P. Mészáros, (2007), arXiv:hep-th/0703070.
- [211] N. Aghanim *et al.* (Planck), (2018), arXiv:1807.06209 [astro-ph.CO].
- [212] K. J. Mack, J. P. Ostriker, and M. Ricotti, *Astrophys. J.* **665**, 1277 (2007), arXiv:astro-ph/0608642.
- [213] F. Capela, M. Pshirkov, and P. Tinyakov, *Phys. Rev.* **D87**, 123524 (2013), arXiv:1301.4984 [astro-ph.CO].
- [214] S. Clesse and J. García-Bellido, *Phys. Dark Univ.* **15**, 142 (2017), arXiv:1603.05234 [astro-ph.CO].
- [215] A. W. Strong, I. V. Moskalenko, and O. Reimer, *Astrophys. J.* **613**, 956 (2004), arXiv:astro-ph/0405441.
- [216] H. Niikura, M. Takada, S. Yokoyama, T. Sumi, and S. Masaki, (2019), arXiv:1901.07120 [astro-ph.CO].
- [217] M. R. S. Hawkins, *Nature* **366**, 242 (1993).
- [218] S. Dong *et al.*, *Astrophys. J.* **664**, 862 (2007), arXiv:astro-ph/0702240 [ASTRO-PH].
- [219] G. F. Marani, R. J. Nemiroff, J. P. Norris, K. Hurley, and J. T. Bonnell, *Astrophys. J. Lett.* **512**, L13 (1999), arXiv:astro-ph/9810391.
- [220] R. J. Nemiroff, G. F. Marani, J. P. Norris, and J. T. Bonnell, *Phys. Rev. Lett.* **86**, 580 (2001), arXiv:astro-ph/0101488 [astro-ph].
- [221] A. Barnacka, J. F. Glicenstein, and R. Moderski, *Phys. Rev.* **D86**, 043001 (2012), arXiv:1204.2056 [astro-ph.CO].
- [222] A. Katz, J. Kopp, S. Sibiryakov, and W. Xue, Submitted to: JCAP (2018), arXiv:1807.11495 [astro-ph.CO].
- [223] B. Paczynski, *Astrophys. J.* **304**, 1 (1986).
- [224] C. Alcock *et al.* (MACHO), *Astrophys. J.* **542**, 281 (2000), arXiv:astro-ph/0001272.
- [225] C. Alcock *et al.* (MACHO), *Astrophys. J. Suppl.* **136**, 439 (2001), arXiv:astro-ph/0003392 [astro-ph].
- [226] C. Hamadache *et al.*, *Astron. Astrophys.* **454**, 185 (2006), arXiv:astro-ph/0601510.
- [227] P. Tisserand *et al.* (EROS-2), *Astron. Astrophys.* **469**, 387 (2007), arXiv:astro-ph/0607207.
- [228] C. Alcock *et al.* (MACHO), *Astrophys. J. Lett.* **550**, L169 (2001), arXiv:astro-ph/0011506.
- [229] S. Calchi-Novati *et al.* (The POINT-AGAPE), *Astron. Astrophys.* **443**, 911 (2005), arXiv:astro-ph/0504188.
- [230] L. Wyrzykowski *et al.*, *Mon. Not. Roy. Astron. Soc.* **397**, 1228 (2009), arXiv:0905.2044 [astro-ph.GA].
- [231] S. Calchi Novati, L. Mancini, G. Scarpetta, and L. Wyrzykowski, *Mon. Not. Roy. Astron. Soc.* **400**, 1625 (2009), arXiv:0908.3836 [astro-ph.GA].

- [232] L. Wyrzykowski *et al.*, Mon. Not. Roy. Astron. Soc. **407**, 189 (2010), arXiv:1004.5247 [astro-ph.GA].
- [233] L. Wyrzykowski *et al.*, Mon. Not. Roy. Astron. Soc. **413**, 493 (2011), arXiv:1012.1154 [astro-ph.GA].
- [234] L. Wyrzykowski *et al.*, Mon. Not. Roy. Astron. Soc. **416**, 2949 (2011), arXiv:1106.2925 [astro-ph.GA].
- [235] S. Calchi Novati, S. Mirzoyan, P. Jetzer, and G. Scarpetta, Mon. Not. Roy. Astron. Soc. **435**, 1582 (2013), arXiv:1308.4281 [astro-ph.GA].
- [236] u. Wyrzykowski and I. Mandel, (2019), arXiv:1904.07789 [astro-ph.SR].
- [237] J. Calcino, J. García-Bellido, and T. M. Davis, Mon. Not. Roy. Astron. Soc. **479**, 2889 (2018), arXiv:1803.09205 [astro-ph.CO].
- [238] M. R. S. Hawkins, Astron. Astrophys. **575**, A107 (2015), arXiv:1503.01935 [astro-ph.GA].
- [239] K. Griest, A. M. Cieplak, and M. J. Lehner, Phys. Rev. Lett. **111**, 181302 (2013).
- [240] K. Griest, A. M. Cieplak, and M. J. Lehner, Astrophys. J. **786**, 158 (2014), arXiv:1307.5798 [astro-ph.CO].
- [241] H. Niihara, M. Takada, N. Yasuda, R. H. Lupton, T. Sumi, S. More, A. More, M. Oguri, and M. Chiba, (2017), arXiv:1701.02151 [astro-ph.CO].
- [242] N. Smyth, S. Profumo, S. English, T. Jeltema, K. McKinnon, and P. Guhathakurta, (2019), arXiv:1910.01285 [astro-ph.CO].
- [243] S. Sugiyama, T. Kurita, and M. Takada, (2019), arXiv:1905.06066 [astro-ph.CO].
- [244] M. Oguri, J. M. Diego, N. Kaiser, P. L. Kelly, and T. Broadhurst, Phys. Rev. **D97**, 023518 (2018), arXiv:1710.00148 [astro-ph.CO].
- [245] M. Zumalacárregui and U. Seljak, Phys. Rev. Lett. **121**, 141101 (2018), arXiv:1712.02240 [astro-ph.CO].
- [246] J. García-Bellido, S. Clesse, and P. Fleury, Phys. Dark Univ. **20**, 95 (2018), arXiv:1712.06574 [astro-ph.CO].
- [247] J. J. Dalcanton, C. R. Canizares, A. Granados, C. C. Steidel, and J. T. Stocke, Astrophys. J. **424**, 550 (1994).
- [248] M. R. S. Hawkins, Astron. Astrophys. (2006), 10.1051/0004-6361:20066283, [Astron. Astrophys.462,581(2007)], arXiv:astro-ph/0611491 [astro-ph].
- [249] E. Zackrisson, N. Bergvall, T. Marquart, and P. Helbig, Astron. Astrophys. **408**, 17 (2003), arXiv:astro-ph/0306434 [astro-ph].
- [250] E. Mediavilla, J. A. Muñoz, E. Falco, V. Motta, E. Guerras, H. Canovas, C. Jean, A. Oscoz, and A. M. Mosquera, Astrophys. J. **706**, 1451 (2009), arXiv:0910.3645.
- [251] E. Mediavilla, J. Jiménez-Vicente, J. A. Muñoz, H. Vives-Arias, and J. Calderón-Infante, Astrophys. J. **836**, L18 (2017), arXiv:1702.00947 [astro-ph.GA].
- [252] M. R. S. Hawkins, Astron. Astrophys. **633**, A107 (2020), arXiv:2001.07633 [astro-ph.GA].
- [253] H. K. Vedantham *et al.*, Astrophys. J. **845**, 89 (2017), arXiv:1702.06582 [astro-ph.HE].
- [254] P. N. Wilkinson *et al.*, Phys. Rev. Lett. **86**, 584 (2001), arXiv:astro-ph/0101328.
- [255] Y. D. Hezaveh *et al.*, Astrophys. J. **823**, 37 (2016), arXiv:1601.01388 [astro-ph.CO].
- [256] M. Karami, A. E. Broderick, S. Rahvar, and M. Reid, Astrophys. J. **833**, 169 (2016), arXiv:1601.05801 [astro-ph.HE].
- [257] K. Schutz and A. Liu, Phys. Rev. **D95**, 023002 (2017), arXiv:1610.04234 [astro-ph.CO].
- [258] J. B. Muñoz, E. D. Kovetz, L. Dai, and M. Kamionkowski, Phys. Rev. Lett. **117**, 091301 (2016), arXiv:1605.00008 [astro-ph.CO].
- [259] J. A. Dror, H. Ramani, T. Trickle, and K. M. Zurek, (2019), arXiv:1901.04490 [astro-ph.CO].
- [260] Y. Bai and N. Orlofsky, (2018), arXiv:1812.01427 [astro-ph.HE].
- [261] B. J. Carr and M. Sakellariadou, Astrophys. J. **516**, 195 (1999).
- [262] C. G. Lacey and J. P. Ostriker, Astrophys. J. **299**, 633 (1985).
- [263] T. Totani, Publ. Astron. Soc. Jap. **62**, L1 (2010), arXiv:0908.3295 [astro-ph.CO].
- [264] B. J. Carr and C. G. Lacey, Astrophys. J. **316**, 23 (1987).
- [265] K. M. Belotsky, A. A. Kirillov, and S. G. Rubin, Phys. Atom. Nucl. **78**, 387 (2015), [Yad. Fiz. **78**, 417–422 (2015)].
- [266] T. Bringmann, P. Scott, and Y. Akrami, Phys. Rev. **D85**, 125027 (2012), arXiv:1110.2484 [astro-ph.CO].
- [267] J. R. Chisholm, Phys. Rev. **D73**, 083504 (2006), arXiv:astro-ph/0509141.
- [268] A. A. Jackson and M. P. Ryan, Nature **245**, 88 (1973).
- [269] B. E. Zhilyaev, Bull. Crim. Astrophys. Observ. **103**, 58 (2007), arXiv:0706.0930 [astro-ph].
- [270] I. B. Khriplovich, A. A. Pomeransky, N. Produit, and G. Y. Ruban, (2008), arXiv:0801.4623 [hep-ex].
- [271] Y. Luo, S. Hanasoge, J. Tromp, and F. Pretorius, Astrophys. J. **751**, 16 (2012), arXiv:1203.3806 [astro-ph.CO].
- [272] A. W. Adams and J. S. Bloom, (2004), arXiv:astro-ph/0405266.
- [273] N. Seto and A. Cooray, Phys. Rev. **D70**, 063512 (2004), arXiv:astro-ph/0405216.
- [274] M. Roncadelli, A. Treves, and R. Turolla, (2009), arXiv:0901.1093 [astro-ph.CO].
- [275] M. A. Abramowicz *et al.*, Astrophys. J. **705**, 659 (2009), arXiv:0810.3140 [astro-ph].
- [276] F. Capela, M. Pshirkov, and P. Tinyakov, Phys. Rev. **D87**, 023507 (2013), arXiv:1209.6021 [astro-ph.CO].
- [277] P. Pani and A. Loeb, J. Cosmol. Astropart. Phys. **1406**, 026 (2014), arXiv:1401.3025 [astro-ph.CO].
- [278] F. Capela, M. Pshirkov, and P. Tinyakov, (2014), arXiv:1402.4671 [astro-ph.CO].
- [279] G. Defillon, E. Granet, P. Tinyakov, and M. H. G. Tytgat, Phys. Rev. **D90**, 103522 (2014), arXiv:1409.0469 [gr-qc].
- [280] R. Ibata, C. Nipoti, A. Sollima, M. Bellazzini, S. Chapman, and E. Dalessandro, Mon. Not. Roy. Astron. Soc. **428**, 3648 (2013), arXiv:1210.7787 [astro-ph.CO].
- [281] J. D. Bradford, M. Geha, R. Muñoz, F. A. Santana, J. D. Simon, P. Côté, P. B. Stetson, E. Kirby, and S. G. Djorgovski, Astrophys. J. **743**, 167 (2011), [Erratum: Astrophys. J.778,85(2013)], arXiv:1110.0484 [astro-ph.CO].
- [282] P. W. Graham, S. Rajendran, and J. Varela, Phys. Rev. **D92**, 063007 (2015), arXiv:1505.04444 [hep-ph].
- [283] P. Montero-Camacho, X. Fang, G. Vasquez, M. Silva, and C. M. Hirata, JCAP **1908**, 031 (2019), arXiv:1906.05950

- [astro-ph.CO].
- [284] G. M. Fuller, A. Kusenkov, and V. Takhistov, Phys. Rev. Lett. **119**, 061101 (2017), arXiv:1704.01129 [astro-ph.HE].
- [285] M. A. Abramowicz and M. Bejger, (2017), arXiv:1704.05931 [astro-ph.HE].
- [286] J. N. Bahcall, P. Hut, and S. Tremaine, Astrophys. J. **290**, 15 (1985).
- [287] M. D. Weinberg, S. L. Shapiro, and I. Wasserman, Astrophys. J. **312**, 367 (1987).
- [288] J. Yoo, J. Chanamé, and A. Gould, Astrophys. J. **601**, 311 (2004), arXiv:astro-ph/0307437.
- [289] D. P. Quinn *et al.*, Mon. Not. Roy. Astron. Soc. Lett. **396**, L11 (2009), arXiv:0903.1644 [astro-ph.GA].
- [290] M. A. Monroy-Rodríguez and C. Allen, Astrophys. J. **790**, 159 (2014), arXiv:1406.5169 [astro-ph.GA].
- [291] B. Moore, Astrophys. J. Lett. **413**, L93 (1993), astro-ph/9306004.
- [292] T. D. Brandt, Astrophys. J. **824**, L31 (2016), arXiv:1605.03665 [astro-ph.GA].
- [293] S. M. Koushiappas and A. Loeb, Phys. Rev. Lett. **119**, 041102 (2017), arXiv:1704.01668 [astro-ph.GA].
- [294] Q. Zhu, E. Vasiliev, Y. Li, and Y. Jing, Mon. Not. Roy. Astron. Soc. **476**, 2 (2018), arXiv:1710.05032 [astro-ph.CO].
- [295] P. Boldrini, Y. Miki, A. Y. Wagner, R. Mohayaee, J. Silk, and A. Arbey, (2019), arXiv:1909.07395 [astro-ph.CO].
- [296] J. Stegmann, P. R. Capelo, E. Bortolas, and L. Mayer, (2019), arXiv:1910.04793 [astro-ph.GA].
- [297] N. Banik, G. Bertone, J. Bovy, and N. Bozorgnia, JCAP **1807**, 061 (2018), arXiv:1804.04384 [astro-ph.CO].
- [298] J. Bovy, D. Erkal, and J. L. Sanders, Mon. Not. Roy. Astron. Soc. **466**, 628 (2017), arXiv:1606.03470 [astro-ph.GA].
- [299] P. Hut and M. J. Rees, Mon. Not. Roy. Astron. Soc. **259**, 27 (1992).
- [300] G. H. Xu and J. P. Ostriker, Astrophys. J. **437**, 184 (1994).
- [301] S. Van den Bergh, Nature (London) **224**, 891 (1969).
- [302] B. J. Carr, “Cosmological density of black holes,” (1978).
- [303] B. Carr and J. Silk, Mon. Not. Roy. Astron. Soc. **478**, 3756 (2018), arXiv:1801.00672 [astro-ph.CO].
- [304] F. Hoyle and J. V. Narlikar, Proceedings of the Royal Society of London Series A **290**, 177 (1966).
- [305] B. J. Carr and M. J. Rees, Mon. Not. Roy. Astron. Soc. **206**, 801 (1984).
- [306] P. Mészáros, Astron. Astrophys. **38**, 5 (1975).
- [307] B. J. Carr, Astron. Astrophys. **56**, 377 (1977).
- [308] K. Freese, R. Price, and D. N. Schramm, Astrophys. J. **275**, 405 (1983).
- [309] B. J. Carr and J. Silk, Astrophys. J. **268**, 1 (1983).
- [310] R. Murgia, G. Scelfo, M. Viel, and A. Raccanelli, Phys. Rev. Lett. **123**, 071102 (2019), arXiv:1903.10509 [astro-ph.CO].
- [311] A. Kashlinsky, Astrophys. J. **823**, L25 (2016), arXiv:1605.04023 [astro-ph.CO].
- [312] A. Kashlinsky, J. C. Mather, K. Helgason, R. G. Arendt, V. Bromm, and S. H. Moseley, Astrophys. J. **804**, 99 (2015), arXiv:1412.5566 [astro-ph.CO].
- [313] K. Helgason, M. Ricotti, A. Kashlinsky, and V. Bromm, Mon. Not. Roy. Astron. Soc. **455**, 282 (2016), arXiv:1505.07226 [astro-ph.CO].
- [314] J. R. Bond, B. J. Carr, and C. J. Hogan, Astrophys. J. **306**, 428 (1986).
- [315] N. Dürchting, Phys. Rev. **D70**, 064015 (2004), arXiv:astro-ph/0406260.
- [316] M. Y. Khlopov, S. G. Rubin, and A. S. Sakharov, J. Astropart. Phys. **23**, 265 (2005), arXiv:astro-ph/0401532.
- [317] T. Bringmann, P. F. Depta, V. Domcke, and K. Schmidt-Hoberg, (2018), arXiv:1808.05910 [astro-ph.CO].
- [318] Y. Ali-Haïmoud, Phys. Rev. Lett. **121**, 081304 (2018), arXiv:1805.05912 [astro-ph.CO].
- [319] G. Ballesteros, P. D. Serpico, and M. Taoso, JCAP **1810**, 043 (2018), arXiv:1807.02084 [astro-ph.CO].
- [320] V. Desjacques and A. Riotto, (2018), arXiv:1806.10414 [astro-ph.CO].
- [321] S. Young and C. T. Byrnes, (2019), arXiv:1910.06077 [astro-ph.CO].
- [322] T. Suyama and S. Yokoyama, PTEP **2019**, 103E02 (2019), arXiv:1906.04958 [astro-ph.CO].
- [323] T. Matsubara, T. Terada, K. Kohri, and S. Yokoyama, (2019), arXiv:1909.04053 [astro-ph.CO].
- [324] M. Raidal, V. Vaskonen, and H. Veermäe, JCAP **1709**, 037 (2017), arXiv:1707.01480 [astro-ph.CO].
- [325] Y. Ali-Haïmoud, E. D. Kovetz, and M. Kamionkowski, Phys. Rev. **D96**, 123523 (2017), arXiv:1709.06576 [astro-ph.CO].
- [326] B. P. Abbott *et al.* (LIGO Scientific, Virgo), Phys. Rev. Lett. **123**, 161102 (2019), arXiv:1904.08976 [astro-ph.CO].
- [327] G. V. Bicknell and R. N. Henriksen, Astrophys. J. **219**, 1043 (1978).
- [328] G. V. Bicknell and R. N. Henriksen, Astrophys. J. **225**, 237 (1978).
- [329] T. Harada, H. Maeda, and B. J. Carr, Phys. Rev. **D77**, 024022 (2008), arXiv:0707.0528 [gr-qc].
- [330] H. Maeda, T. Harada, and B. J. Carr, Phys. Rev. **D77**, 024023 (2008), arXiv:0707.0530 [gr-qc].
- [331] B. J. Carr, T. Harada, and H. Maeda, Class. Quant. Grav. **27**, 183101 (2010), arXiv:1003.3324 [gr-qc].
- [332] B. J. Carr, Mon. Not. Roy. Astron. Soc. **194**, 639 (1981).
- [333] Y. Ali-Haïmoud and M. Kamionkowski, Phys. Rev. **D95**, 043534 (2017), arXiv:1612.05644 [astro-ph.CO].
- [334] B. Horowitz, (2016), arXiv:1612.07264 [astro-ph.CO].
- [335] D. Aloni, K. Blum, and R. Flauger, JCAP **1705**, 017 (2017), arXiv:1612.06811 [astro-ph.CO].
- [336] L. Chen, Q.-G. Huang, and K. Wang, J. Cosmol. Astropart. Phys. **1612**, 044 (2016), arXiv:1608.02174 [astro-ph.CO].
- [337] V. Poulin, P. D. Serpico, F. Calore, S. Clesse, and K. Kohri, Phys. Rev. **D96**, 083524 (2017), arXiv:1707.04206 [astro-ph.CO].
- [338] P. D. Serpico, V. Poulin, D. Inman, and K. Kohri, (2020), arXiv:2002.10771 [astro-ph.CO].
- [339] D. Gaggero, G. Bertone, N. F. Calore, R. M. T. Connors, M. Lovell, S. Markoff, and E. Storm, Phys. Rev. Lett. **118**, 241101 (2017), arXiv:1612.00457 [astro-ph.HE].
- [340] J. Manshanden, D. Gaggero, G. Bertone, R. M. T. Connors, and M. Ricotti, (2018), arXiv:1812.07967 [astro-ph.HE].
- [341] T. Kawaguchi, M. Kawasaki, T. Takayama, M. Yamaguchi, and J. Yokoyama, Mon. Not. Roy. Astron. Soc. **388**, 1426 (2008), arXiv:0711.3886 [astro-ph].

- [342] Y. Inoue and A. Kusenko, JCAP **1710**, 034 (2017), arXiv:1705.00791 [astro-ph.CO].
- [343] A. Ewall-Wice, T. C. Chang, J. Lazio, O. Dore, M. Seiffert, and R. A. Monsalve, (2018), arXiv:1803.01815 [astro-ph.CO].
- [344] A. Hektor, G. Hutsi, L. Marzola, M. Raidal, V. Vaskonen, and H. Veermäe, Phys. Rev. **D98**, 023503 (2018), arXiv:1803.09697 [astro-ph.CO].
- [345] O. Mena, S. Palomares-Ruiz, P. Villanueva-Domingo, and S. J. Witte, Phys. Rev. **D100**, 043540 (2019), arXiv:1906.07735 [astro-ph.CO].
- [346] Yu. N. Eroshenko, Astron. Lett. **42**, 347 (2016), [Pisma Astron. Zh.42,no.6,359(2016)], arXiv:1607.00612 [astro-ph.HE].
- [347] A. A. Abdo *et al.* (Fermi-LAT), Phys. Rev. Lett. **104**, 101101 (2010), arXiv:1002.3603 [astro-ph.HE].
- [348] T. Nakama, K. Kohri, and J. Silk, Phys. Rev. **D99**, 123530 (2019), arXiv:1905.04477 [astro-ph.CO].
- [349] G. Bertone, A. M. Coogan, D. Gaggero, B. J. Kavanagh, and C. Weniger, (2019), arXiv:1905.01238 [hep-ph].
- [350] K. T. Abe, H. Tashiro, and T. Tanaka, (2019), arXiv:1901.06809 [astro-ph.CO].
- [351] J. Chluba, A. L. Erickcek, and I. Ben-Dayan, Astrophys. J. **758**, 76 (2012), arXiv:1203.2681 [astro-ph.CO].
- [352] B. J. Carr and J. E. Lidsey, Phys. Rev. **D48**, 543 (1993).
- [353] J. D. Barrow and P. Coles, Mon. Not. Roy. Astron. Soc. **248**, 52 (1991).
- [354] K. Kohri, T. Nakama, and T. Suyama, Phys. Rev. **D90**, 083514 (2014), arXiv:1405.5999 [astro-ph.CO].
- [355] T. Nakama, T. Suyama, and J. Yokoyama, Phys. Rev. **D94**, 103522 (2016), arXiv:1609.02245 [gr-qc].
- [356] T. Nakama, B. Carr, and J. Silk, Phys. Rev. **D97**, 043525 (2018), arXiv:1710.06945 [astro-ph.CO].
- [357] M. H. Abitbol, J. Chluba, J. C. Hill, and B. R. Johnson, Mon. Not. Roy. Astron. Soc. **471**, 1126 (2017), arXiv:1705.01534 [astro-ph.CO].
- [358] B. J. Carr, Astron. Astrophys. **89**, 6 (1980).
- [359] J. R. Bond and B. J. Carr, Mon. Not. Roy. Astron. Soc. **207**, 585 (1984).
- [360] T. Nakamura, M. Sasaki, T. Tanaka, and K. S. Thorne, Astrophys. J. Lett. **487**, L139 (1997), arXiv:astro-ph/9708060.
- [361] K. Ioka, T. Tanaka, and T. Nakamura, Phys. Rev. **D60**, 083512 (1999), arXiv:astro-ph/9809395.
- [362] K. T. Inoue and T. Tanaka, Phys. Rev. Lett. **91**, 021101 (2003), arXiv:gr-qc/0303058.
- [363] B. Abbott *et al.* (LIGO), Astrophys. J. **659**, 918 (2007), arXiv:astro-ph/0608606.
- [364] N. Bartolo, D. Bertacca, V. De Luca, G. Franciolini, S. Matarrese, M. Peloso, A. Ricciardone, A. Riotto, and G. Tasinato, (2019), arXiv:1909.12619 [astro-ph.CO].
- [365] Y.-F. Wang, Q.-G. Huang, T. G. F. Li, and S. Liao, (2019), arXiv:1910.07397 [astro-ph.CO].
- [366] S. Bird, I. Cholis, J. B. Muñoz, Y. Ali-Haïmoud, M. Kamionkowski, E. D. Kovetz, A. Raccanelli, and A. G. Riess, Phys. Rev. Lett. **116**, 201301 (2016), arXiv:1603.00464 [astro-ph.CO].
- [367] Yu. N. Eroshenko, (2016), arXiv:1604.04932 [astro-ph.CO].
- [368] M. Sasaki, T. Suyama, T. Tanaka, and S. Yokoyama, Phys. Rev. Lett. **117**, 061101 (2016), arXiv:1603.08338 [astro-ph.CO].
- [369] M. Raidal, C. Spethmann, V. Vaskonen, and H. Veermäe, (2018), arXiv:1812.01930 [astro-ph.CO].
- [370] B. P. Abbott *et al.* (Virgo, LIGO Scientific), (2018), arXiv:1808.04771 [astro-ph.CO].
- [371] S. Wang, T. Terada, and K. Kohri, Phys. Rev. **D99**, 103531 (2019), arXiv:1903.05924 [astro-ph.CO].
- [372] A. D. Gow, C. T. Byrnes, A. Hall, and J. A. Peacock, (2019), arXiv:1911.12685 [astro-ph.CO].
- [373] J. M. Diego, (2019), arXiv:1911.05736 [astro-ph.CO].
- [374] R. Saito and J. Yokoyama, Phys. Rev. Lett. **102**, 161101 (2009), [Erratum: Phys. Rev. Lett. **107**, 069901 (2011)], arXiv:0812.4339 [astro-ph].
- [375] R. Saito and J. Yokoyama, Prog. Theor. Phys. **123**, 867 (2010), [Erratum: Prog. Theor. Phys. **126**, 351 (2011)], arXiv:0912.5317 [astro-ph.CO].
- [376] E. Bugaev and P. Klimai, Phys. Rev. **D81**, 023517 (2010), arXiv:0908.0664 [astro-ph.CO].
- [377] H. Assadullahi and D. Wands, Phys. Rev. **D81**, 023527 (2010), arXiv:0907.4073 [astro-ph.CO].
- [378] E. Bugaev and P. Klimai, Phys. Rev. **D83**, 083521 (2011), arXiv:1012.4697 [astro-ph.CO].
- [379] T. Nakama and T. Suyama, Phys. Rev. **D92**, 121304 (2015), arXiv:1506.05228 [gr-qc].
- [380] T. Nakama and T. Suyama, Phys. Rev. **D94**, 043507 (2016), arXiv:1605.04482 [gr-qc].
- [381] K. Kohri and T. Terada, Phys. Rev. **D97**, 123532 (2018), arXiv:1804.08577 [gr-qc].
- [382] K. Inomata, K. Kohri, T. Nakama, and T. Terada, JCAP **1910**, 071 (2019), arXiv:1904.12878 [astro-ph.CO].
- [383] K. Inomata, K. Kohri, T. Nakama, and T. Terada, Phys. Rev. **D100**, 043532 (2019), arXiv:1904.12879 [astro-ph.CO].
- [384] J. C. Hidalgo, (2007), arXiv:0708.3875 [astro-ph].
- [385] J. C. Hidalgo, (2009), arXiv:0910.1876 [astro-ph.CO].
- [386] N. Bartolo, V. De Luca, G. Franciolini, M. Peloso, D. Racco, and A. Riotto, (2018), arXiv:1810.12224 [astro-ph.CO].
- [387] N. Bartolo, V. De Luca, G. Franciolini, M. Peloso, and A. Riotto, (2018), arXiv:1810.12218 [astro-ph.CO].
- [388] R.-g. Cai, S. Pi, and M. Sasaki, (2018), arXiv:1810.11000 [astro-ph.CO].
- [389] R.-G. Cai, S. Pi, and M. Sasaki, (2019), arXiv:1909.13728 [astro-ph.CO].
- [390] Z.-C. Chen, C. Yuan, and Q.-G. Huang, (2019), arXiv:1910.12239 [astro-ph.CO].
- [391] R.-G. Cai, S. Pi, S.-J. Wang, and X.-Y. Yang, (2019), 10.1088/1475-7516/2019/10/059, [JCAP1910,no.10,059(2019)], arXiv:1907.06372 [astro-ph.CO].
- [392] V. Korol, I. Mandel, M. C. Miller, R. P. Church, and M. B. Davies, (2019), arXiv:1911.03483 [astro-ph.HE].
- [393] J. Li and Q.-G. Huang, Eur. Phys. J. **C78**, 980 (2018), arXiv:1806.01440 [astro-ph.CO].
- [394] C.-M. Yoo, T. Harada, J. Garriga, and K. Kohri, PTEP **2018**, 123E01 (2018), arXiv:1805.03946 [astro-ph.CO].
- [395] A. Kalaja, N. Bellomo, N. Bartolo, D. Bertacca, S. Matarrese, I. Musco, A. Raccanelli, and L. Verde, JCAP **1910**, 031 (2019), arXiv:1908.03596 [astro-ph.CO].

- [396] K. Ando, M. Kawasaki, and H. Nakatsuka, Phys. Rev. **D98**, 083508 (2018), arXiv:1805.07757 [astro-ph.CO].
- [397] M. Kawasaki and H. Nakatsuka, Phys. Rev. **D99**, 123501 (2019), arXiv:1903.02994 [astro-ph.CO].
- [398] C. Germani and R. K. Sheth, (2019), arXiv:1912.07072 [astro-ph.CO].
- [399] T. Suyama and S. Yokoyama, (2019), arXiv:1912.04687 [astro-ph.CO].
- [400] G. Sato-Polito, E. D. Kovetz, and M. Kamionkowski, Phys. Rev. **D100**, 063521 (2019), arXiv:1904.10971 [astro-ph.CO].
- [401] F. Hasegawa and M. Kawasaki, Phys. Rev. **D98**, 043514 (2018), arXiv:1711.00990 [astro-ph.CO].
- [402] A. M. Green, Phys. Rev. **D94**, 063530 (2016), arXiv:1609.01143 [astro-ph.CO].
- [403] B. Carr, M. Raidal, T. Tenkanen, V. Vaskonen, and H. Veermäe, Phys. Rev. D **96**, 023514 (2017), arXiv:1705.05567.
- [404] K. Kannike, L. Marzola, M. Raidal, and H. Veermäe, J. Cosmol. Astropart. Phys. **1709**, 020 (2017), arXiv:1705.06225 [astro-ph.CO].
- [405] F. Kühnel and K. Freese, Phys. Rev. **D95**, 083508 (2017), arXiv:1701.07223 [astro-ph.CO].
- [406] I. Musco and J. C. Miller, Class. Quant. Grav. **30**, 145009 (2013), arXiv:1201.2379 [gr-qc].
- [407] A. G. Polnarev and M. Y. Khlopov, Sov. Phys. Usp. **28**, 213 (1985).
- [408] T. Harada, C.-M. Yoo, K. Kohri, K.-i. Nakao, and S. Jhingan, Astrophys. J. **833**, 61 (2016), arXiv:1609.01588 [astro-ph.CO].
- [409] T. Harada, C.-M. Yoo, K. Kohri, and K.-I. Nakao, Phys. Rev. **D96**, 083517 (2017), arXiv:1707.03595 [gr-qc].
- [410] K. Kohri and T. Terada, Class. Quant. Grav. **35**, 235017 (2018), arXiv:1802.06785 [astro-ph.CO].
- [411] B. Carr, T. Tenkanen, and V. Vaskonen, Phys. Rev. **D96**, 063507 (2017), arXiv:1706.03746 [astro-ph.CO].